



# Modélisation numérique et expérimentale en sciences de la Terre : Le cas de la convection thermique

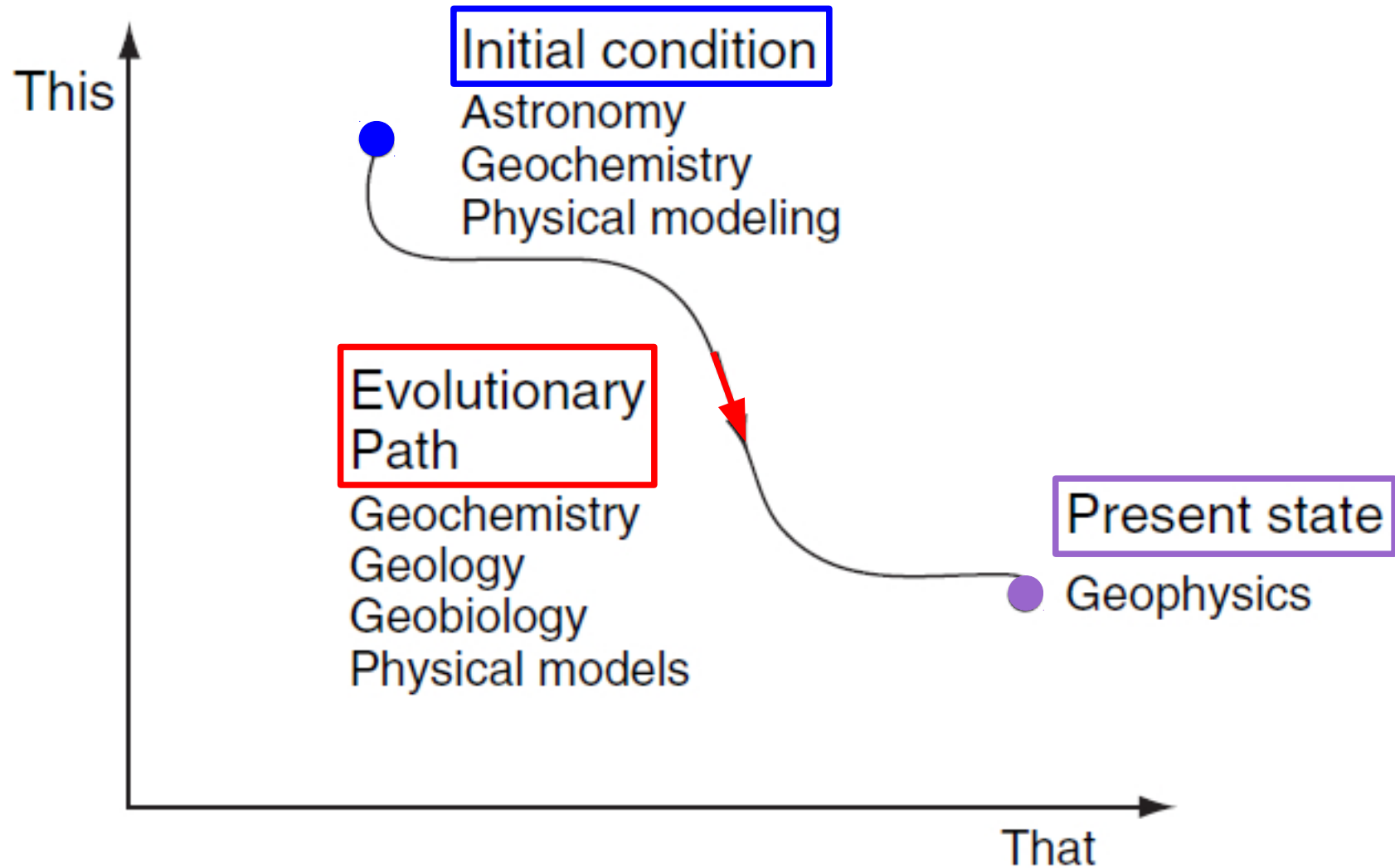
**Cinzia G. Farnetani**

Institut de Physique du Globe de Paris  
Sorbonne Paris Cite, Université Paris Diderot, UMR 7154, Paris, France



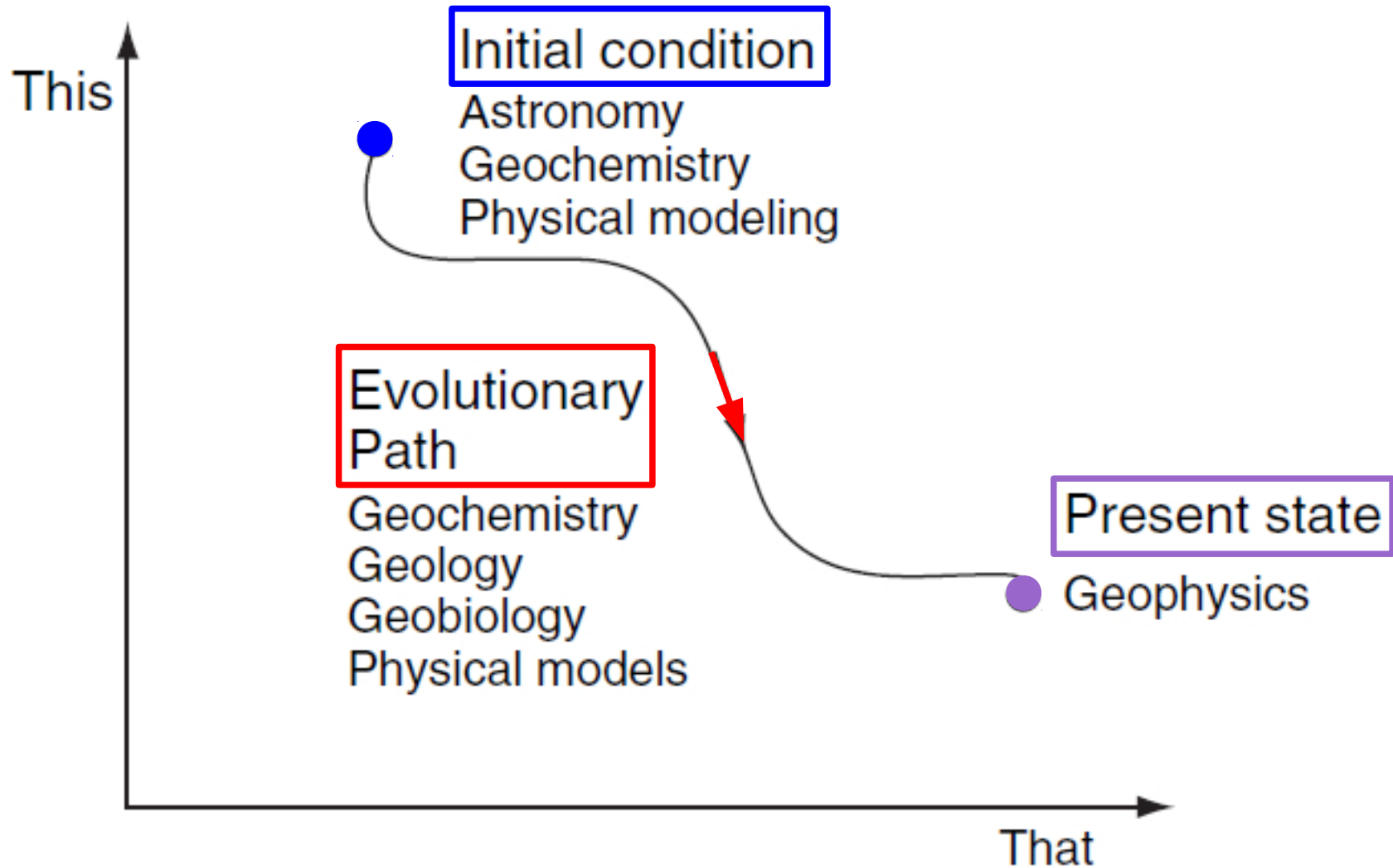
Labex

**UnivEarthS**



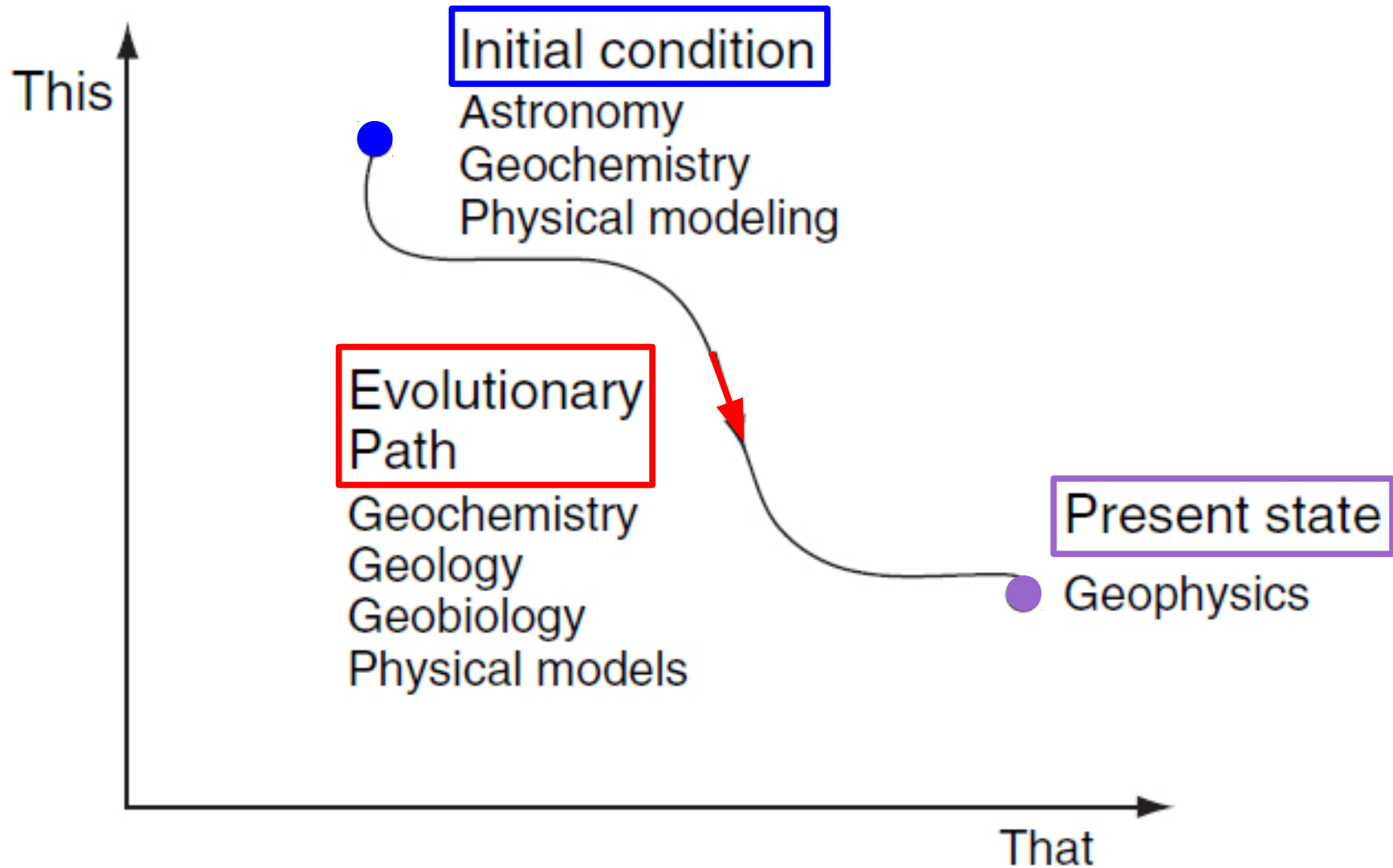
Stevenson's [2007] figure conveys the idea that we have an initial condition, an evolutionary path, a present state.

*This-That (?!?) it does not matter*



### Initial condition

- nature and origin of Earth's constitutive material (i.e., our 'cosmic heritage')
- the physics of the formation processes

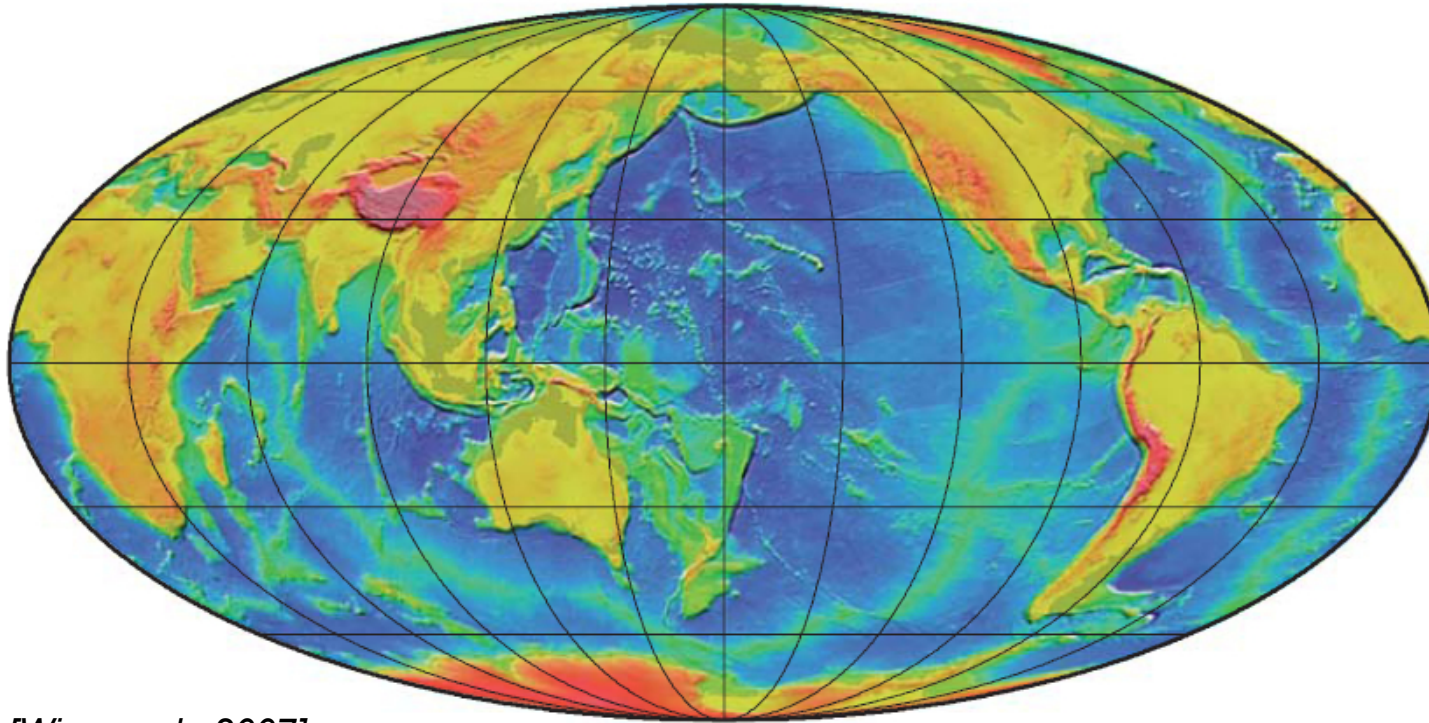


### Evolutionary path

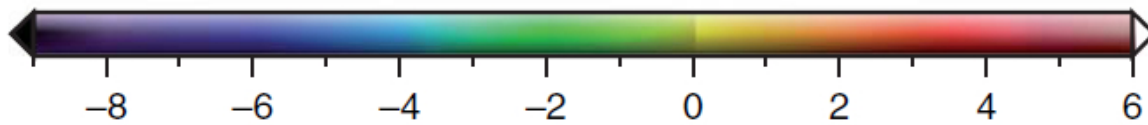
-processes in the Earth's interior, e.g., mantle convection and plate tectonics

Let's start from the **Present state**

# The Earth's topography and bathymetry

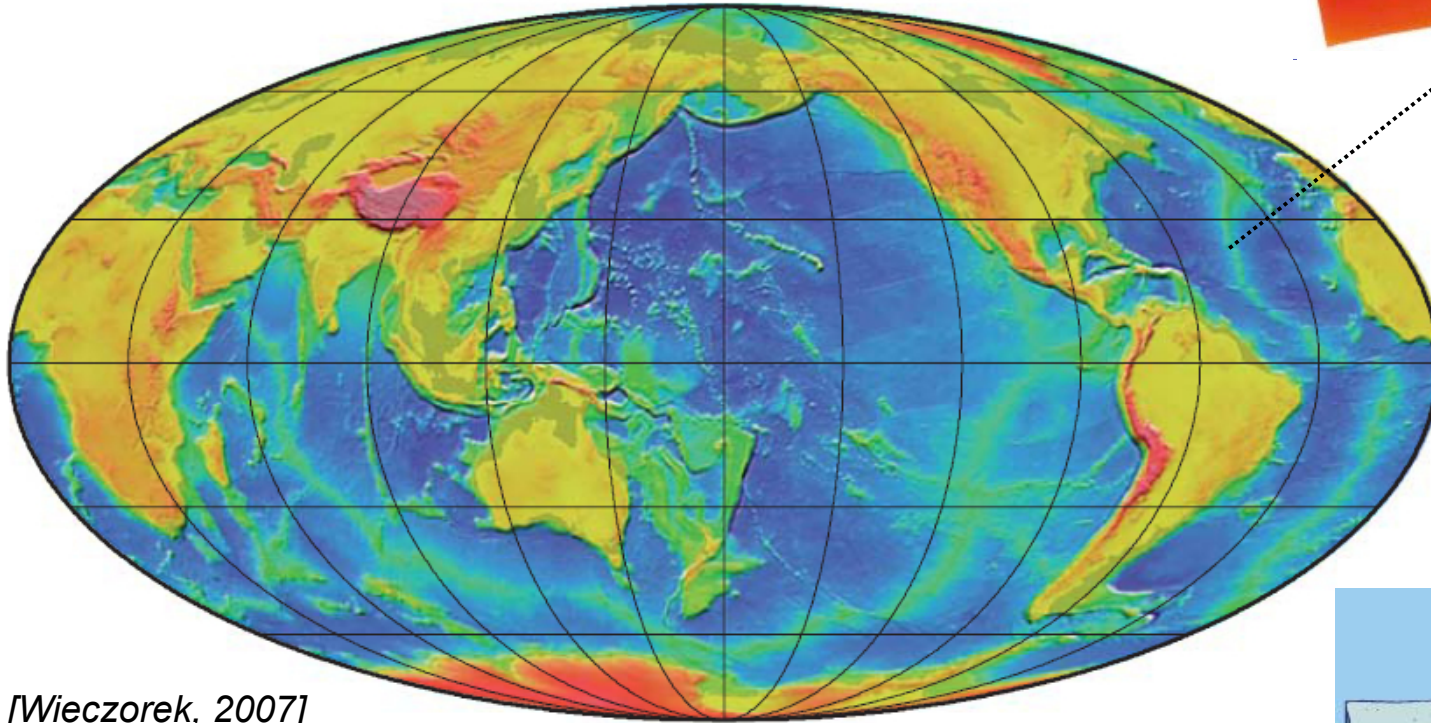
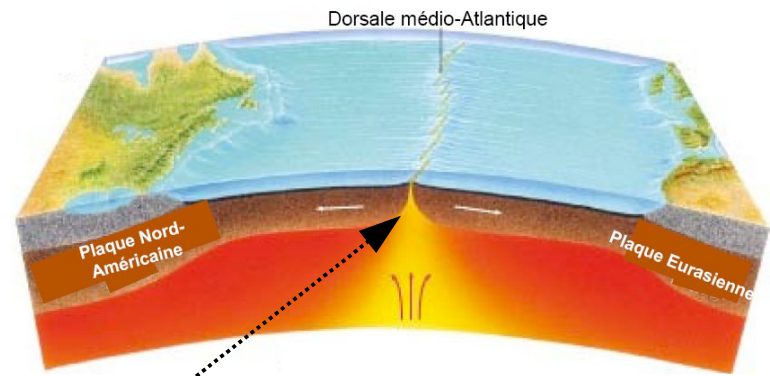


[Wieczorek, 2007]



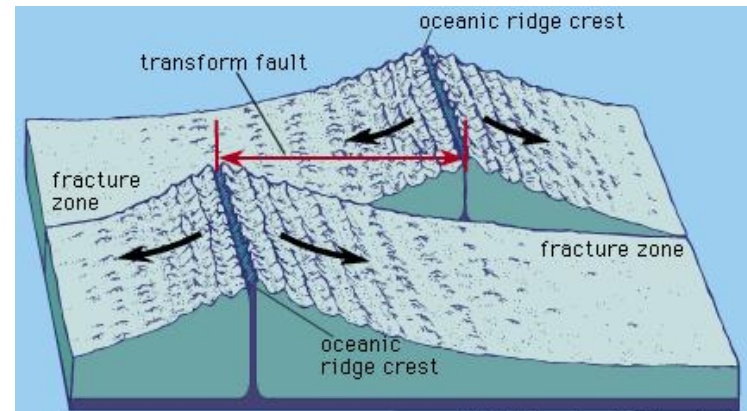
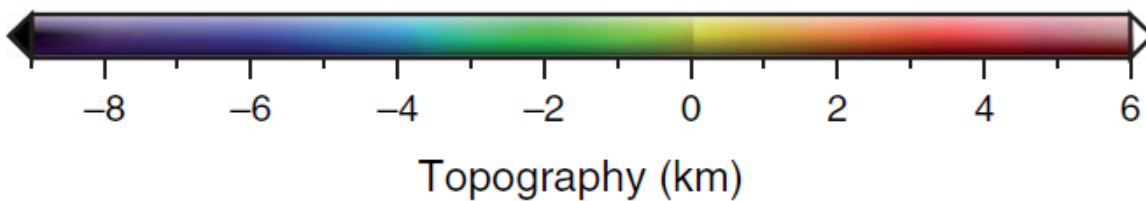
Topography (km)

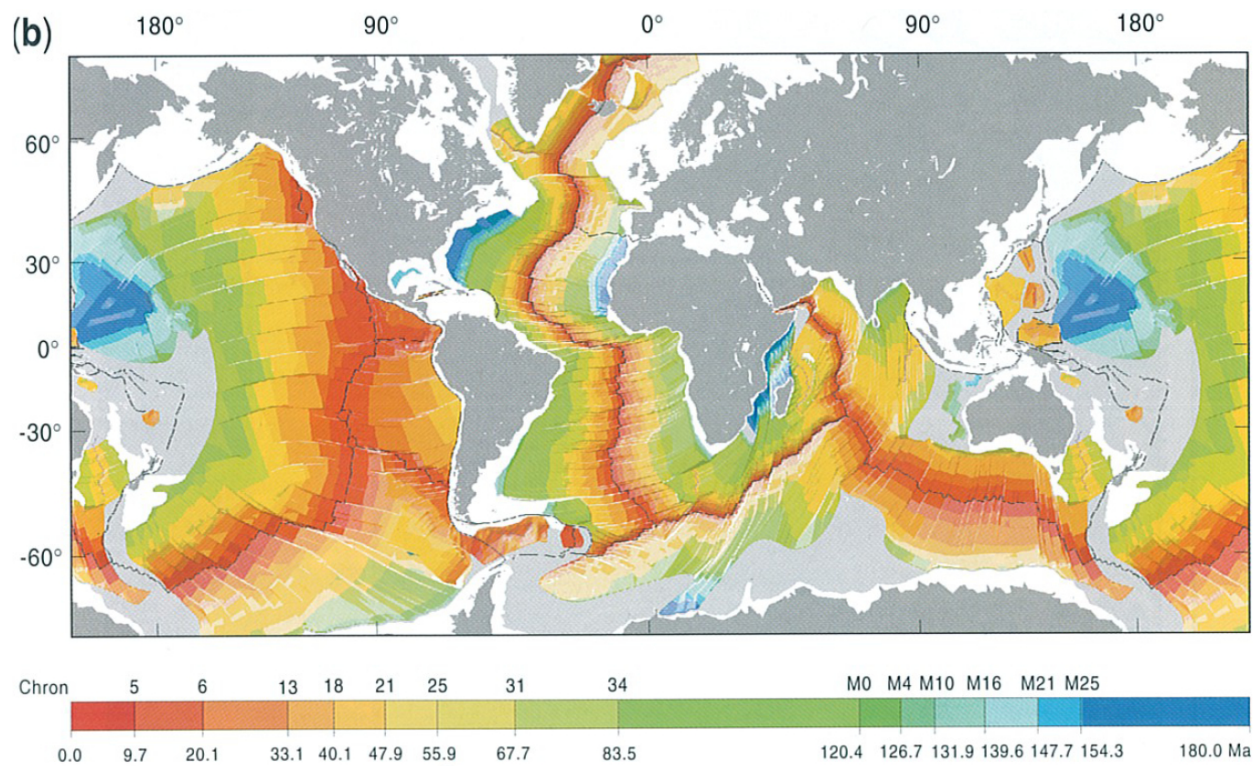
# I. Spreading Ridges



>60000 km of **spreading ridges**, where  $\sim 3 \text{ km}^2 \text{ yr}^{-1}$  of (basaltic) oceanic crust are 'freshly' formed

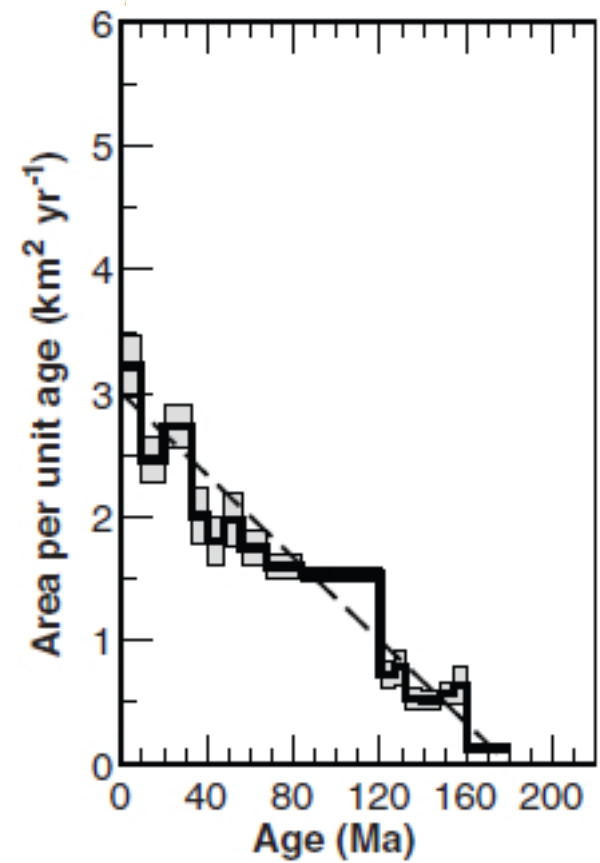
[Wieczorek, 2007]



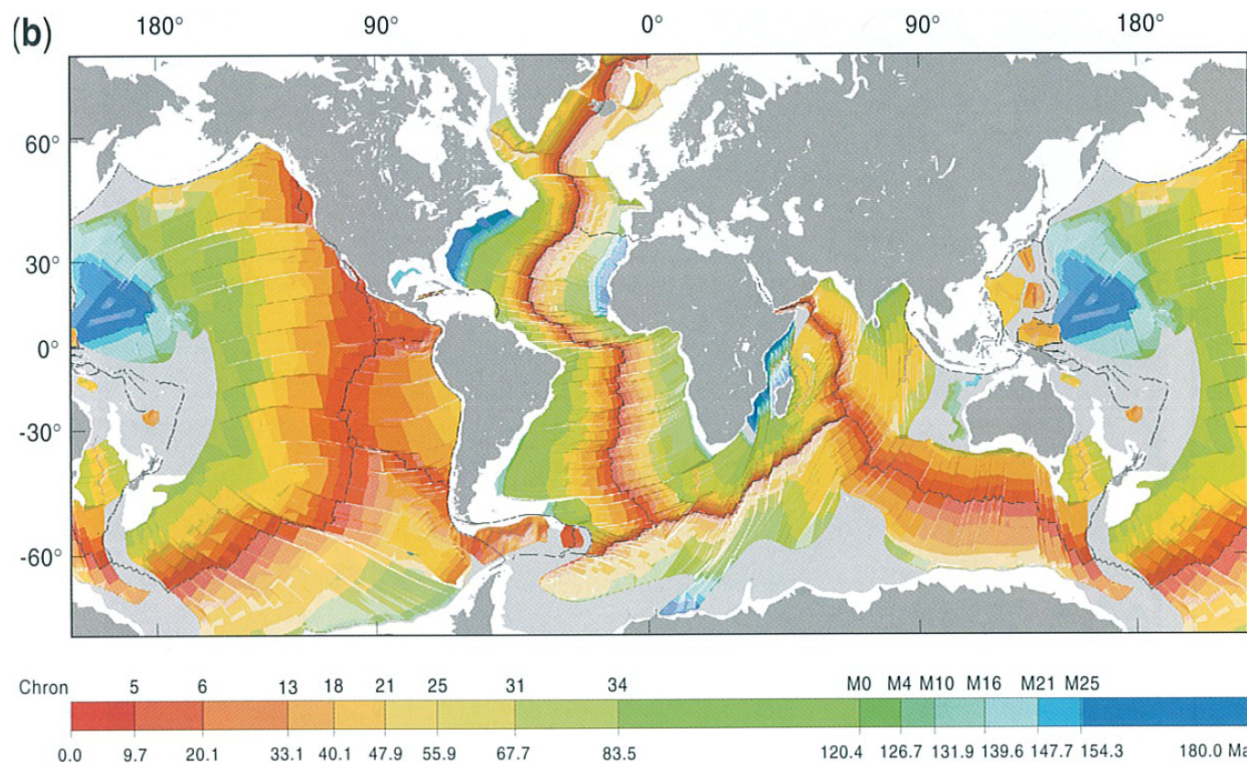


## Ages of the ocean floor

### Area-Age distribution

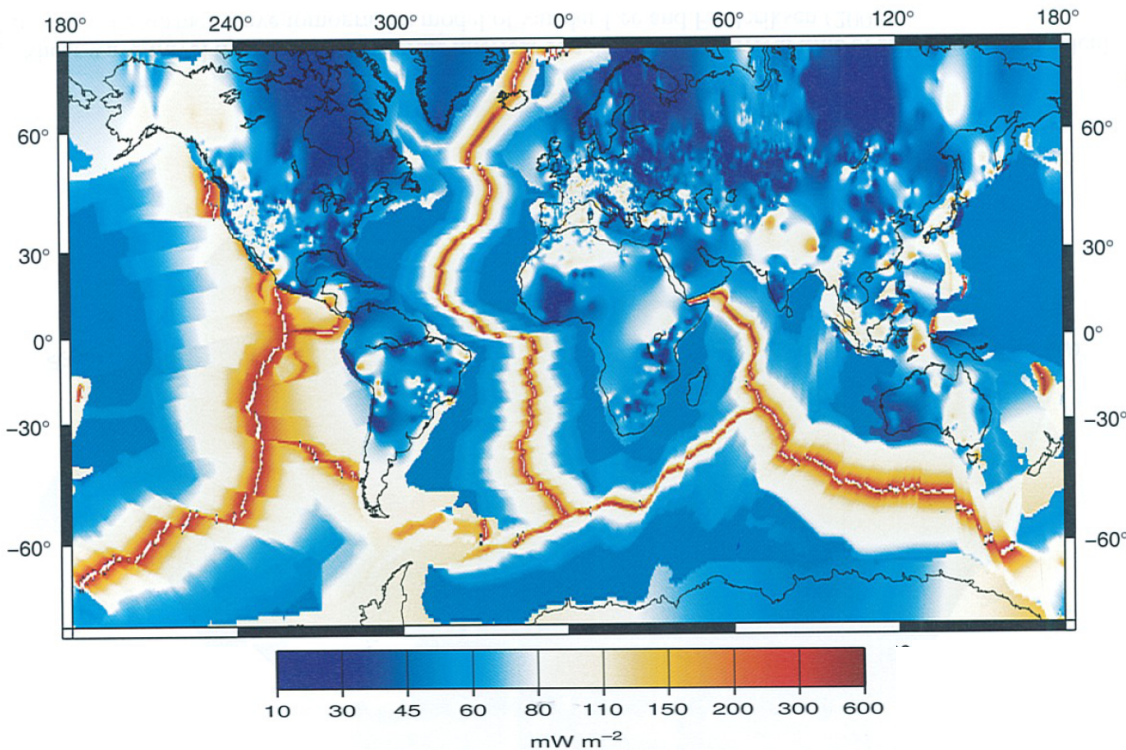


[Coltice et al., 2012]  
see also Labrosse & Jaupart, 2007



## Ages of the ocean floor

Thickness of the lithosphere is proportional to  $(\text{age})^{-1/2}$



## Global heat flow map

Current average heat flow in the ocean basin is  $\sim 100$  (mW/m<sup>2</sup>)

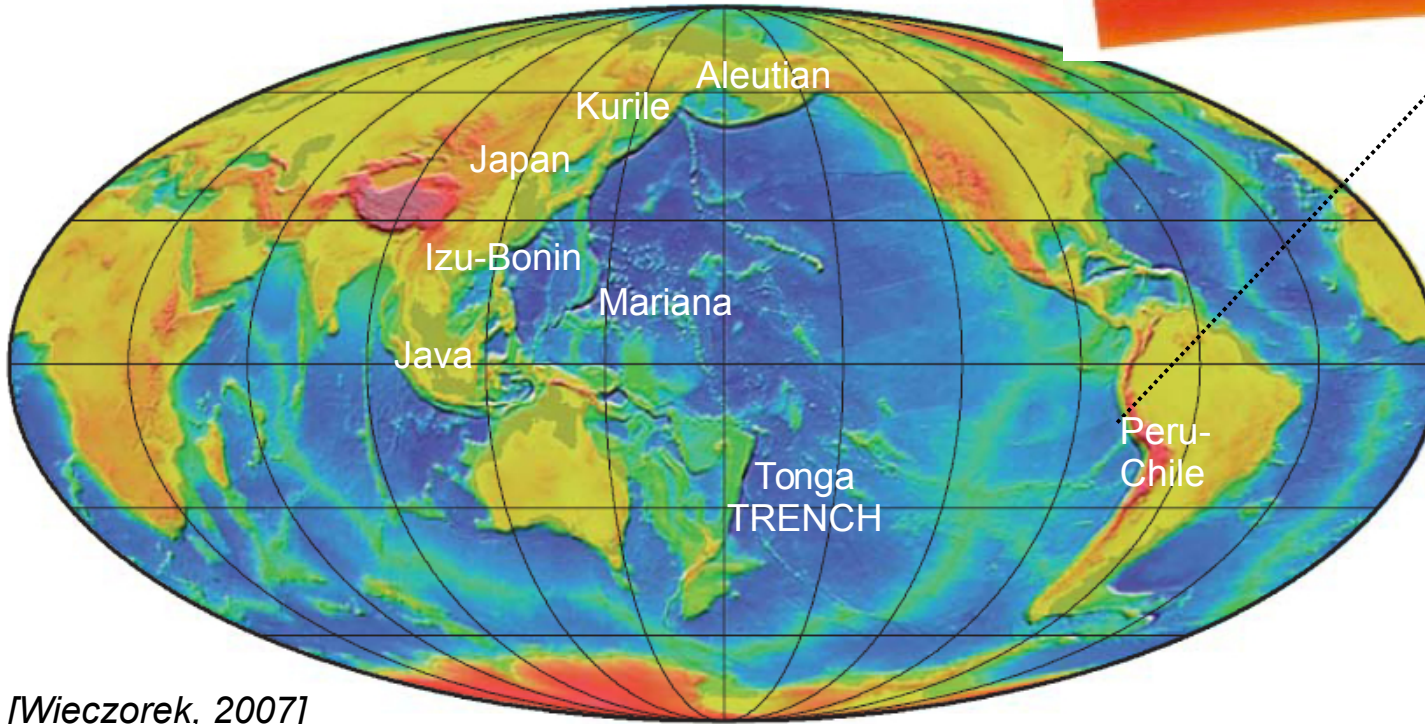
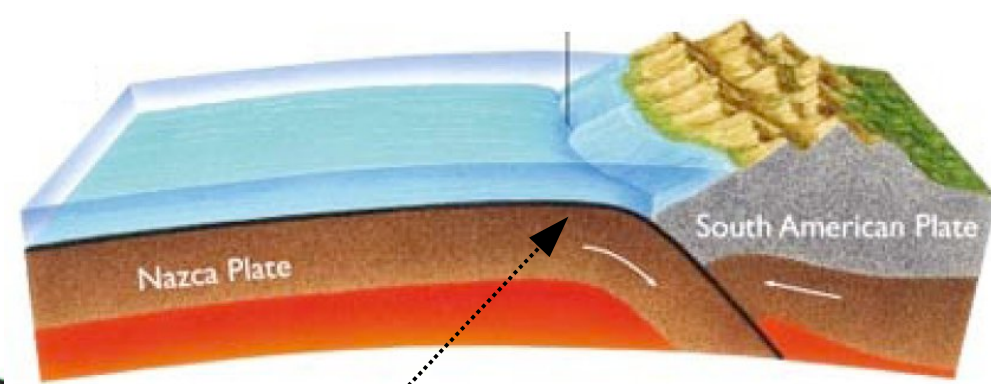
Total heat flow from the oceans  
 $Q_{\text{oceans}} \sim 29$  TW  $>$   $Q_{\text{continents}} \sim 14$  TW

Most of the heat is lost because of sea-floor spreading

[Jaupart & Mareschal book 2011]



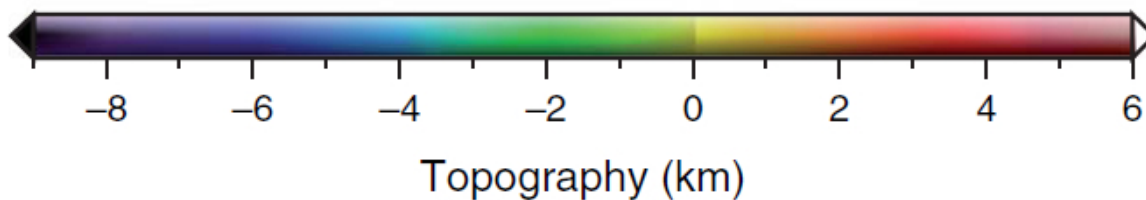
## II. Subduction zones



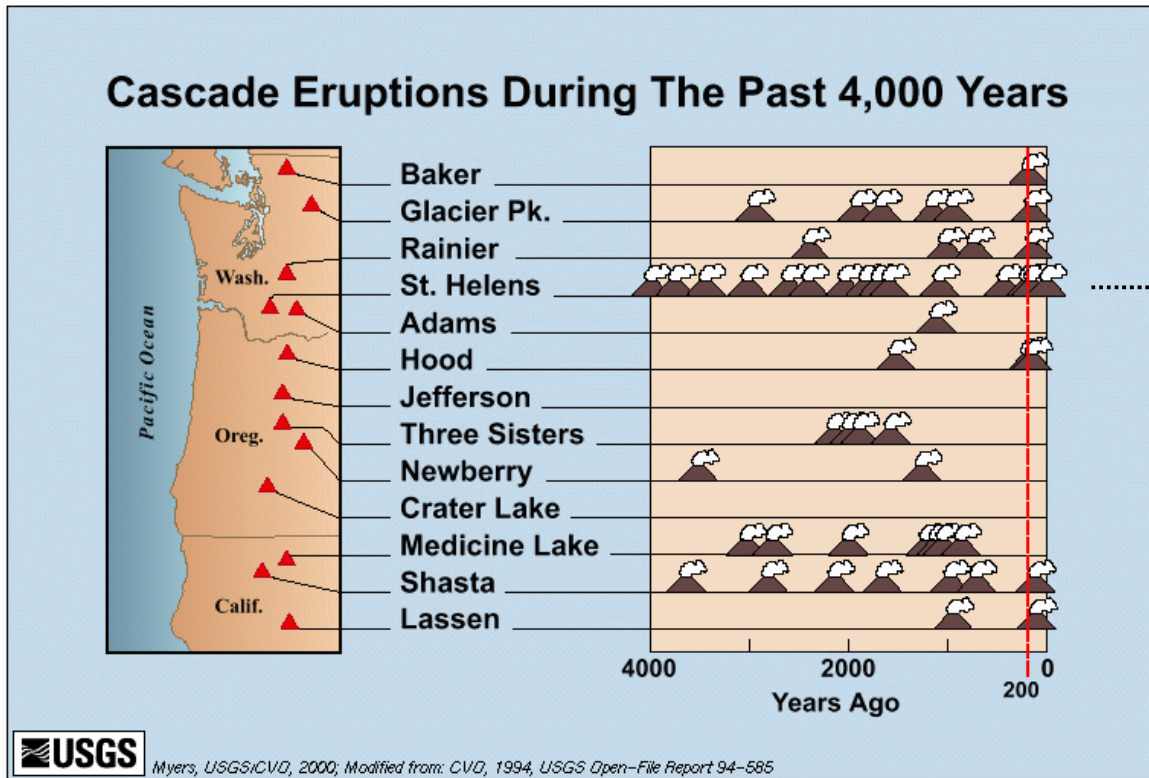
Deep trenches indicate **Subduction zones**, where the oceanic lithosphere is subducted.

Magmatism creates continental crust.

[Wieczorek, 2007]



# Subduction zones are characterized by explosive volcanoes

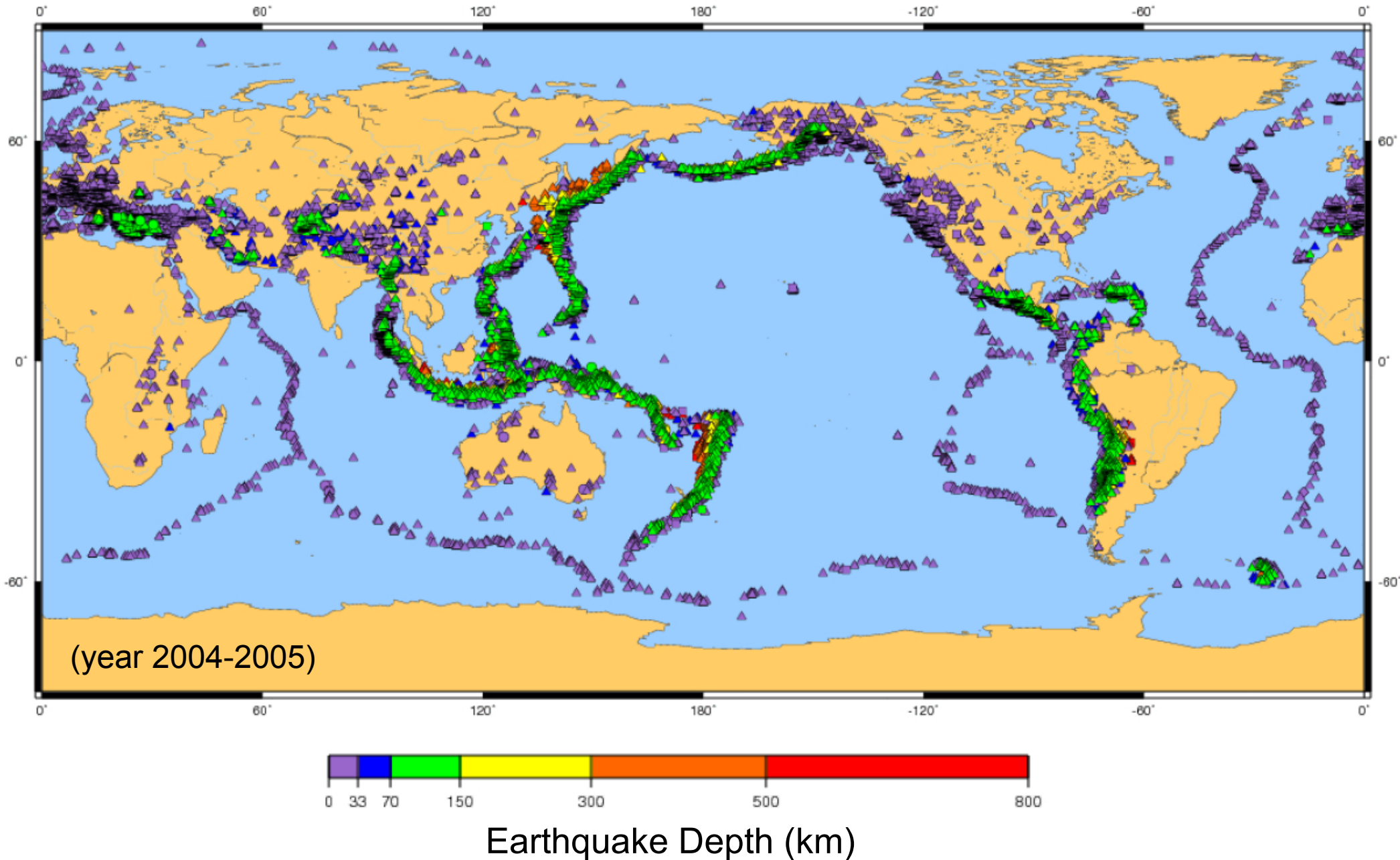


**1980 Mt St. Helens altitude changed from 2950 to 2549 m**

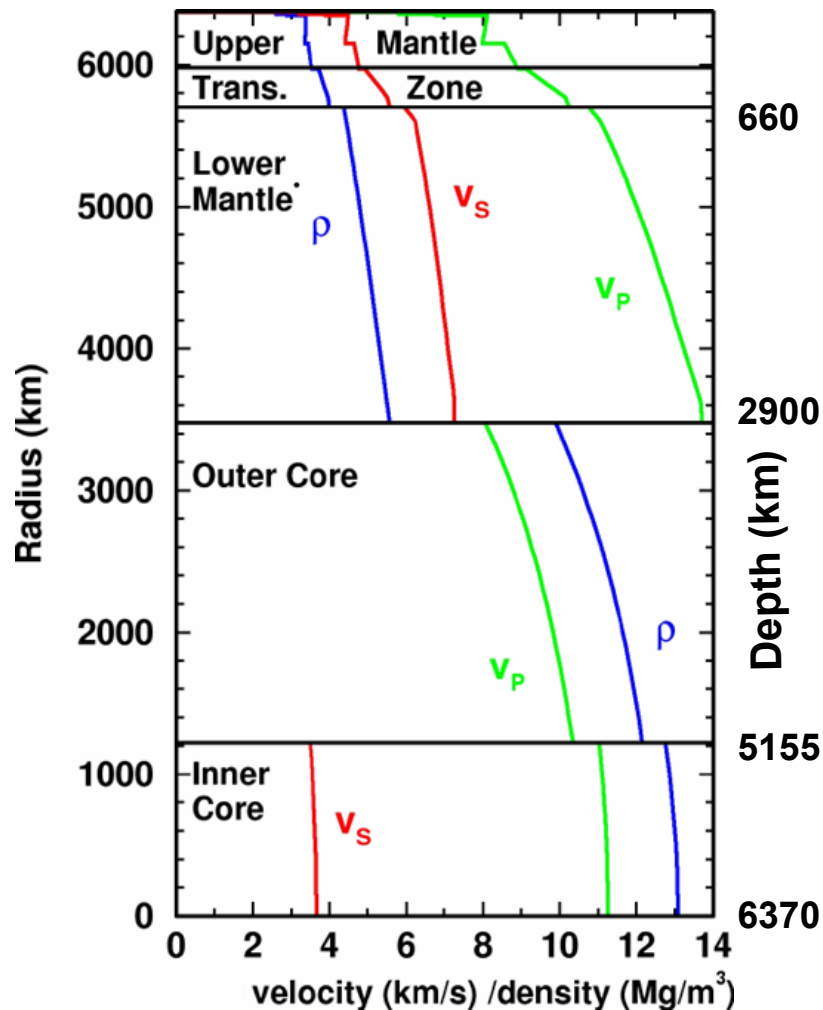
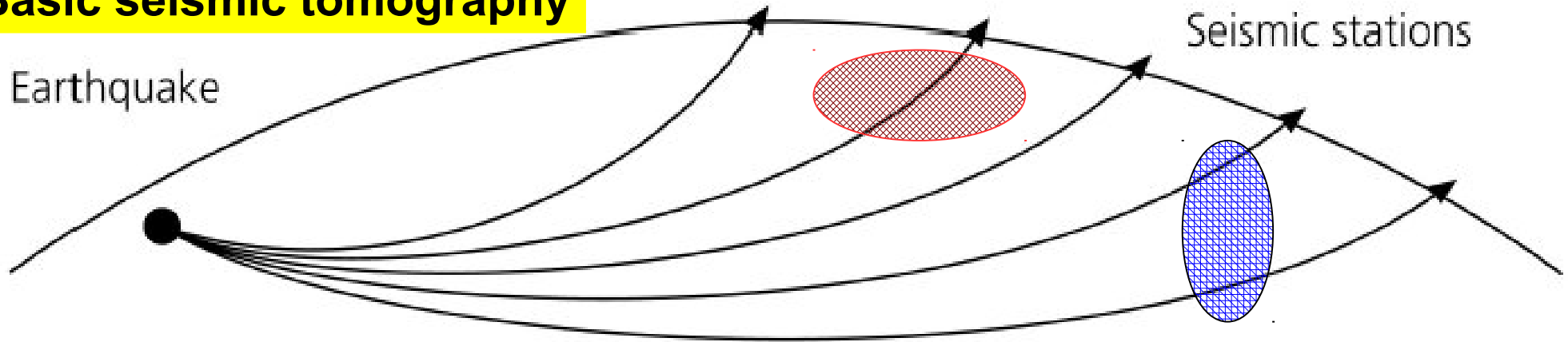


# Subduction zones are seismically active

90 % of all seismic energy is liberated at subduction zones



# Basic seismic tomography



- PREM the reference model for seismic velocity vs. depth
- Calculate for each seismic path the theoretical arrival time.
- Compare it with observed arrival time.
- Find seismic velocity anomalies along each path

**Negative anomaly  $\Delta V < 0$   
suggests  $\Delta T > 0$  (hot zones)**

**Positive anomaly  $\Delta V > 0$   
suggests  $\Delta T < 0$  (cold zones)**

# Tomographic images across subduction zones

We see slabs into the lower mantle

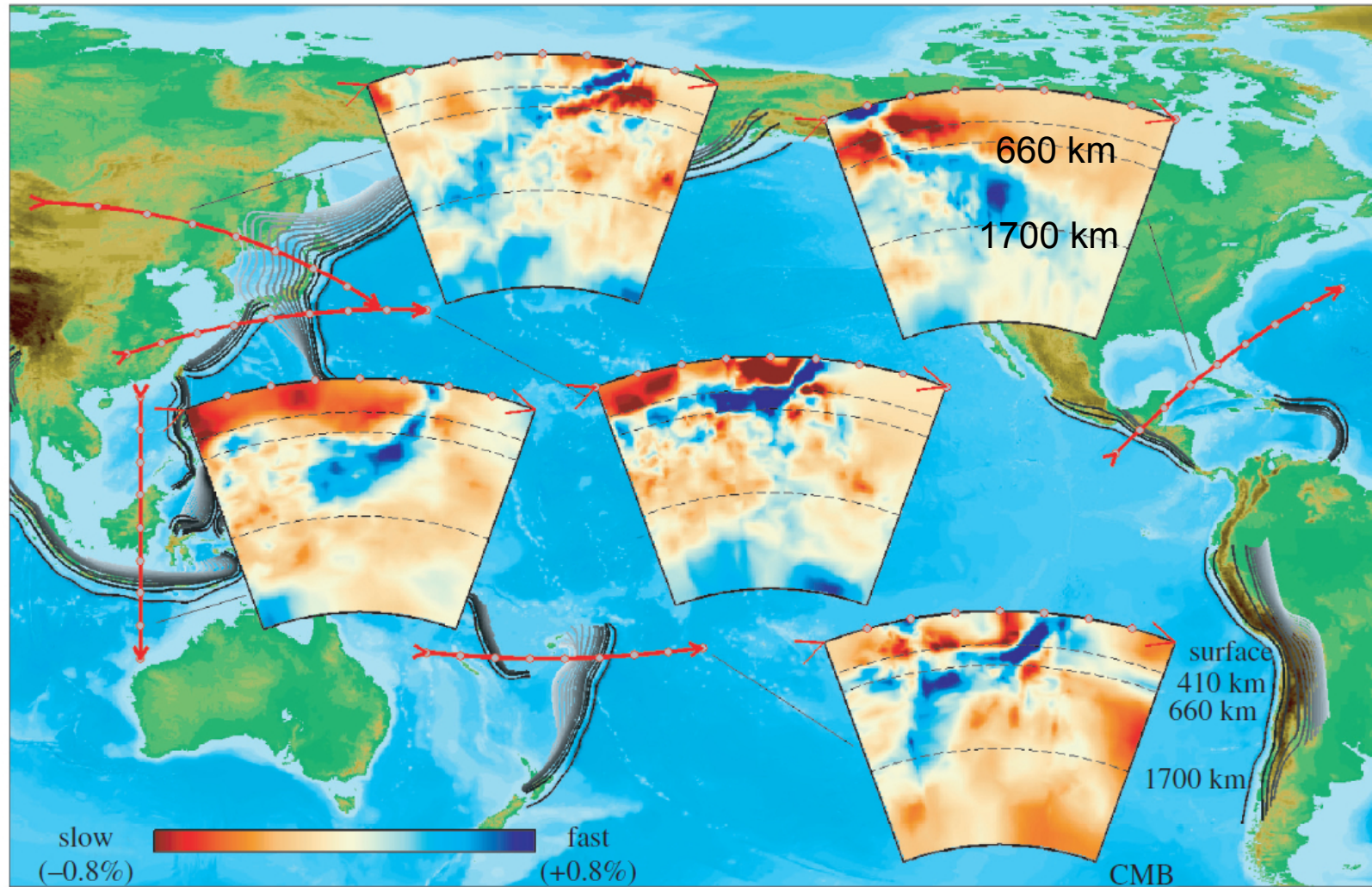
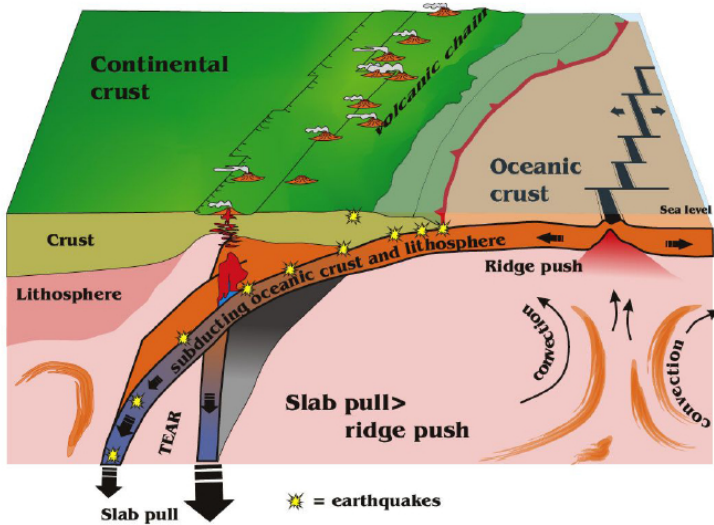


Figure 2. Series of mantle cross-sections through the recent P-wave model of Kárason & van der Hilst (2000) to illustrate the structural complexity in the upper-mantle transition zone and the regional variation in the fate of the slabs. Dashed lines are drawn at depths of 410, 660 and 1700 km, respectively. The model is based on short-period, routinely processed P, pP and PKP travel-time residuals (Engdahl *et al.* 1998) and a large number of PP-P and PKP-Pdiff differential times measured by waveform cross-correlation from long-period seismograms.

# Subduction zones and forces that drive plate motion

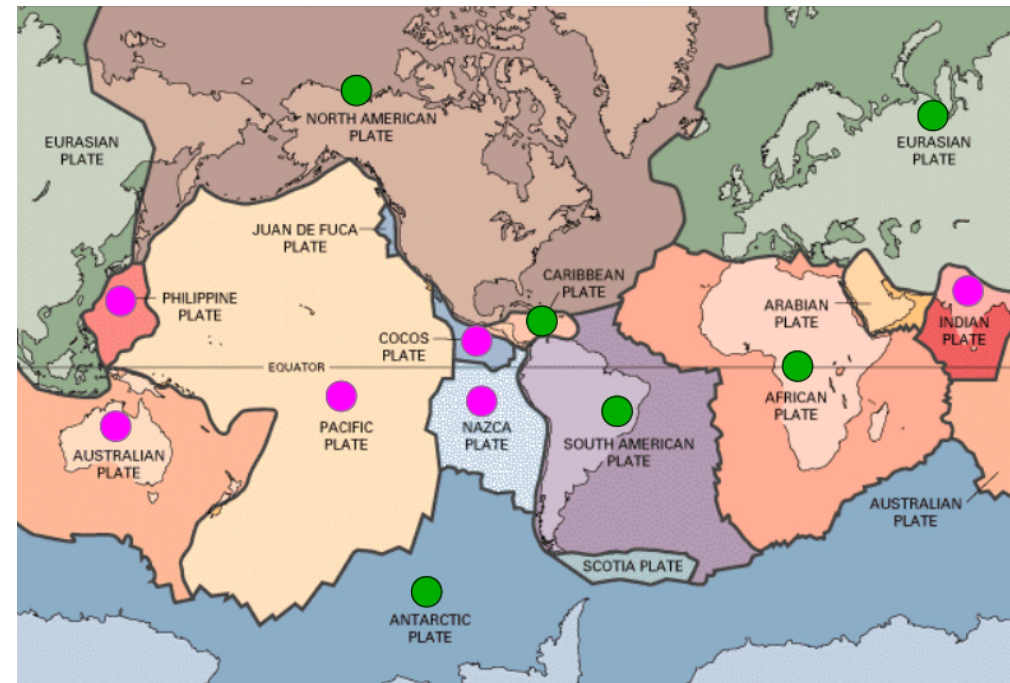
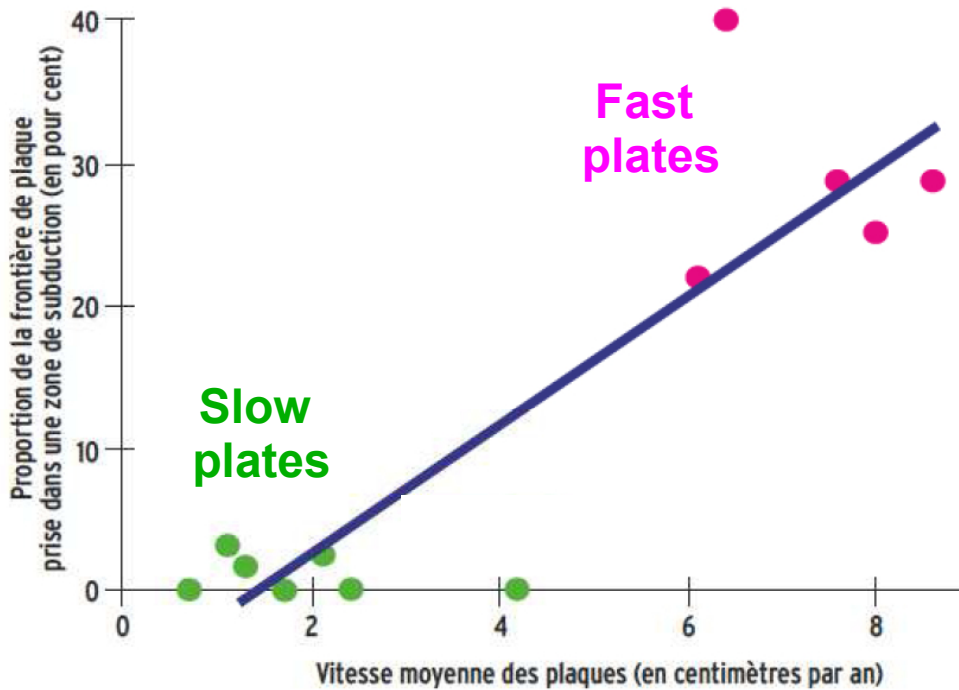


Ridge push and Slab pull forces

$$F_{\text{Ridge push}} \sim 10\% F_{\text{Slab pull}}$$

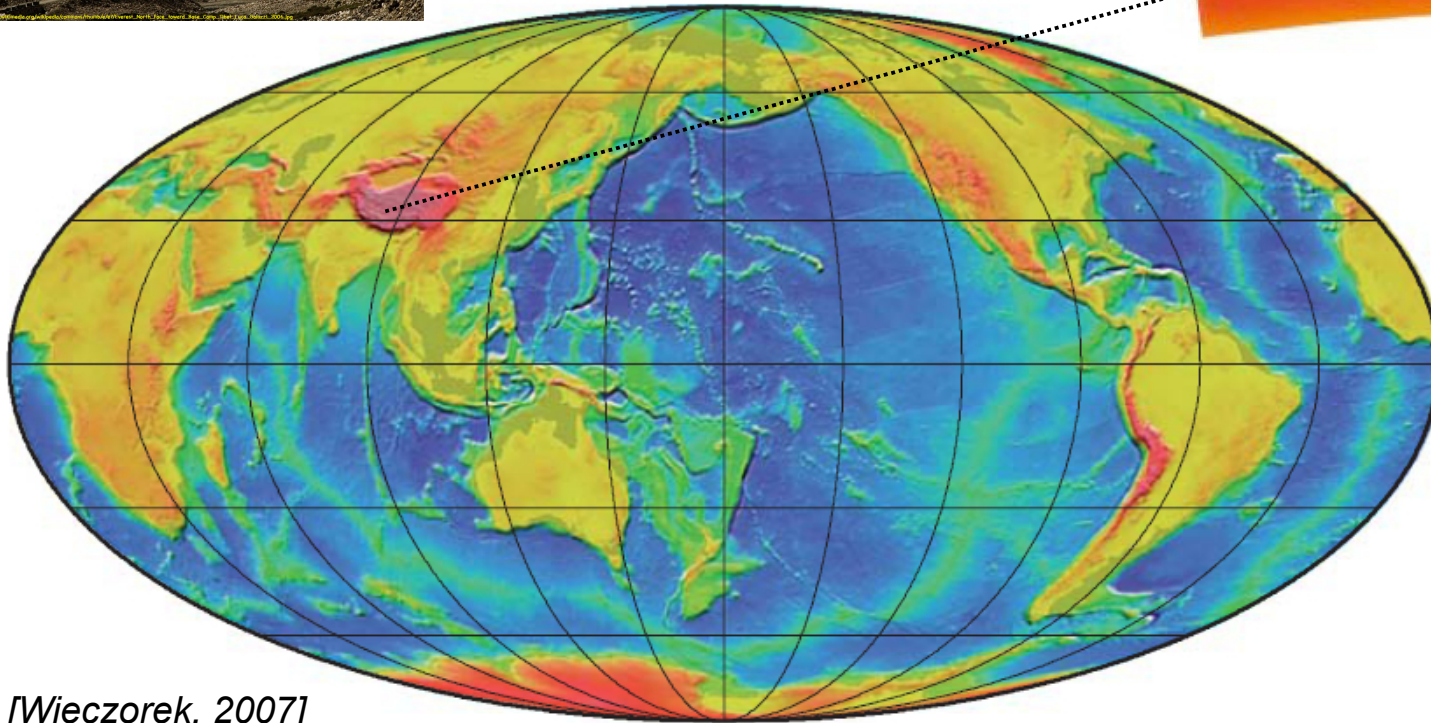
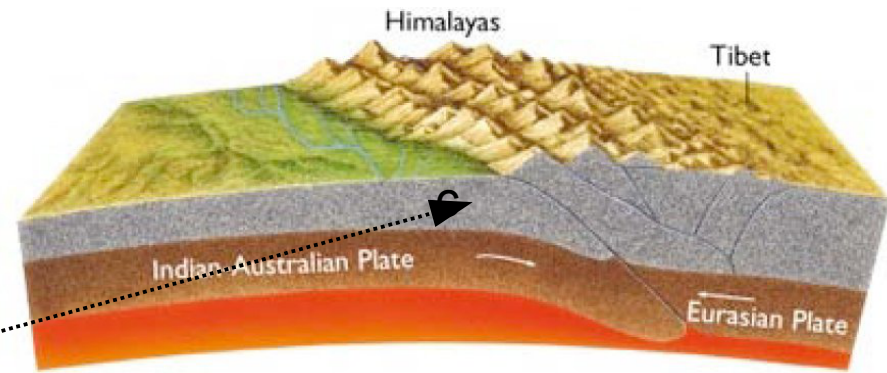
Passive upwelling at ridges is supported by seismic tomography

> Subduction zones at plate edges and > plate velocity

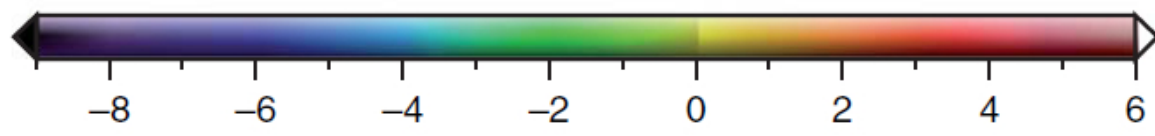




### III. Continental collision zones

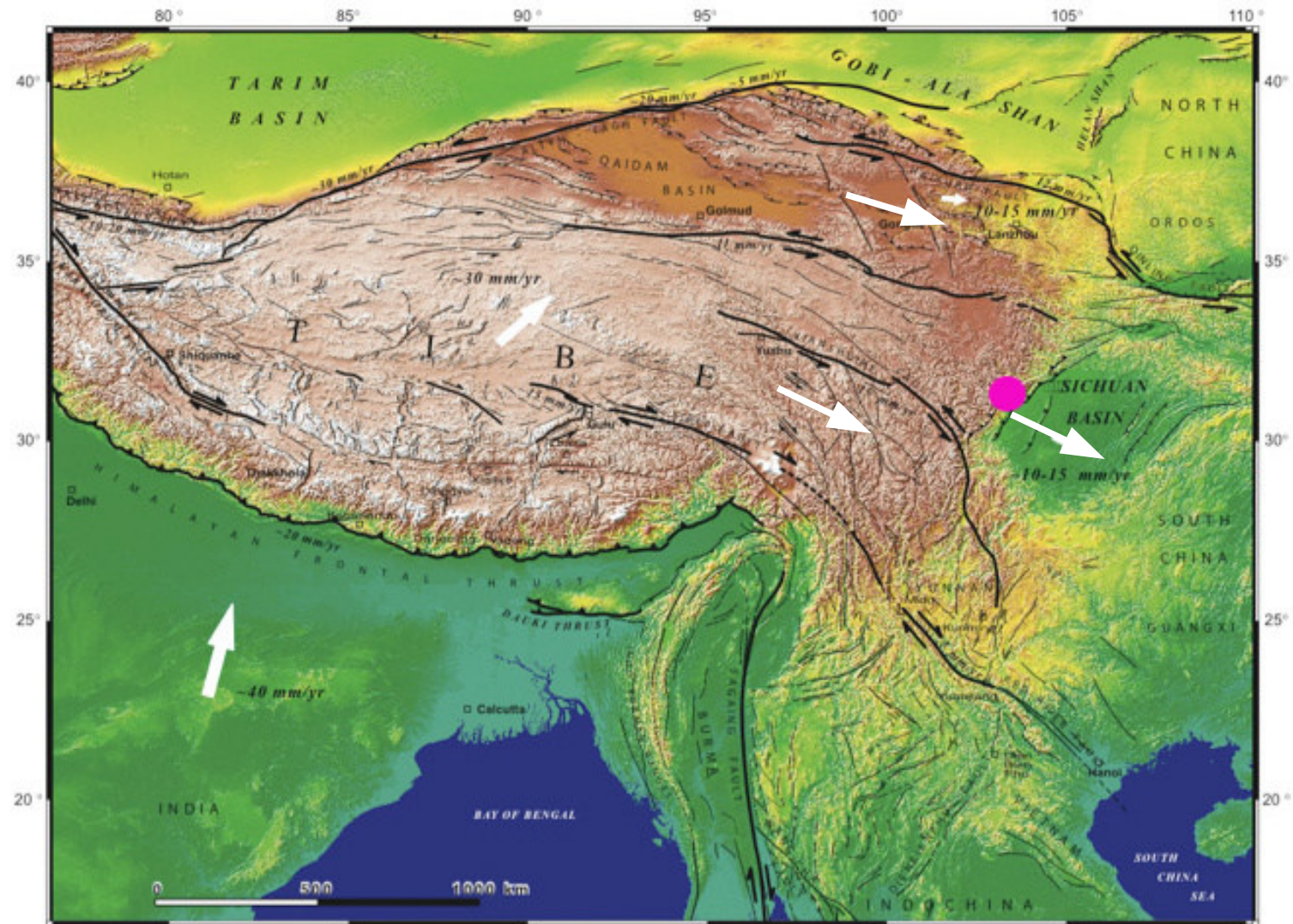
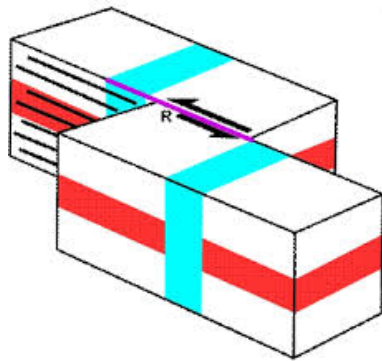


[Wieczorek, 2007]



Topography (km)

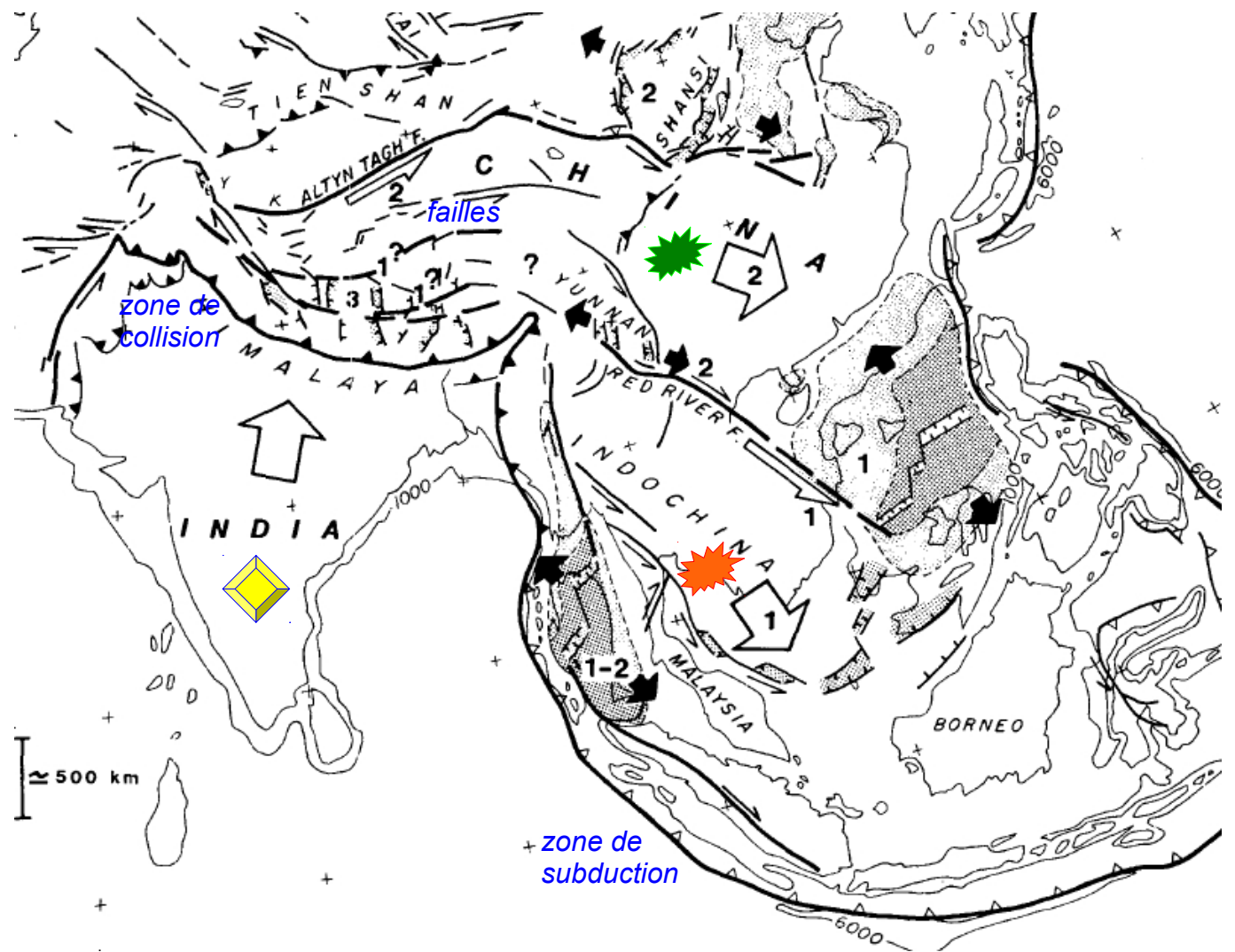
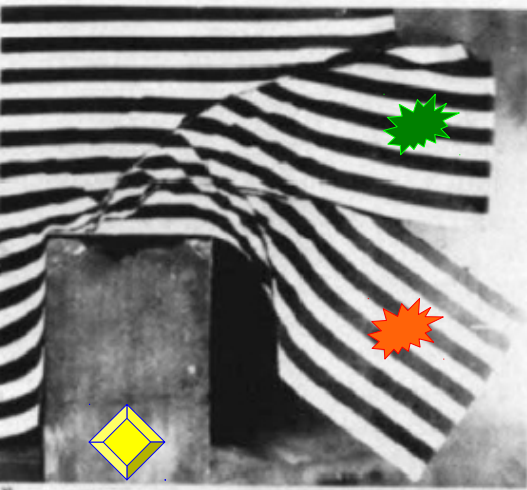
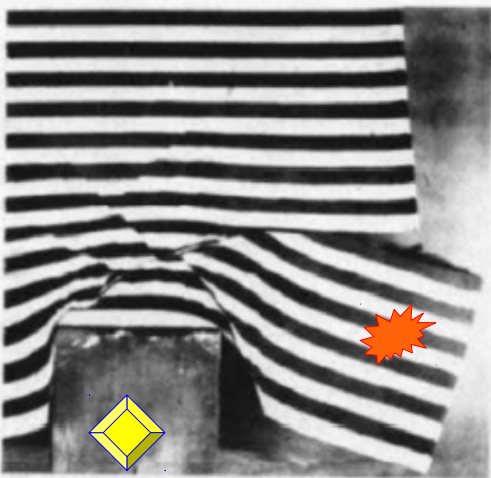
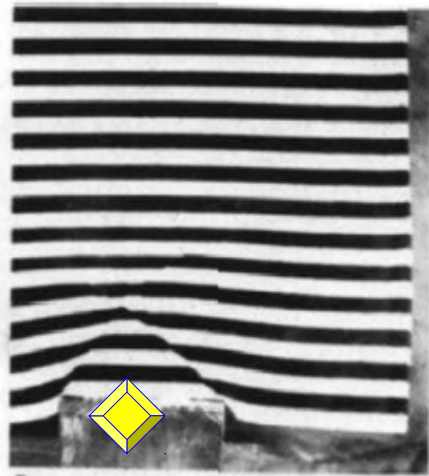







d'après Tapponnier et al., Science, 2001

**La convergence (~2000 km de raccourcissement crustale) est absorbée**  
 par les plissements des roches  
 par les chevauchements  
 par les failles décrochantes

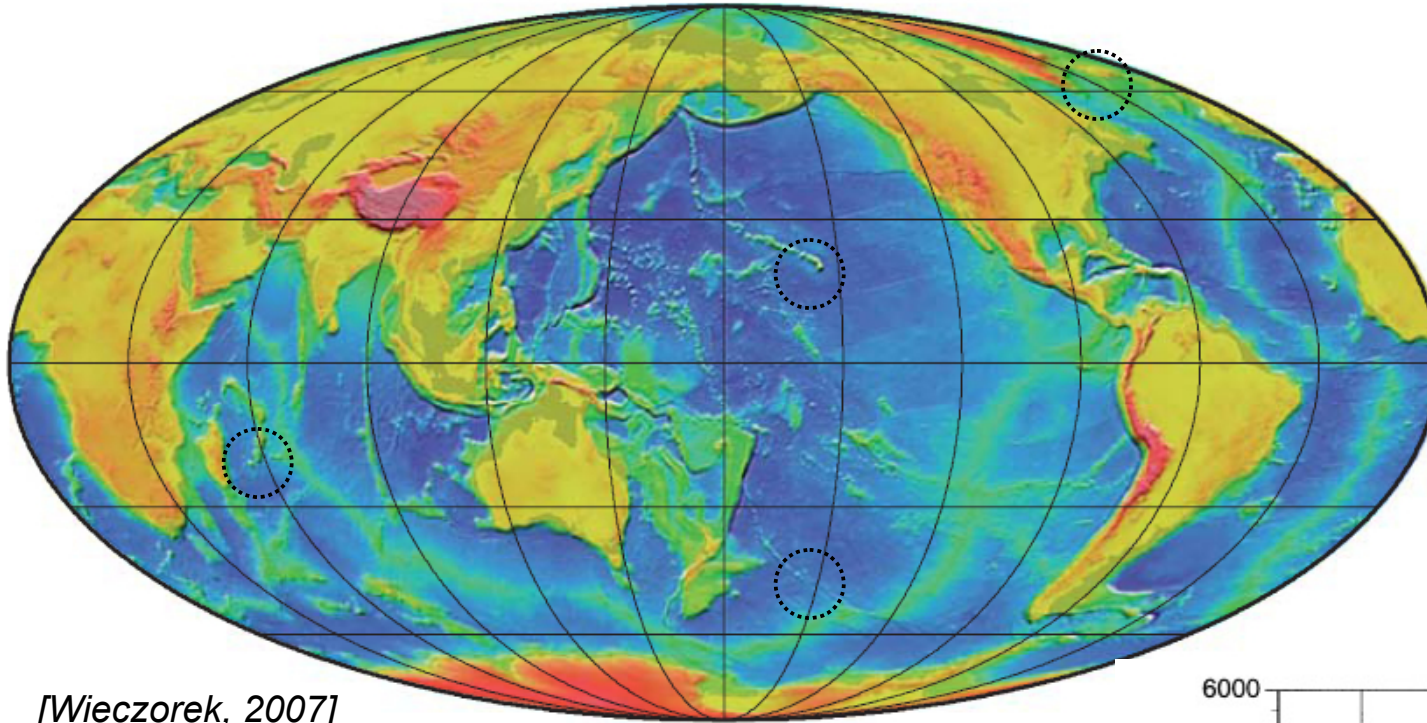




### Expériences de Tapponnier et al. 1982

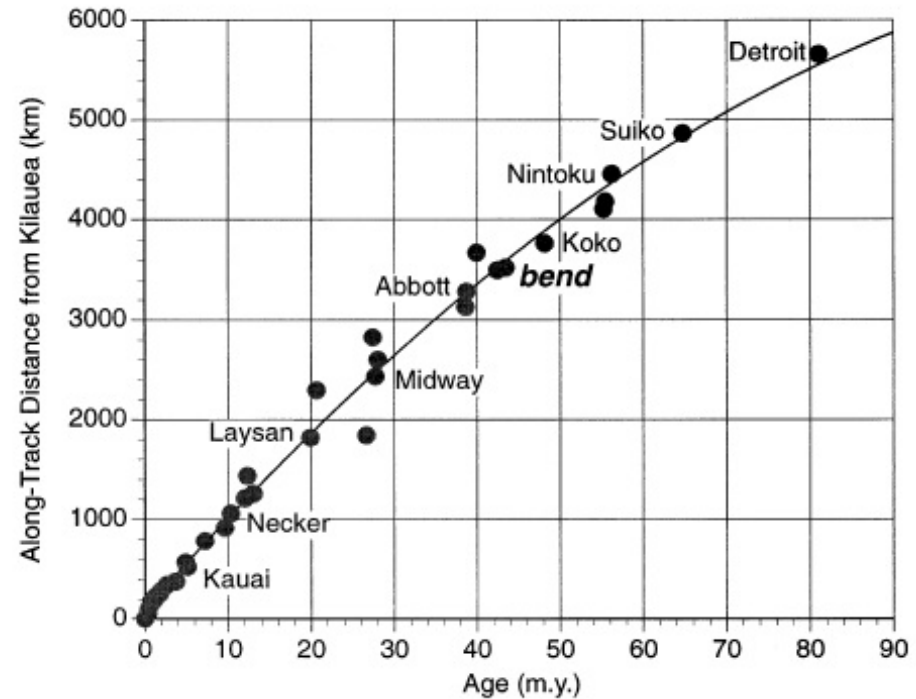
A' coté : étapes d'indentation d'un bloc rigide dans un bloc de plasticine, libre de se déformer. La carte montre la tectonique d'extrusion en Indochine il y a 50-20 Ma (  ) et de la Chine depuis 20 Ma (  ) suite à la collision de l'Inde (  )

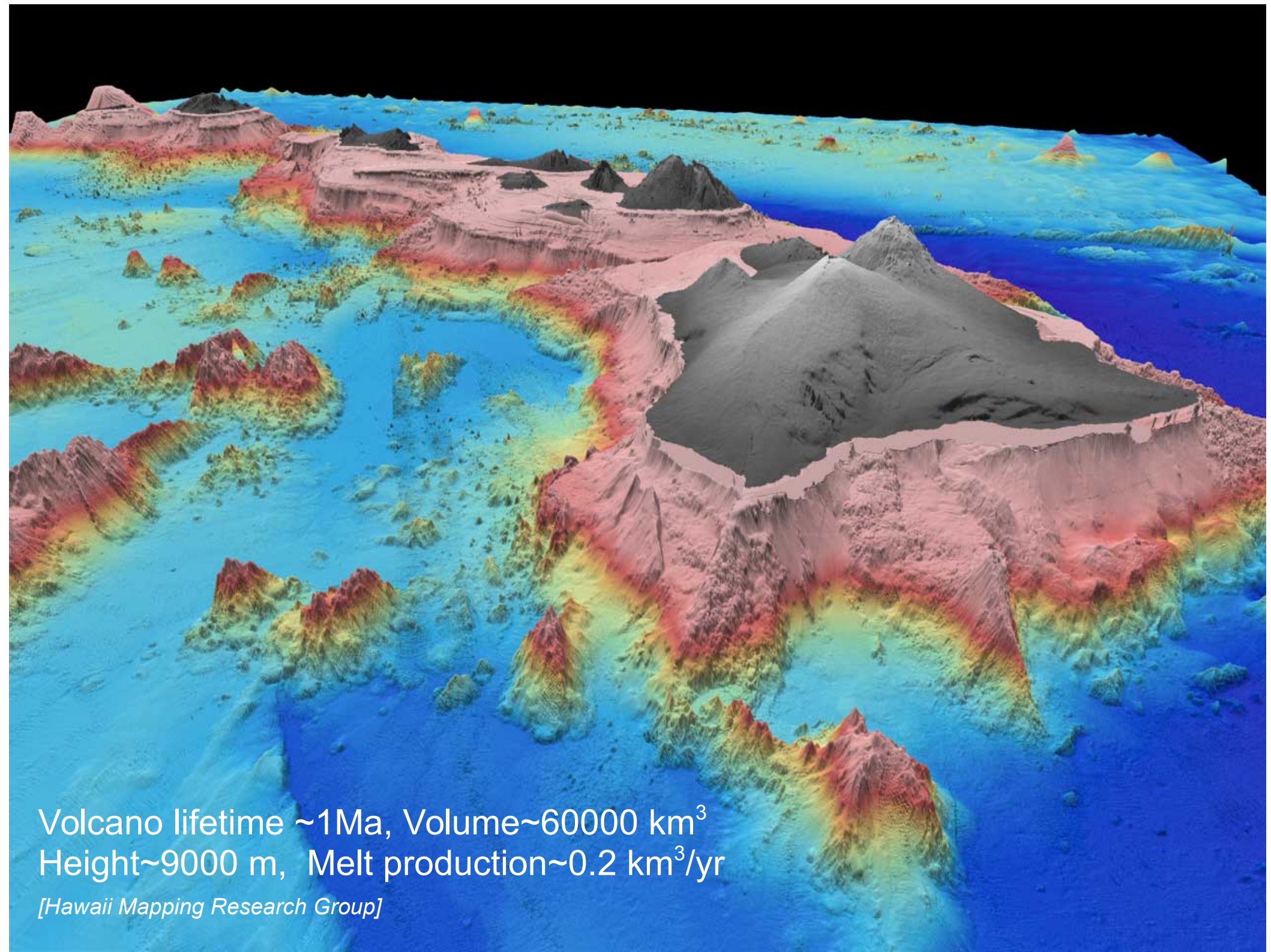
# IV. Intraplate volcanism



[Wieczorek, 2007]

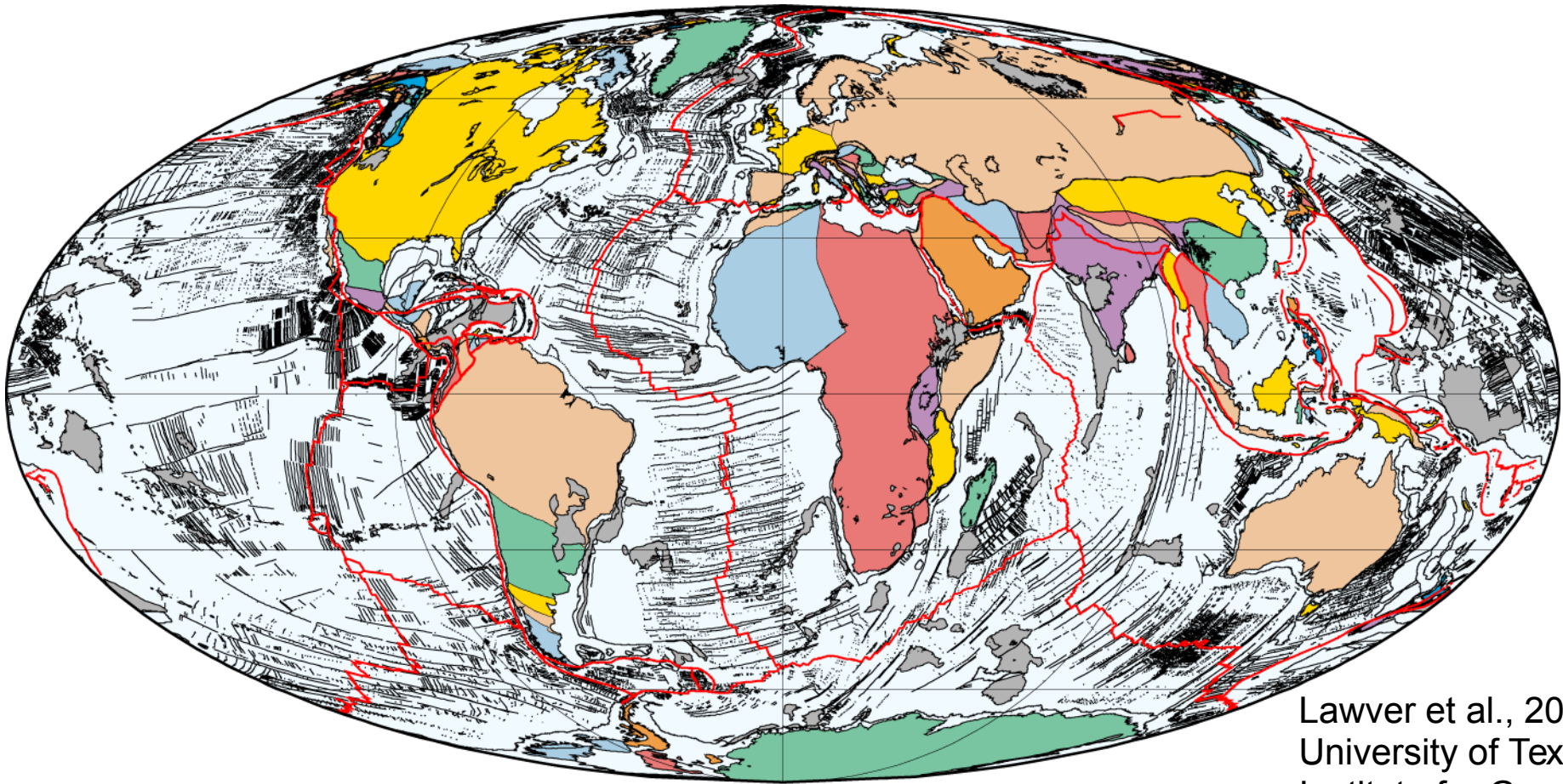
**Active hot-spots**  
**Extinct, submerged volcanic chain**  
**Submerged oceanic plateaux**





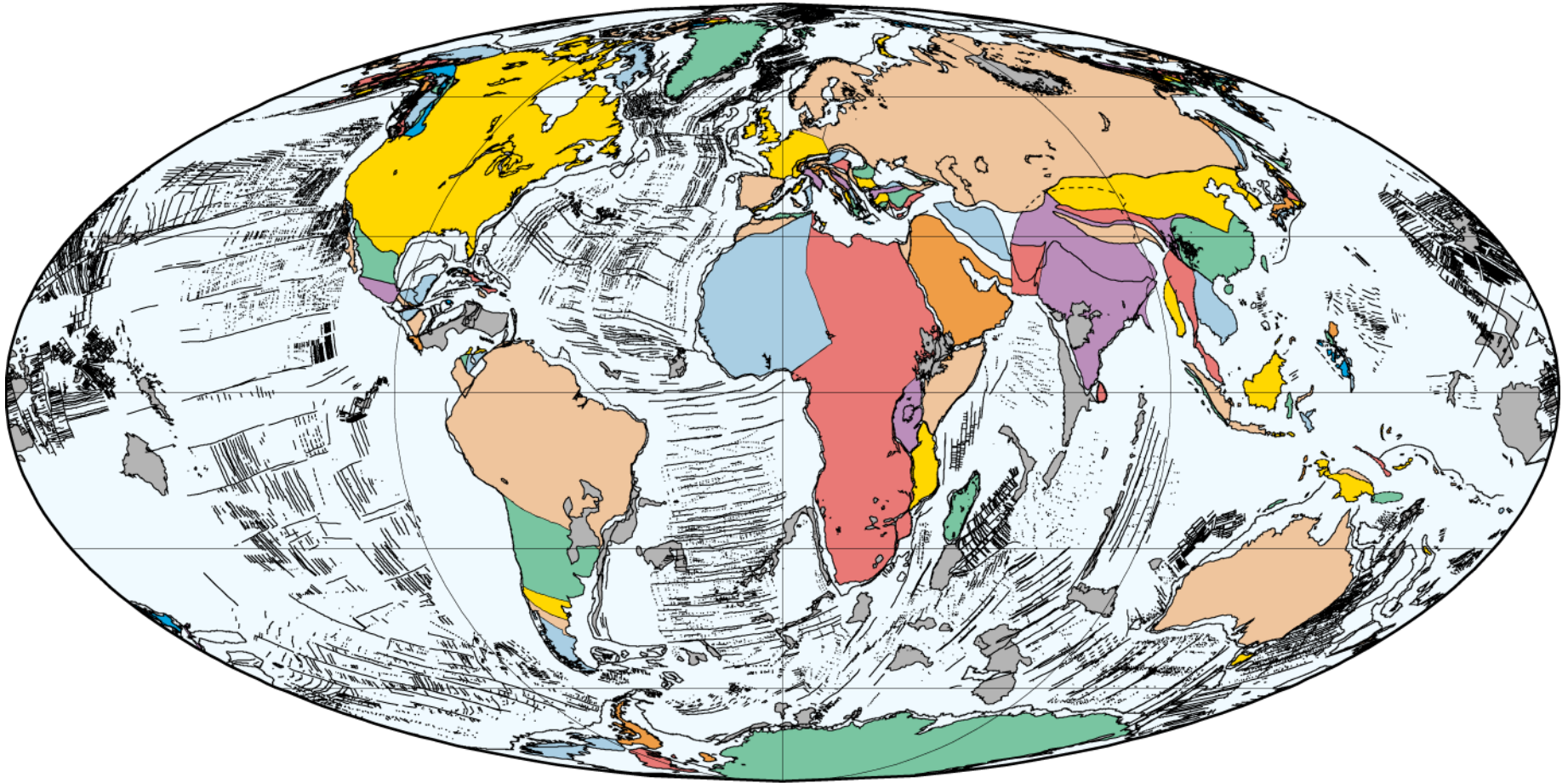
Volcano lifetime  $\sim 1\text{Ma}$ , Volume  $\sim 60000\text{ km}^3$   
Height  $\sim 9000\text{ m}$ , Melt production  $\sim 0.2\text{ km}^3/\text{yr}$

*[Hawaii Mapping Research Group]*



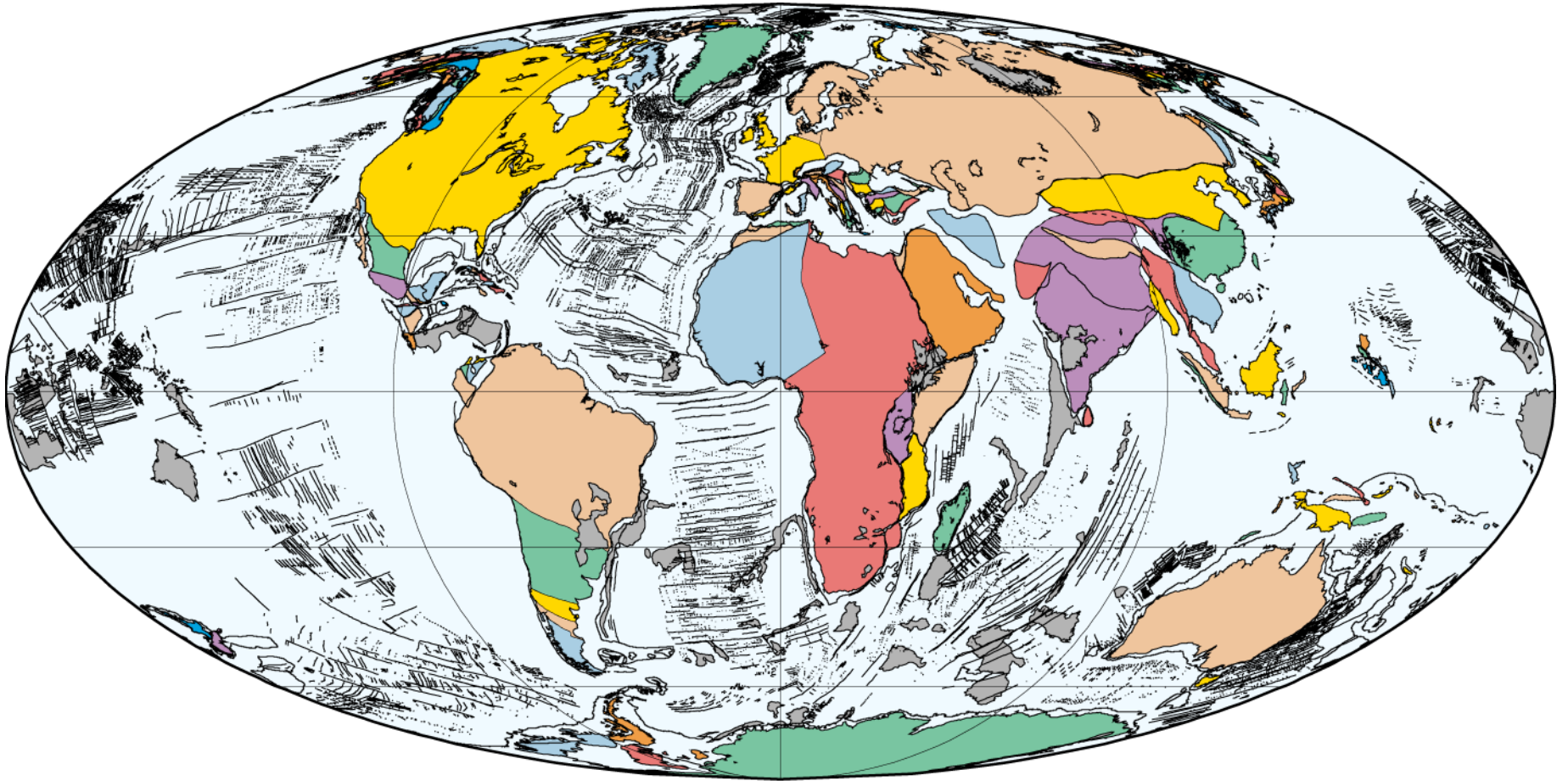
Lawver et al., 2002,  
University of Texas  
Institute for Geophysics

0 Ma  
Present Day



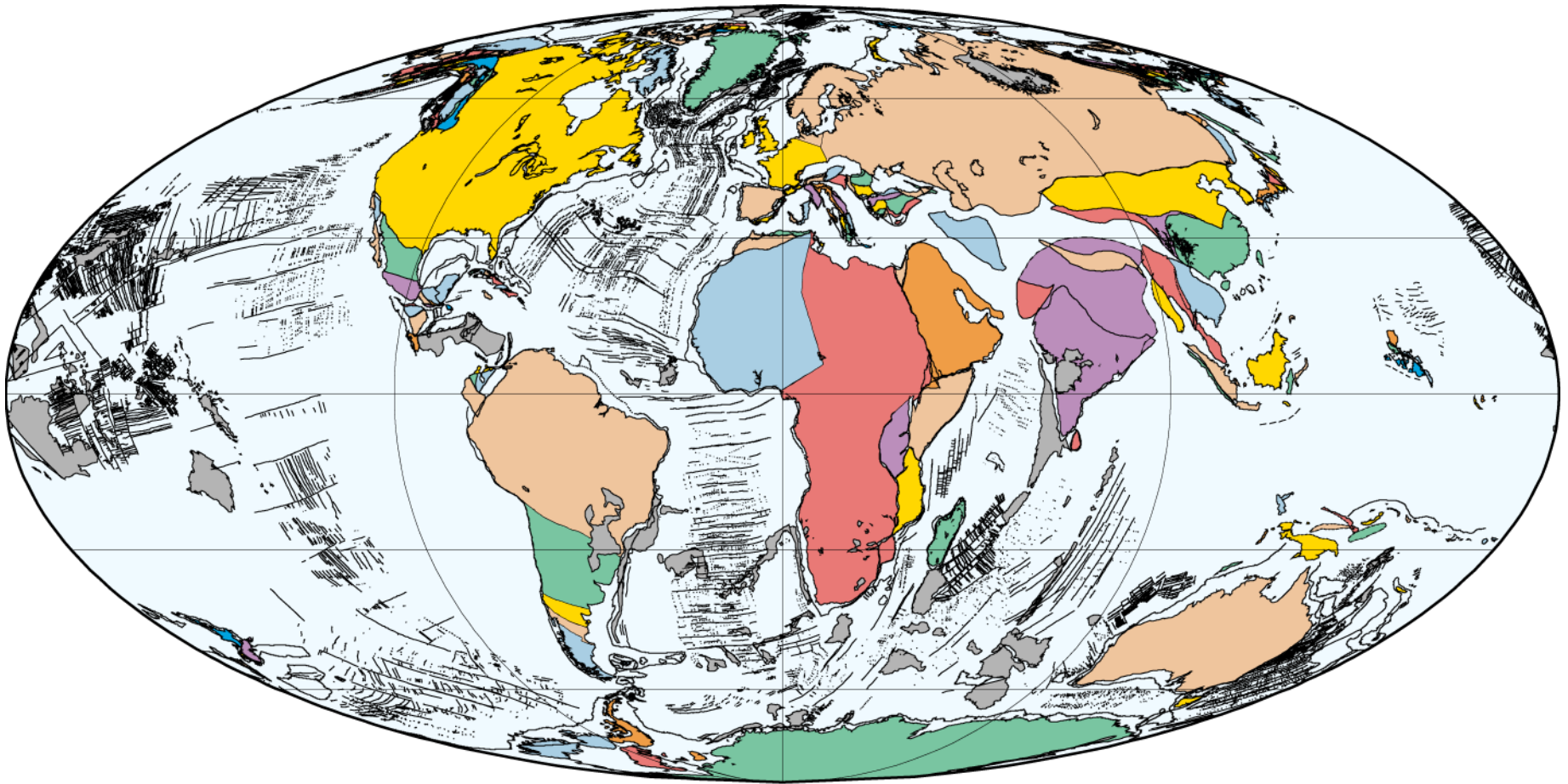
20 Ma  
Early Miocene

PLATES/UTIG  
August 2002



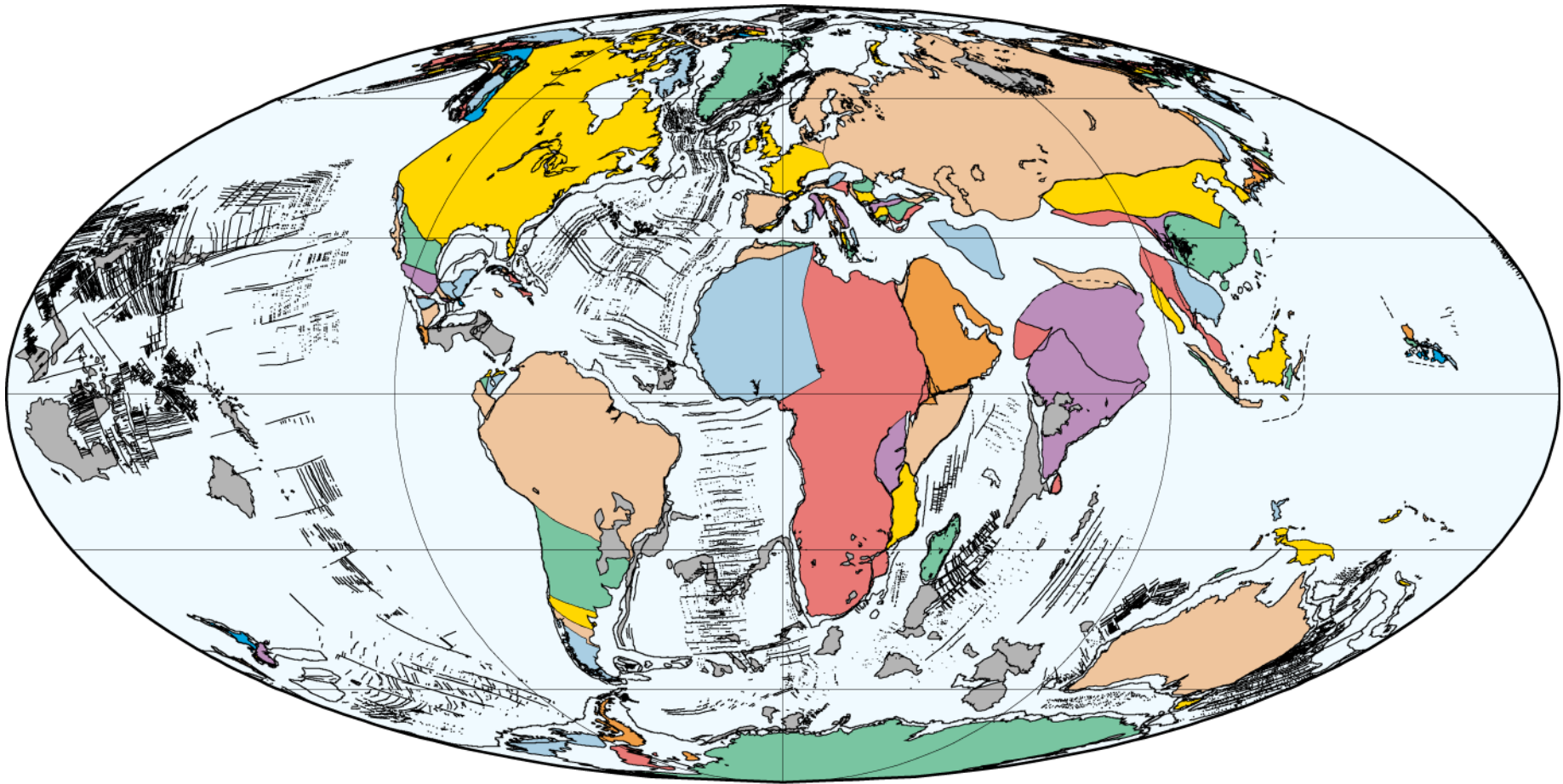
30 Ma  
Early Oligocene

PLATES/UTIG  
August 2002



40 Ma  
Middle Eocene

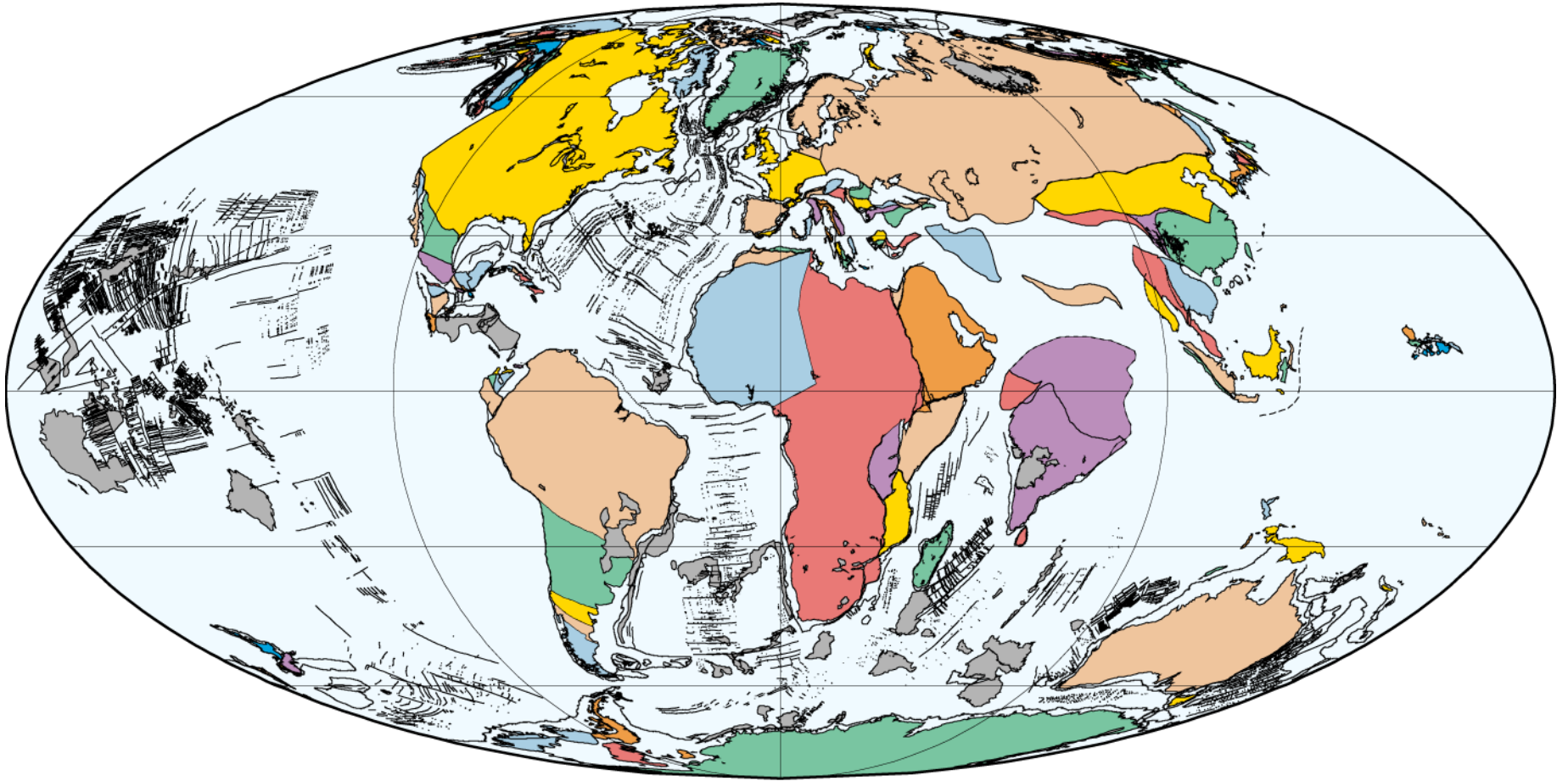
PLATES/UTIG  
August 2002



50 Ma  
Early Eocene

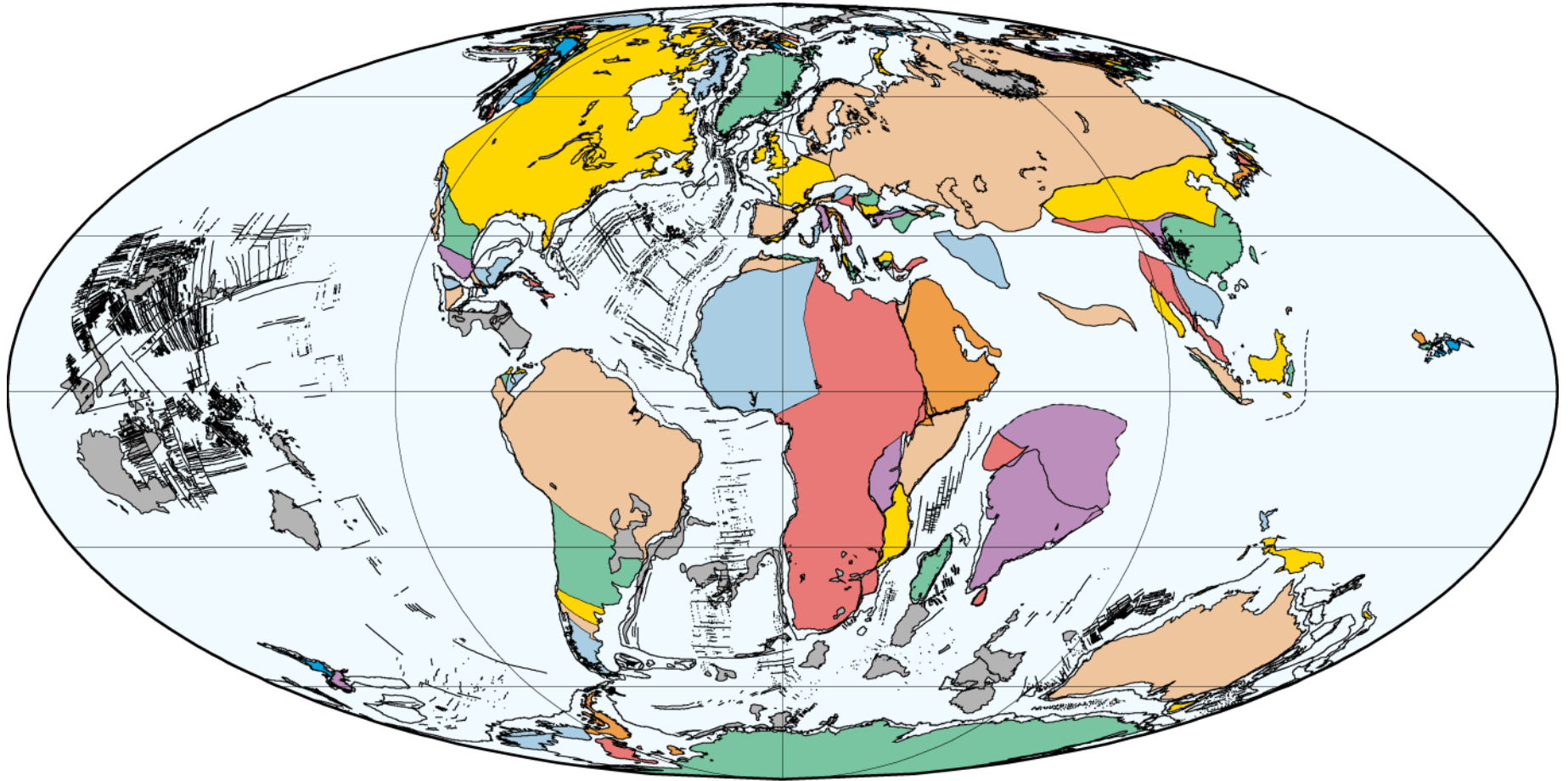
PLATES/UTIG  
August 2002





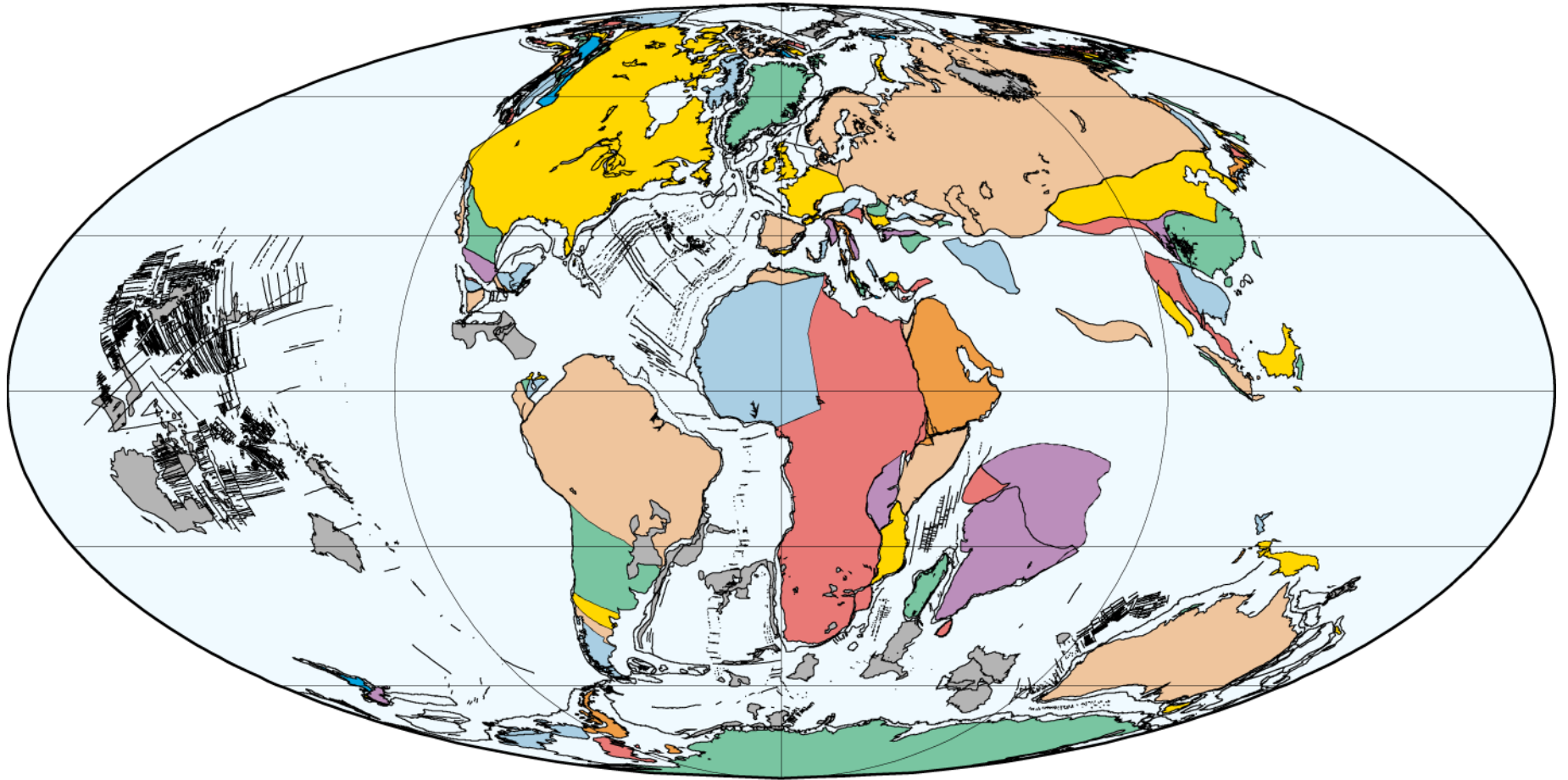
60 Ma  
Late Paleocene

PLATES/UTIG  
August 2002



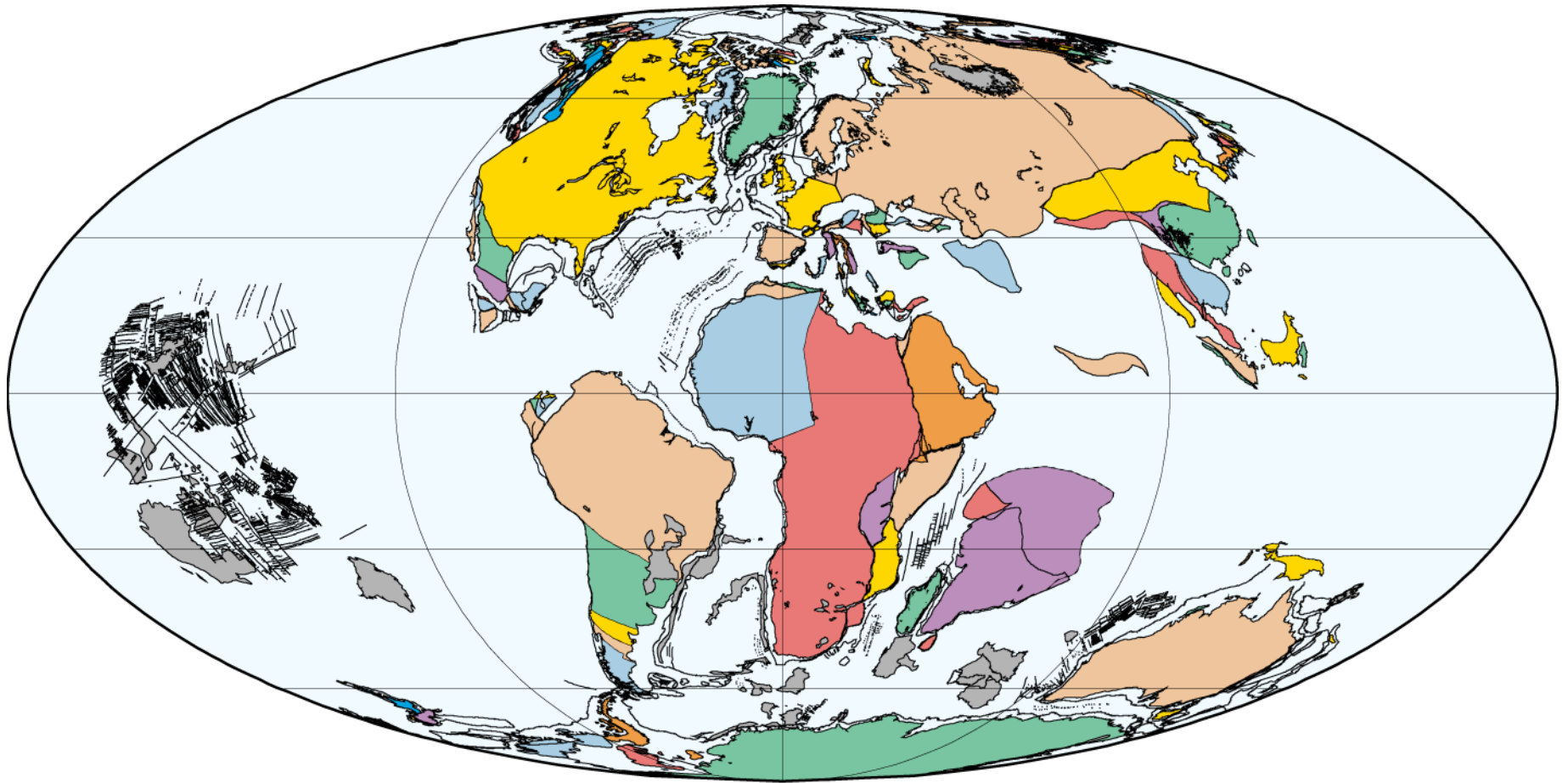
70 Ma  
Maastrichtian (Late Cretaceous)

PLATES/UTIG  
August 2002



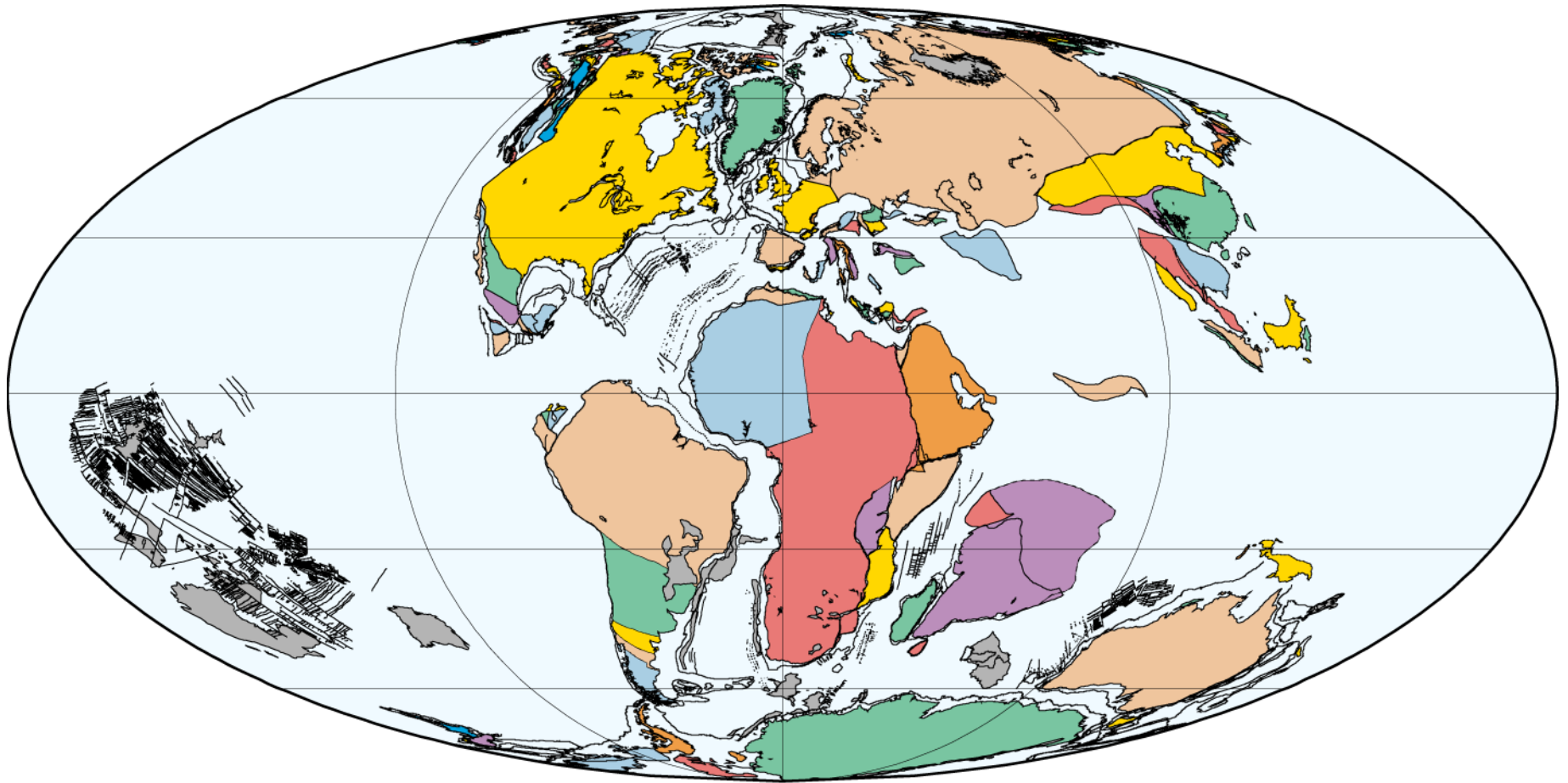
80 Ma  
Campanian (Late Cretaceous)

PLATES/UTIG  
August 2002



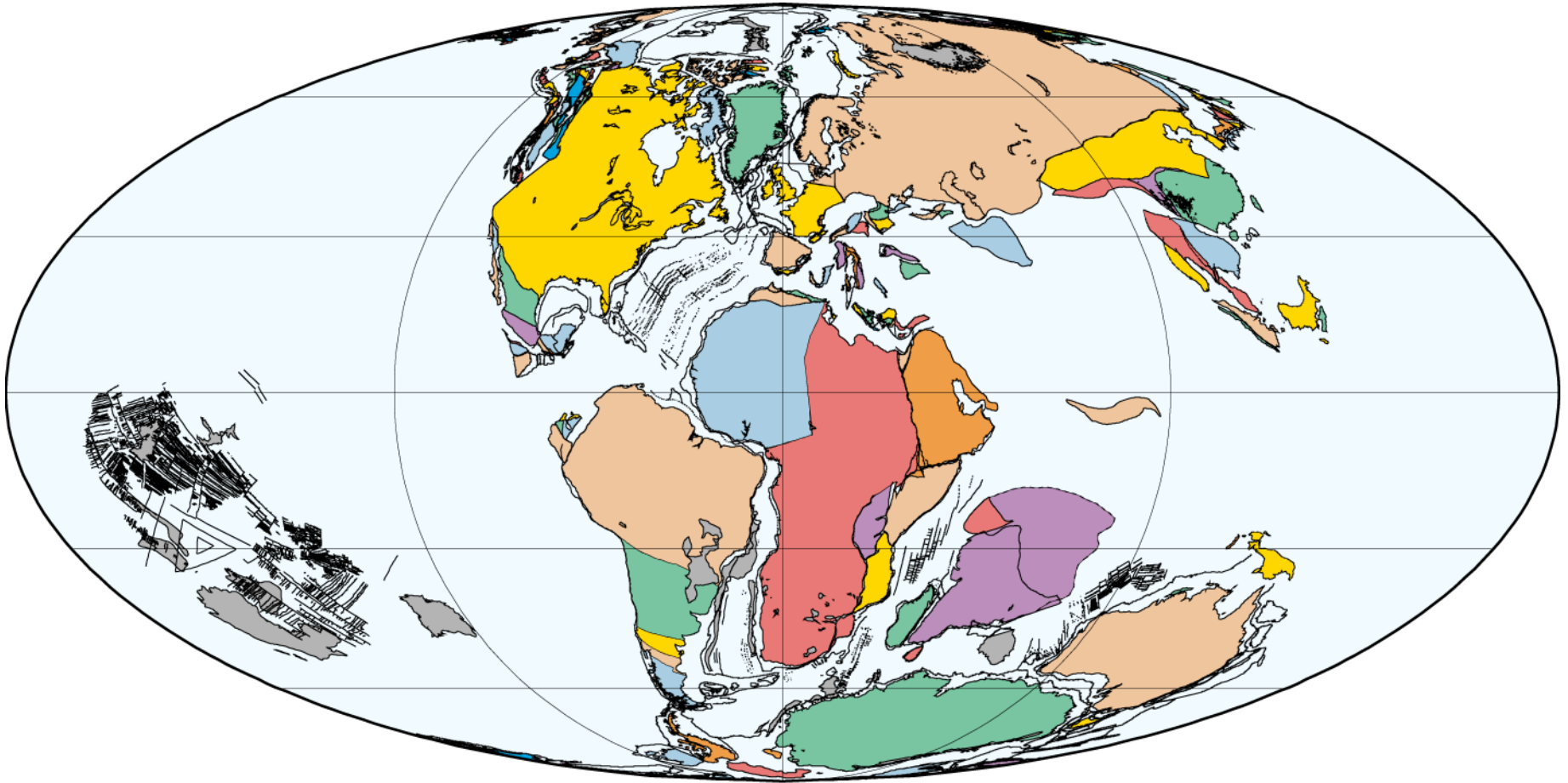
90 Ma  
Turonian (Late Cretaceous)

PLATES/UTIG  
August 2002



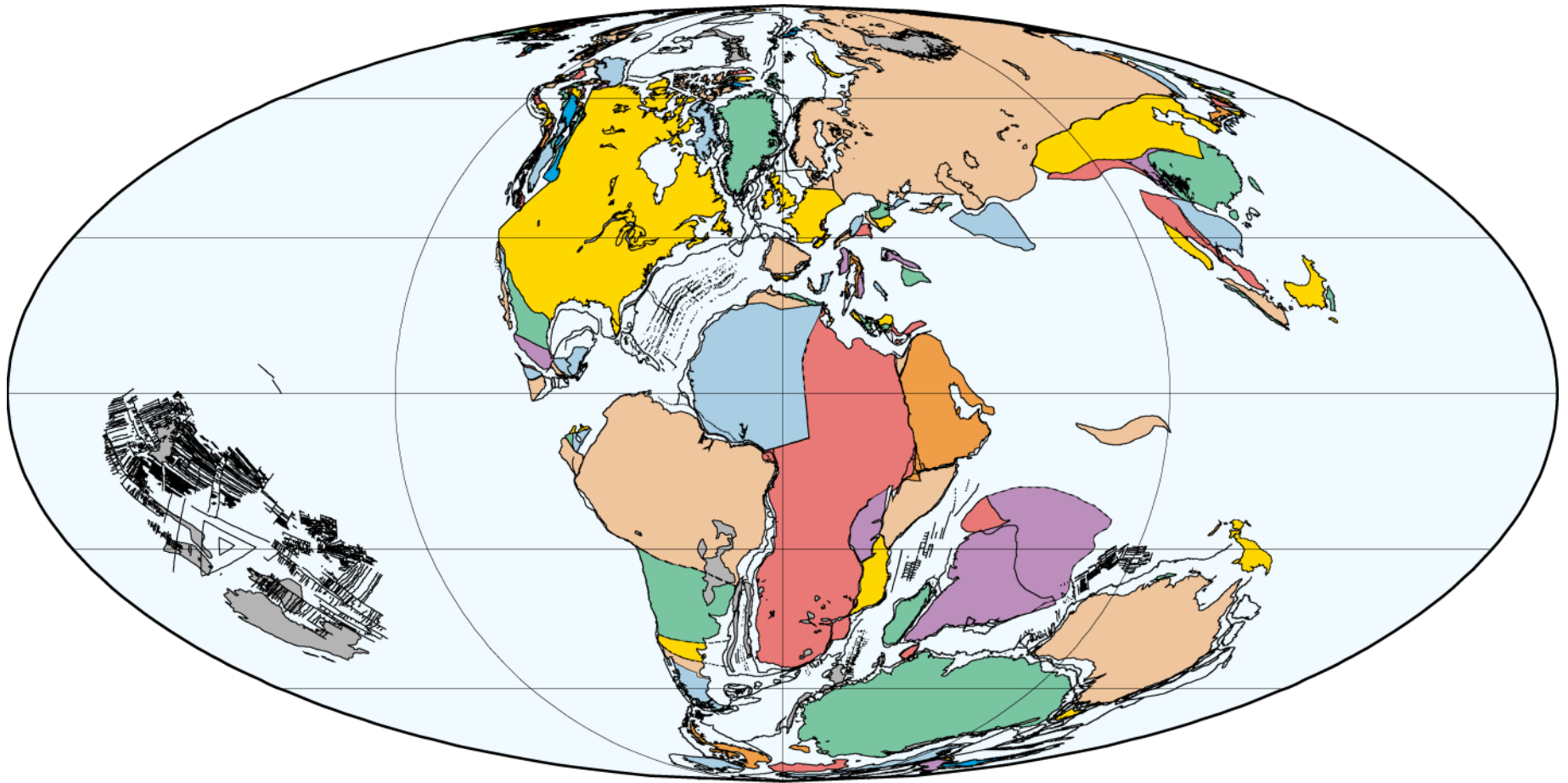
100 Ma  
Late Albian (Early Cretaceous)

PLATES/UTIG  
August 2002



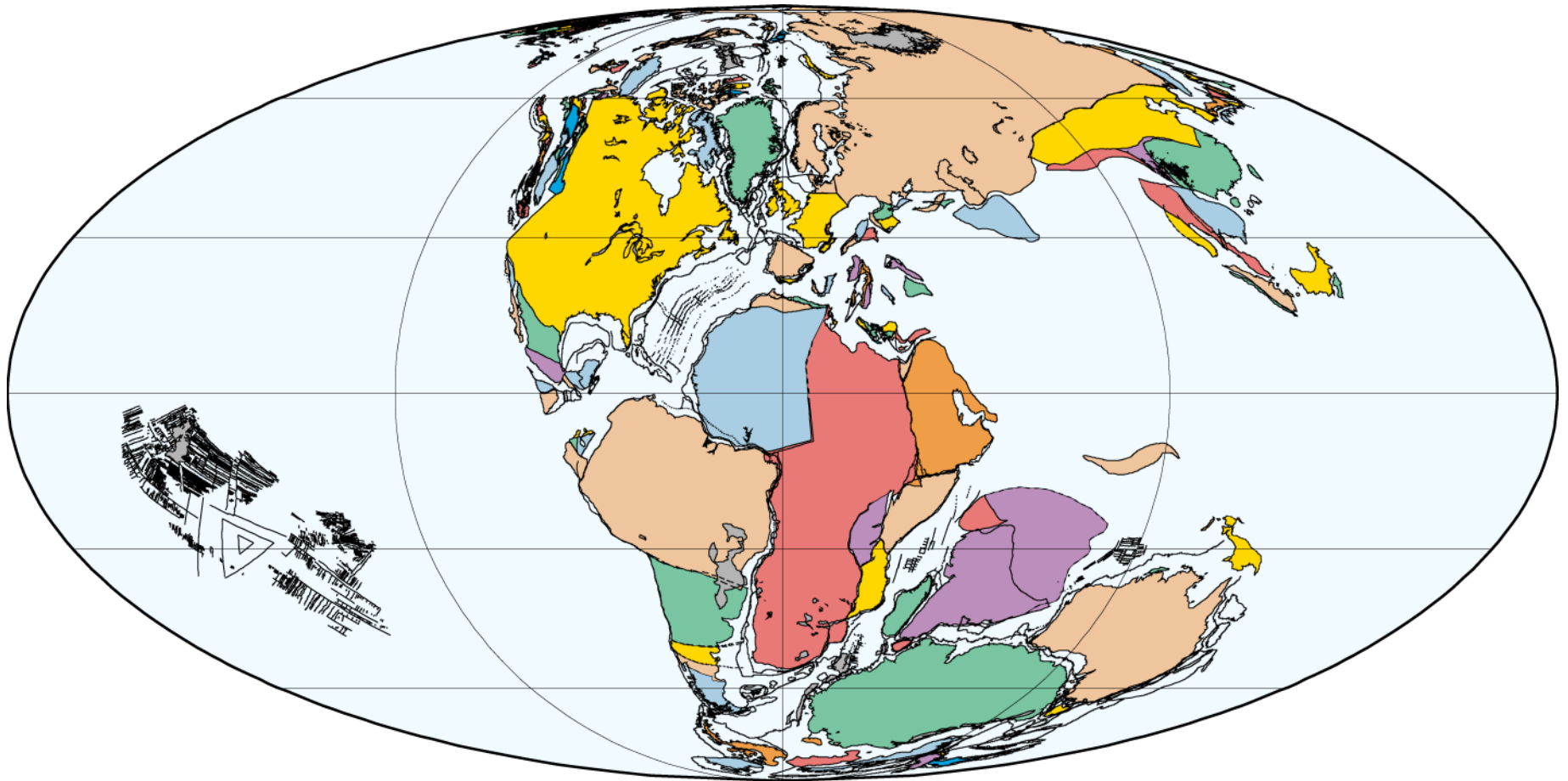
110 Ma  
Early Albian (Early Cretaceous)

PLATES/UTIG  
August 2002



120 Ma  
Aptian (Early Cretaceous)

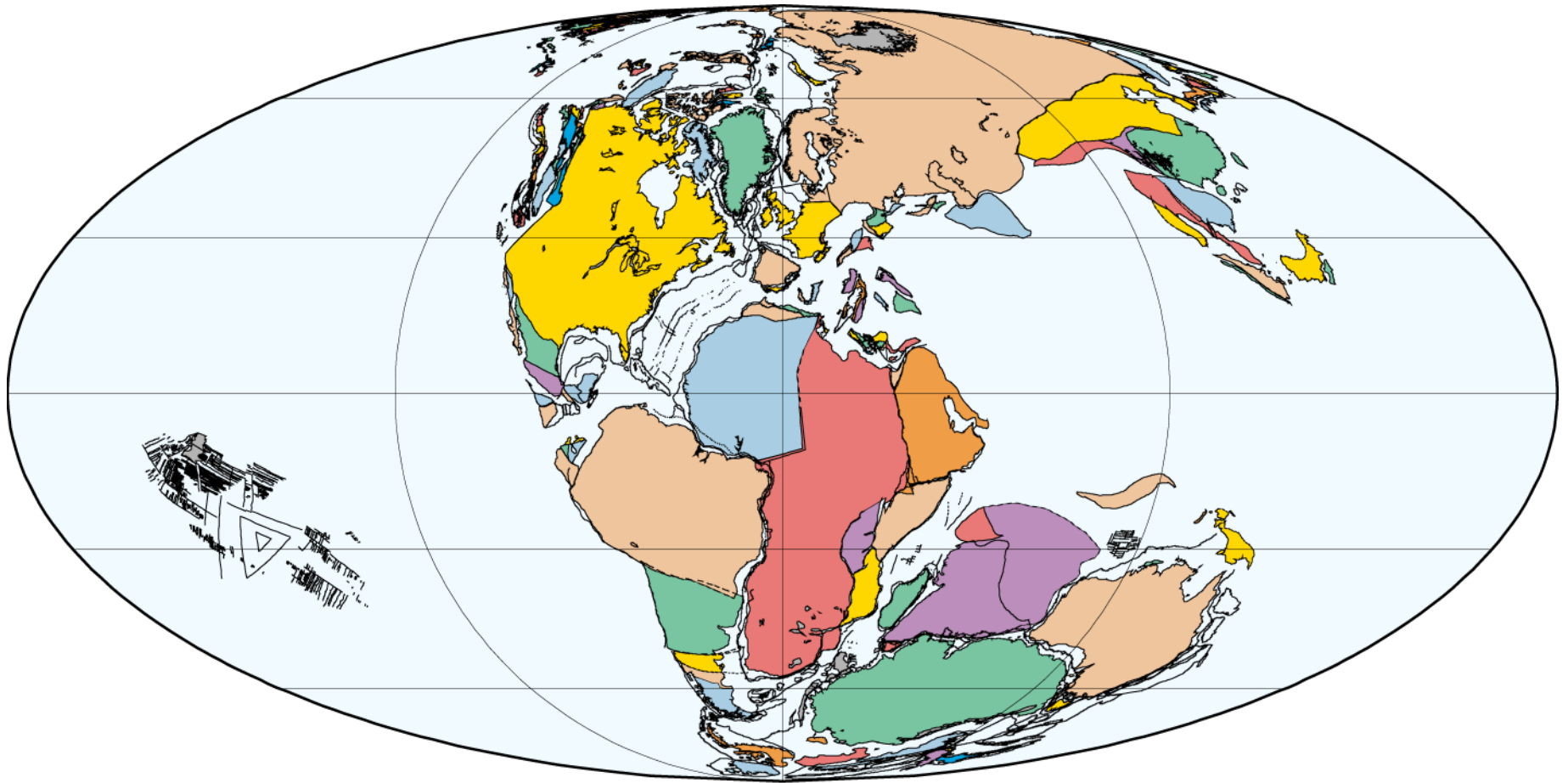
PLATES/UTIG  
August 2002



130 Ma  
Hauterivian (Early Cretaceous)

PLATES/UTIG  
August 2002

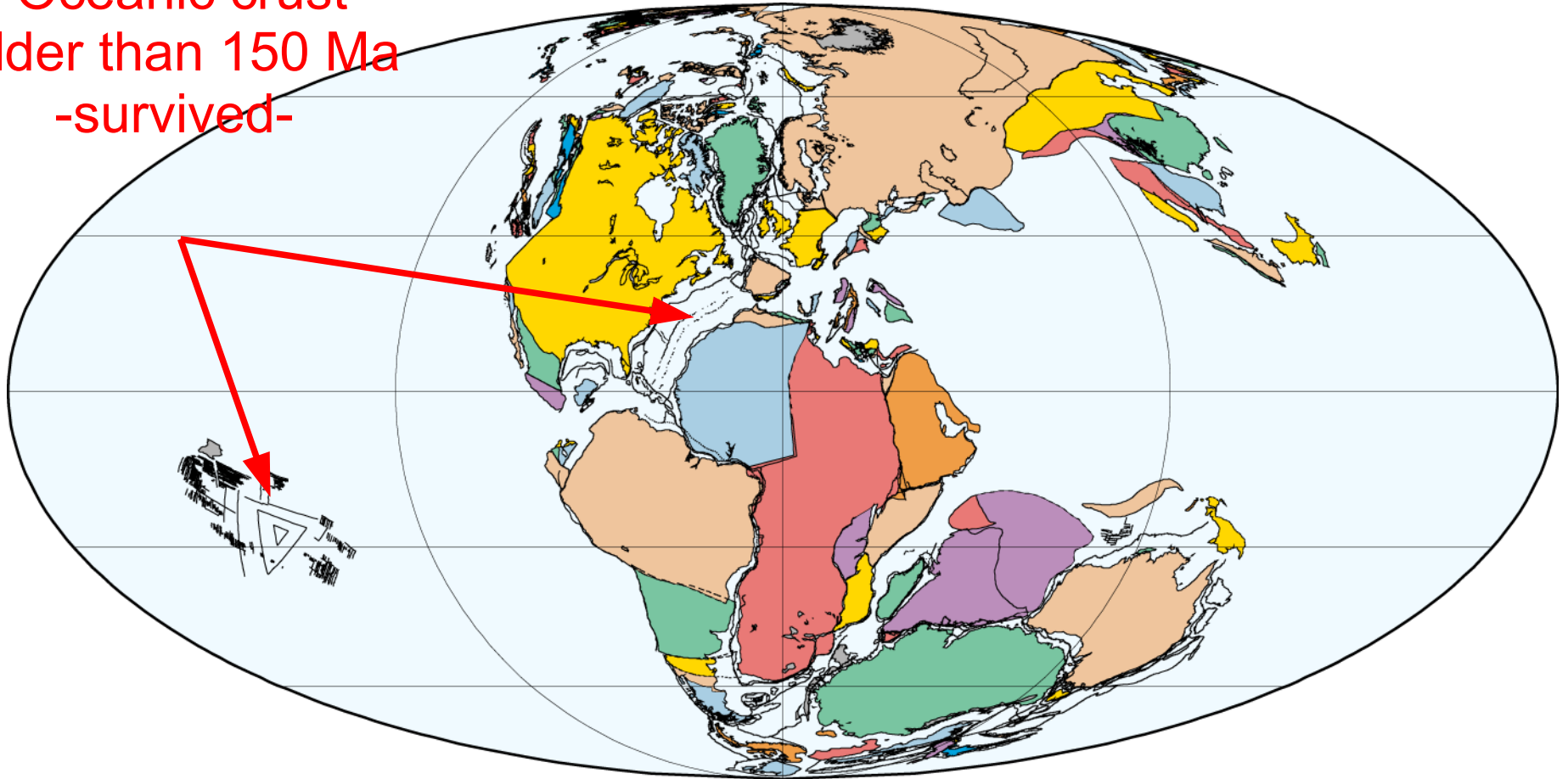




140 Ma  
Ryazanian (Early Cretaceous)

PLATES/UTIG  
August 2002

Oceanic crust  
older than 150 Ma  
-survived-

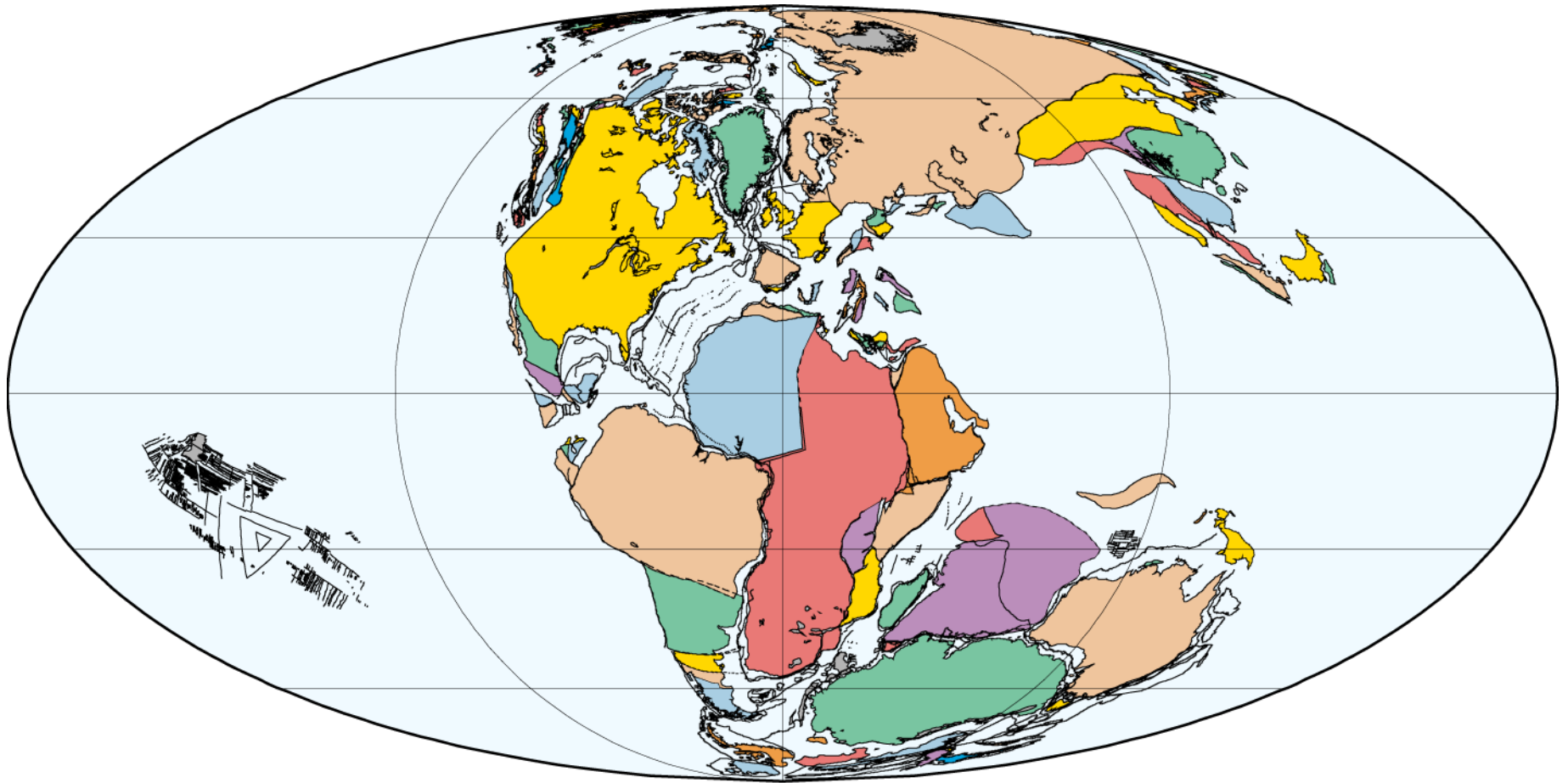


150 Ma  
Volgian (Late Jurassic)

PLATES/UTIG  
August 2002

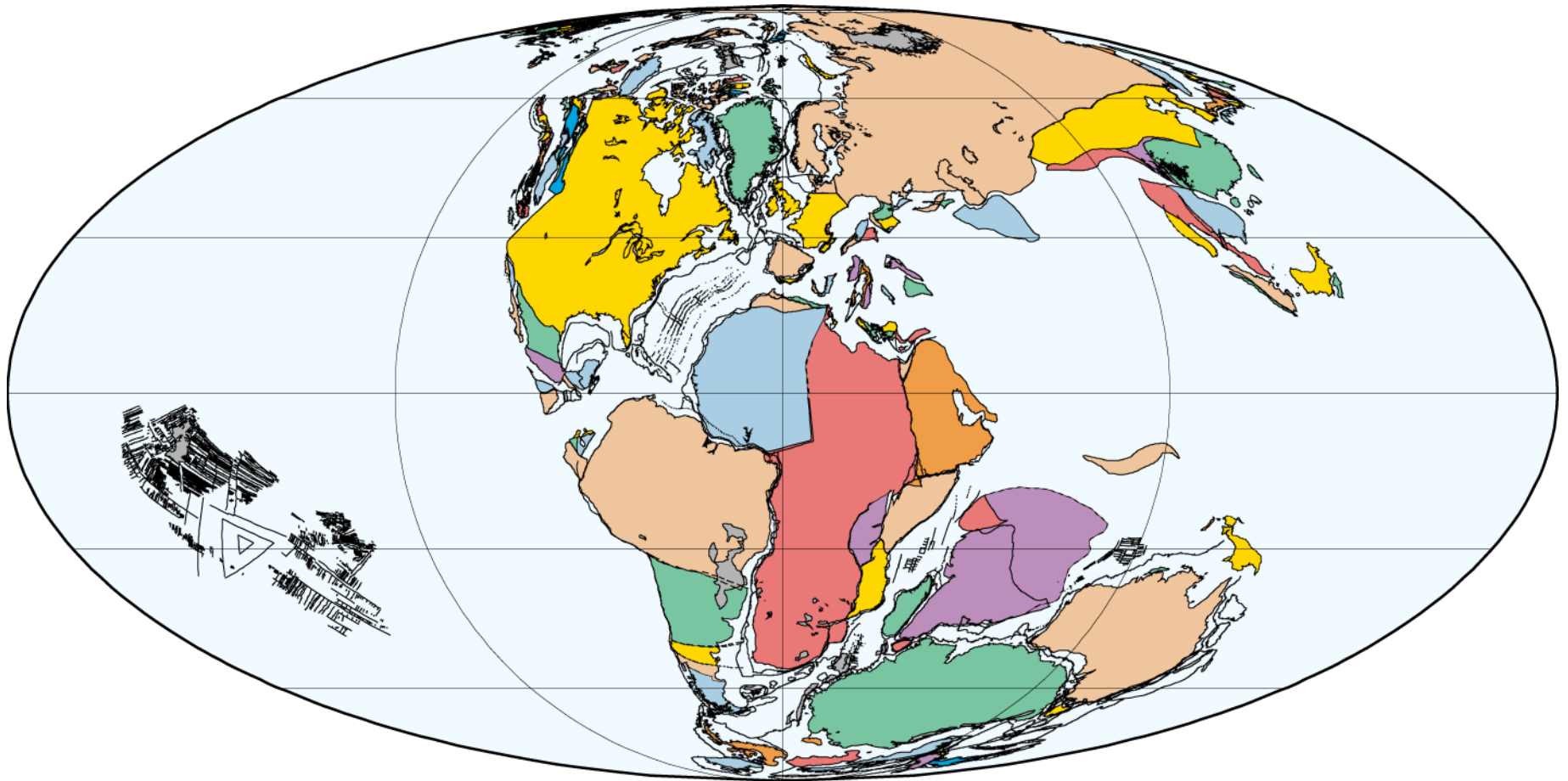
45

Note : the supercontinent Pangea formed ~400Ma ago and started to break ~180Ma ago  
Before Pangea other supercontinents formed, e.g., Rodinia ~1 Ga ago, Columbia ~2 Ga ago



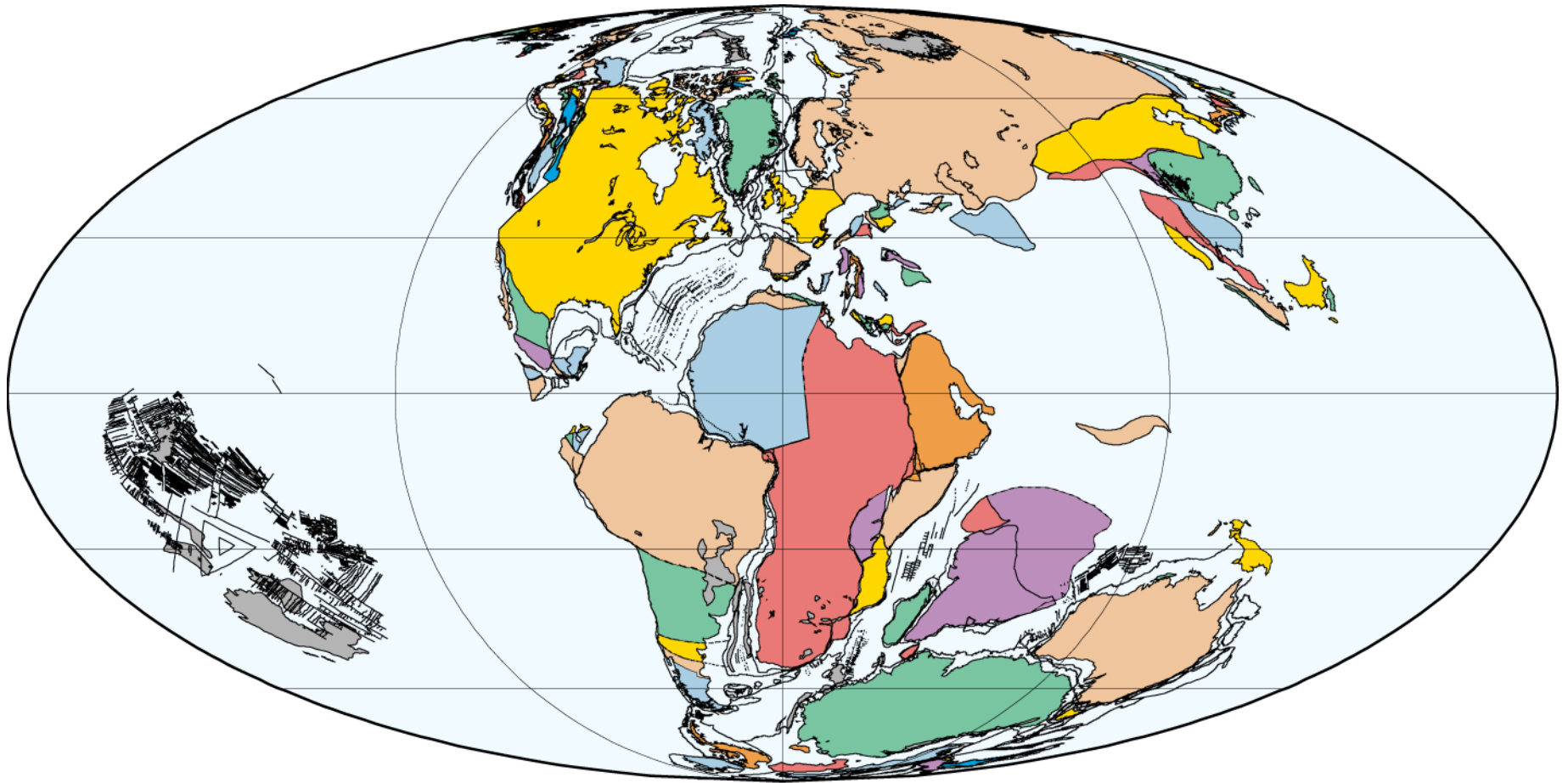
140 Ma  
Ryazanian (Early Cretaceous)

PLATES/UTIG  
August 2002



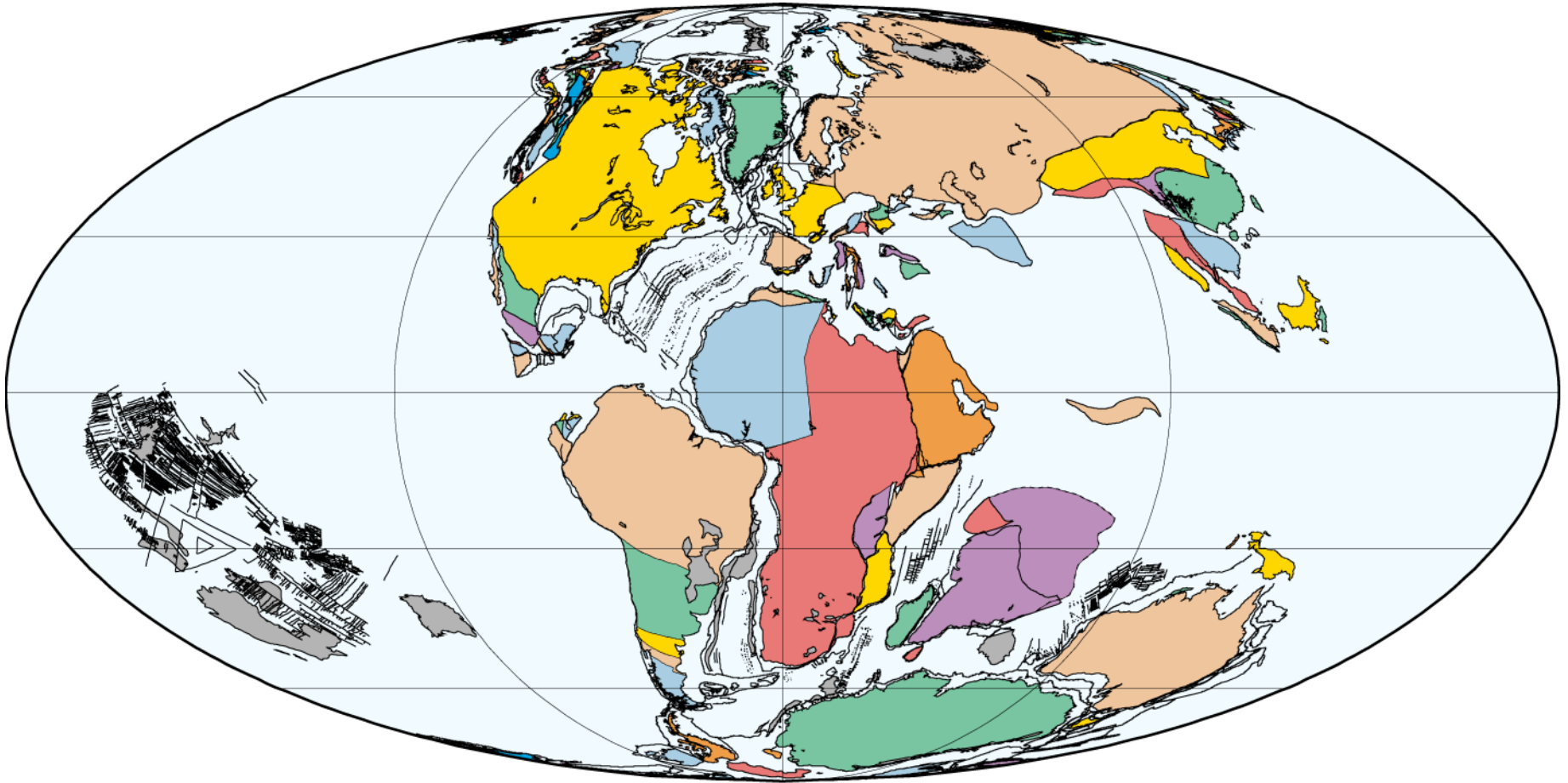
130 Ma  
Hauterivian (Early Cretaceous)

PLATES/UTIG  
August 2002



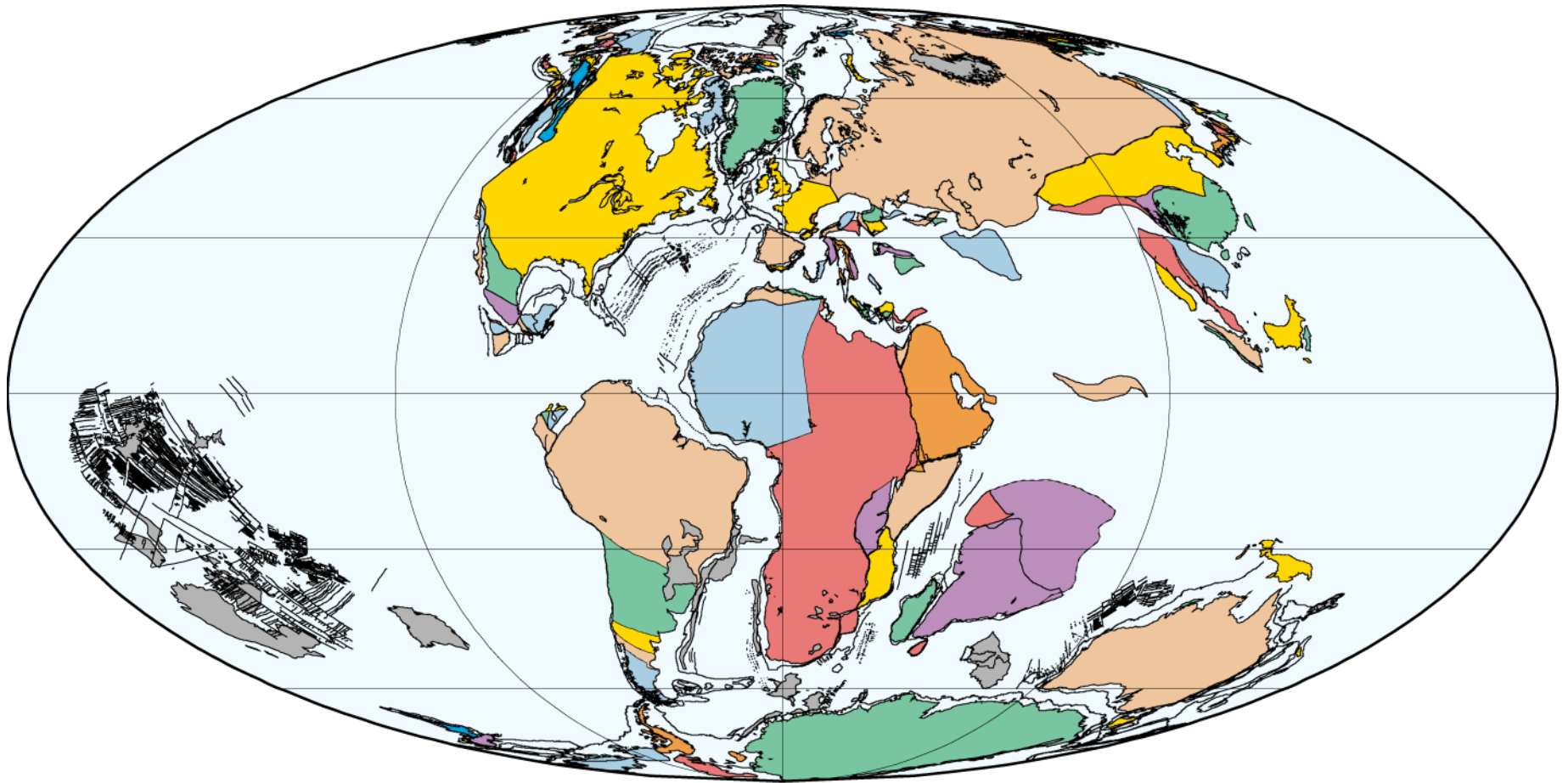
120 Ma  
Aptian (Early Cretaceous)

PLATES/UTIG  
August 2002



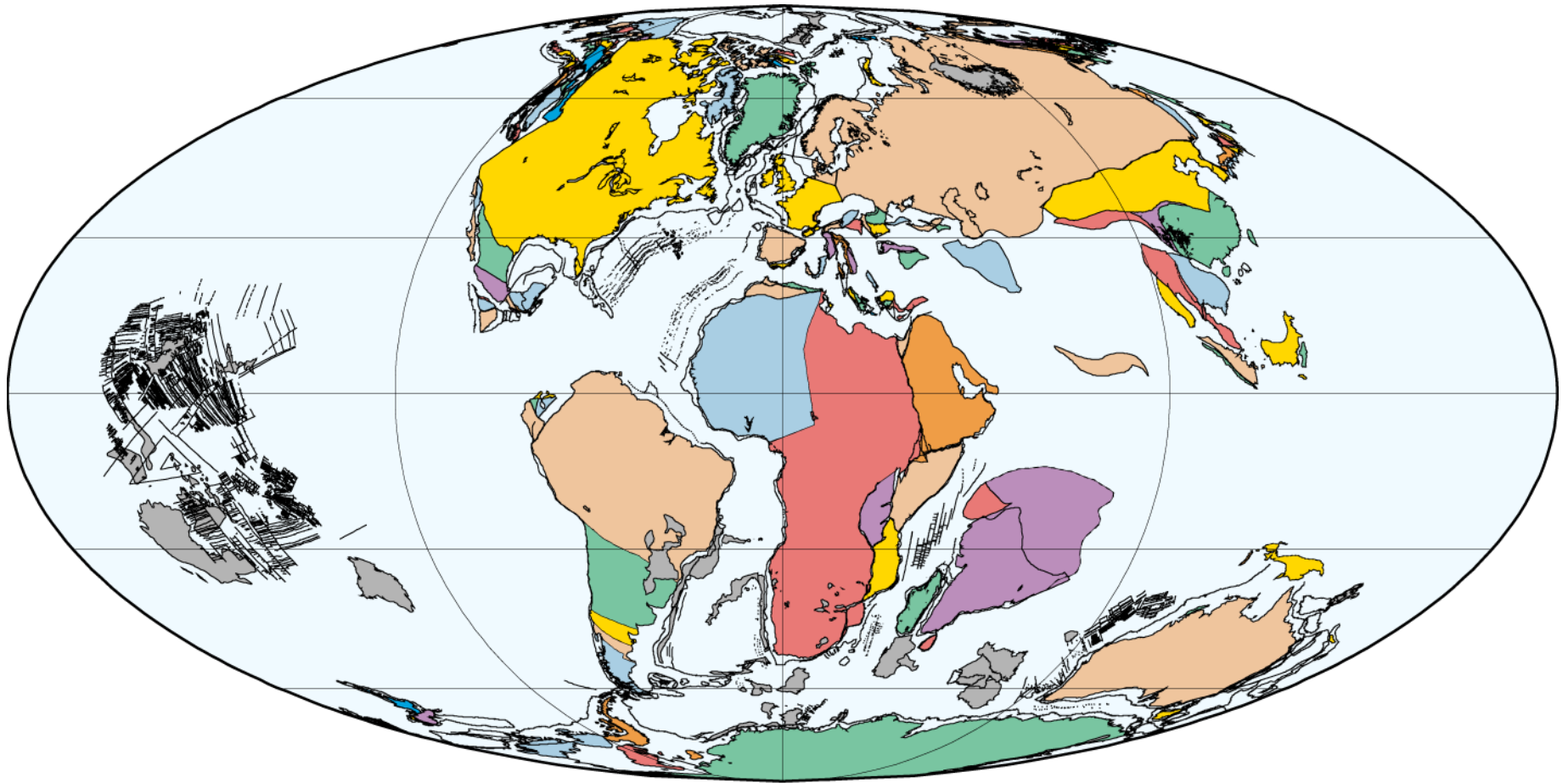
110 Ma  
Early Albian (Early Cretaceous)

PLATES/UTIG  
August 2002



100 Ma  
Late Albian (Early Cretaceous)

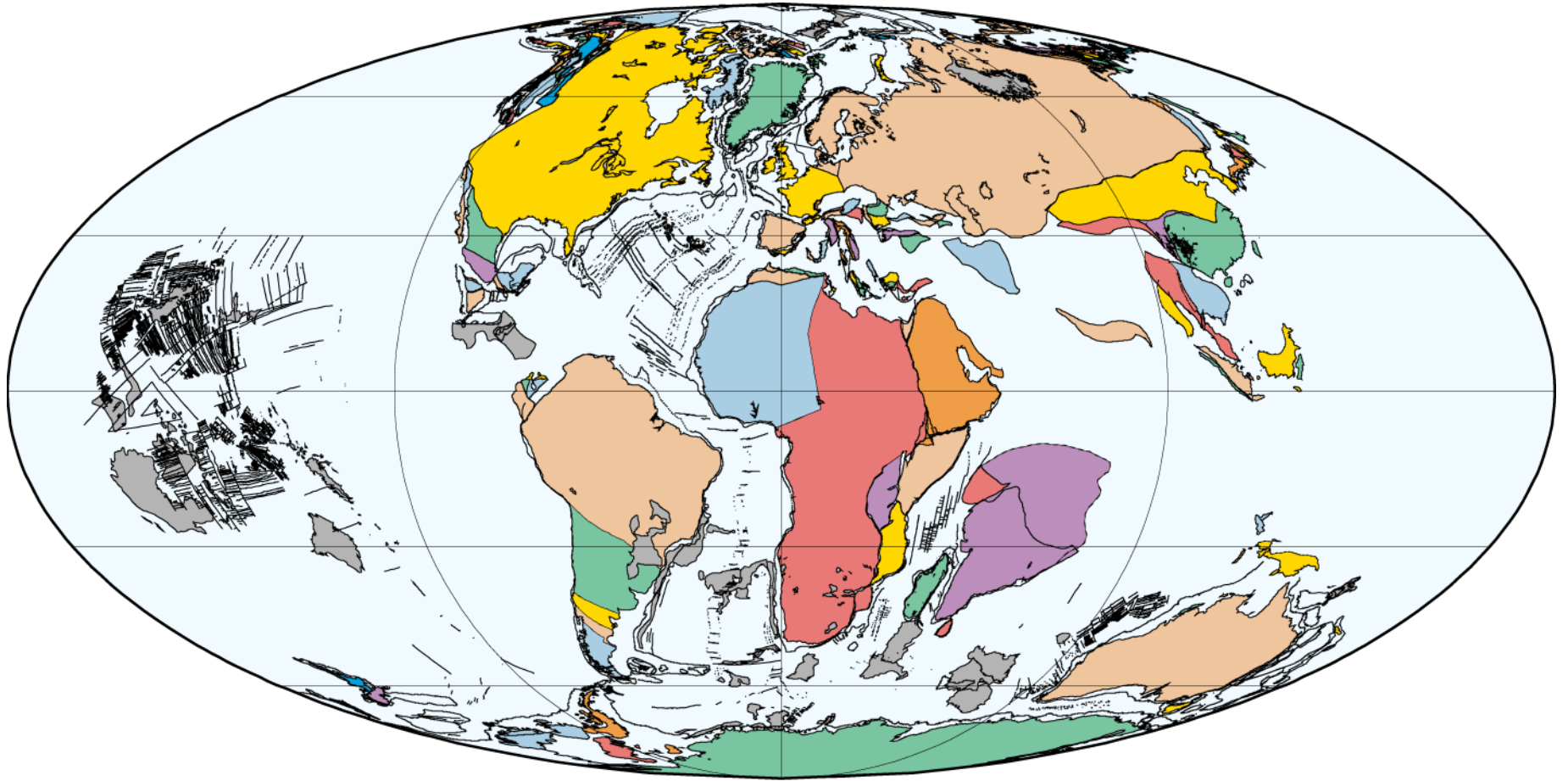
PLATES/UTIG  
August 2002



90 Ma  
Turonian (Late Cretaceous)

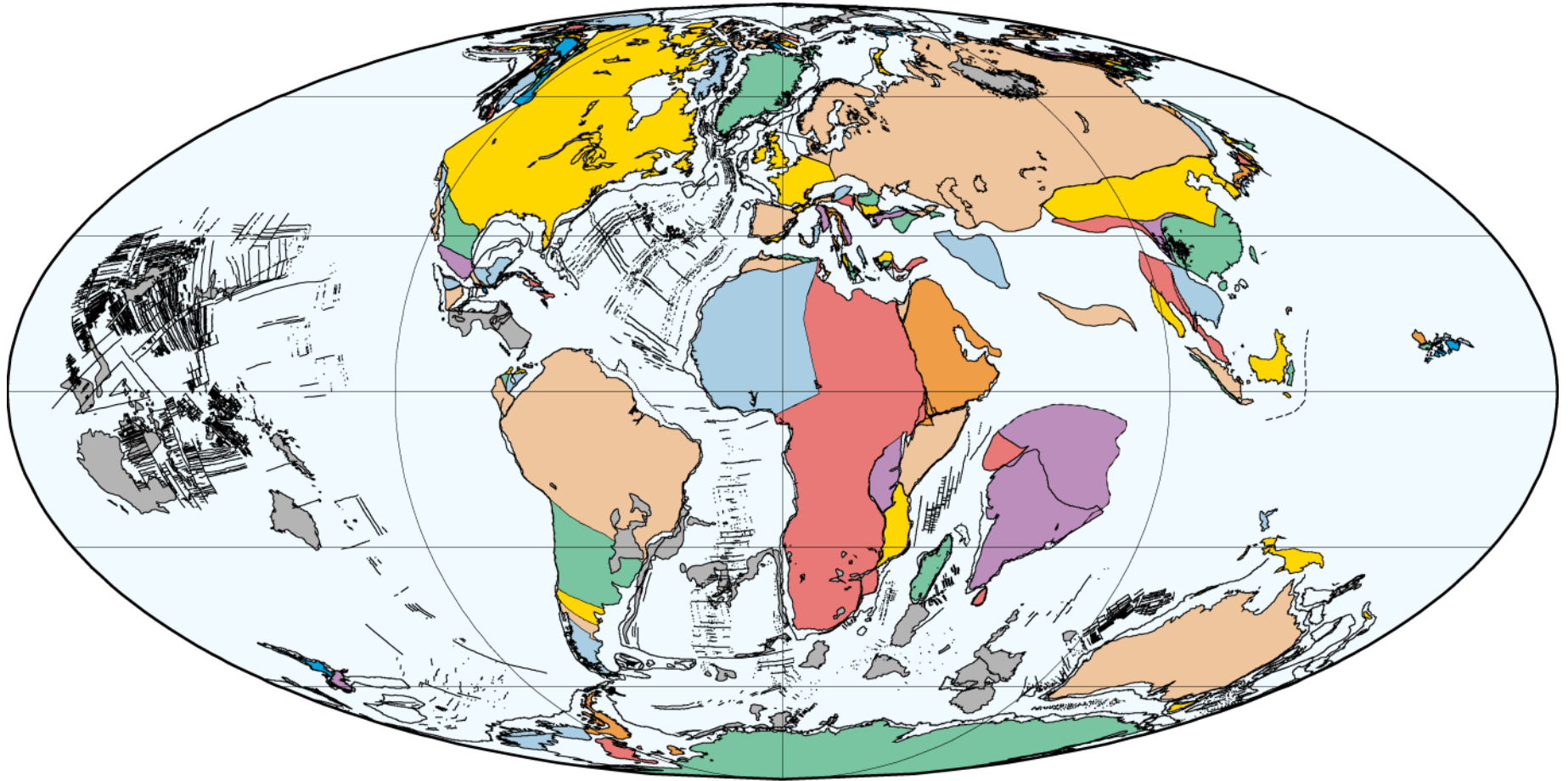
PLATES/UTIG  
August 2002





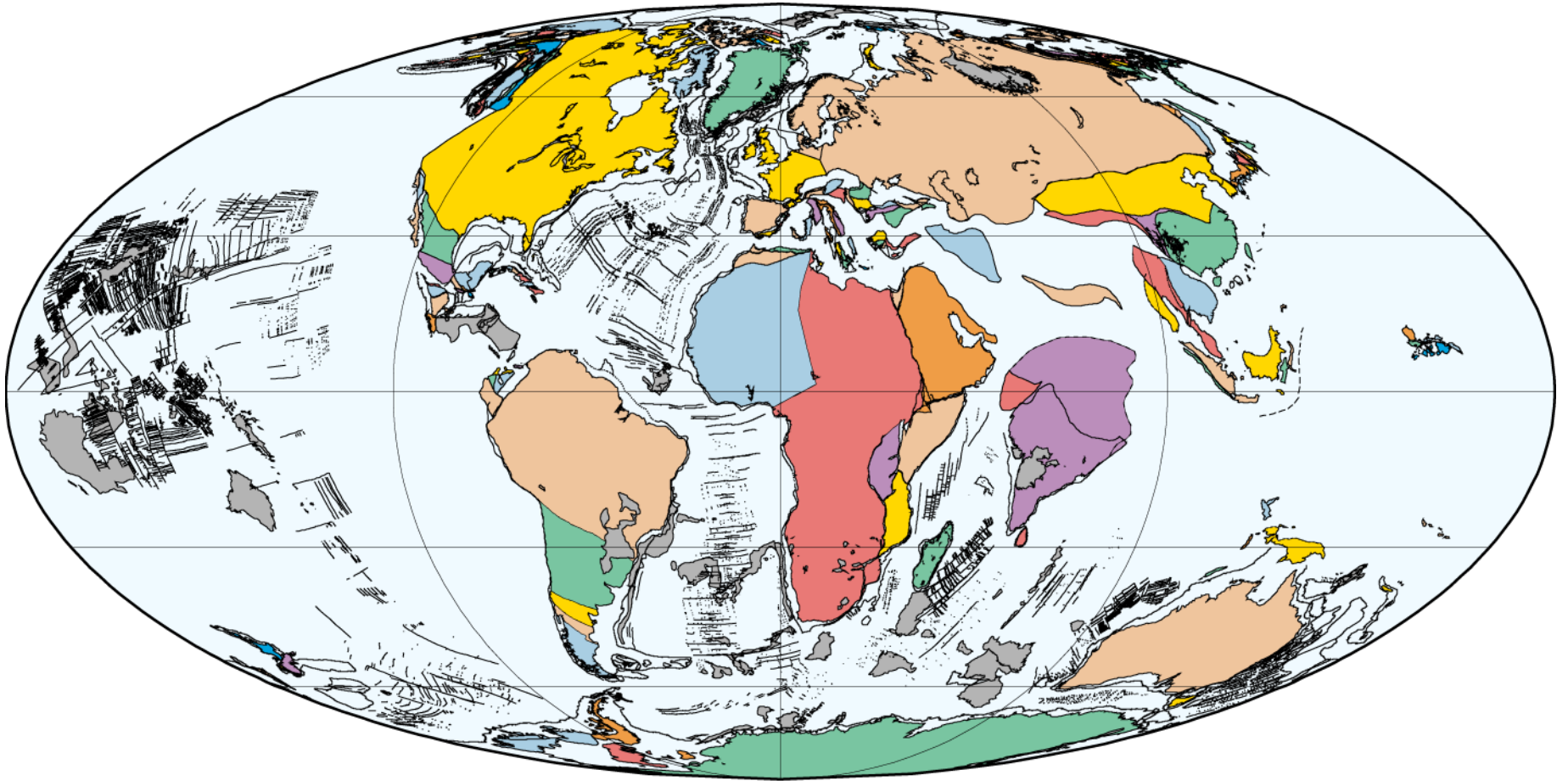
80 Ma  
Campanian (Late Cretaceous)

PLATES/UTIG  
August 2002



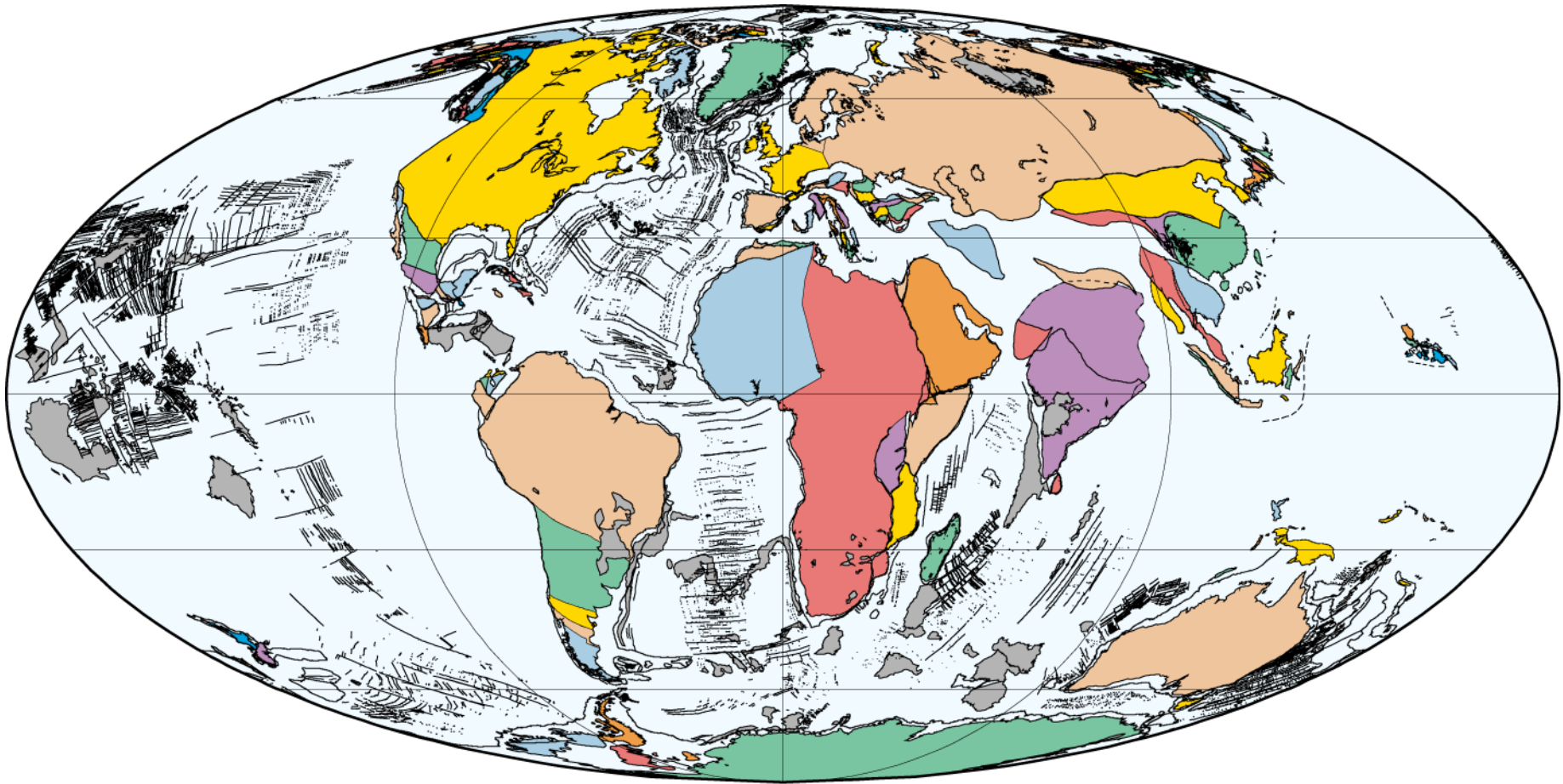
70 Ma  
Maastrichtian (Late Cretaceous)

PLATES/UTIG  
August 2002



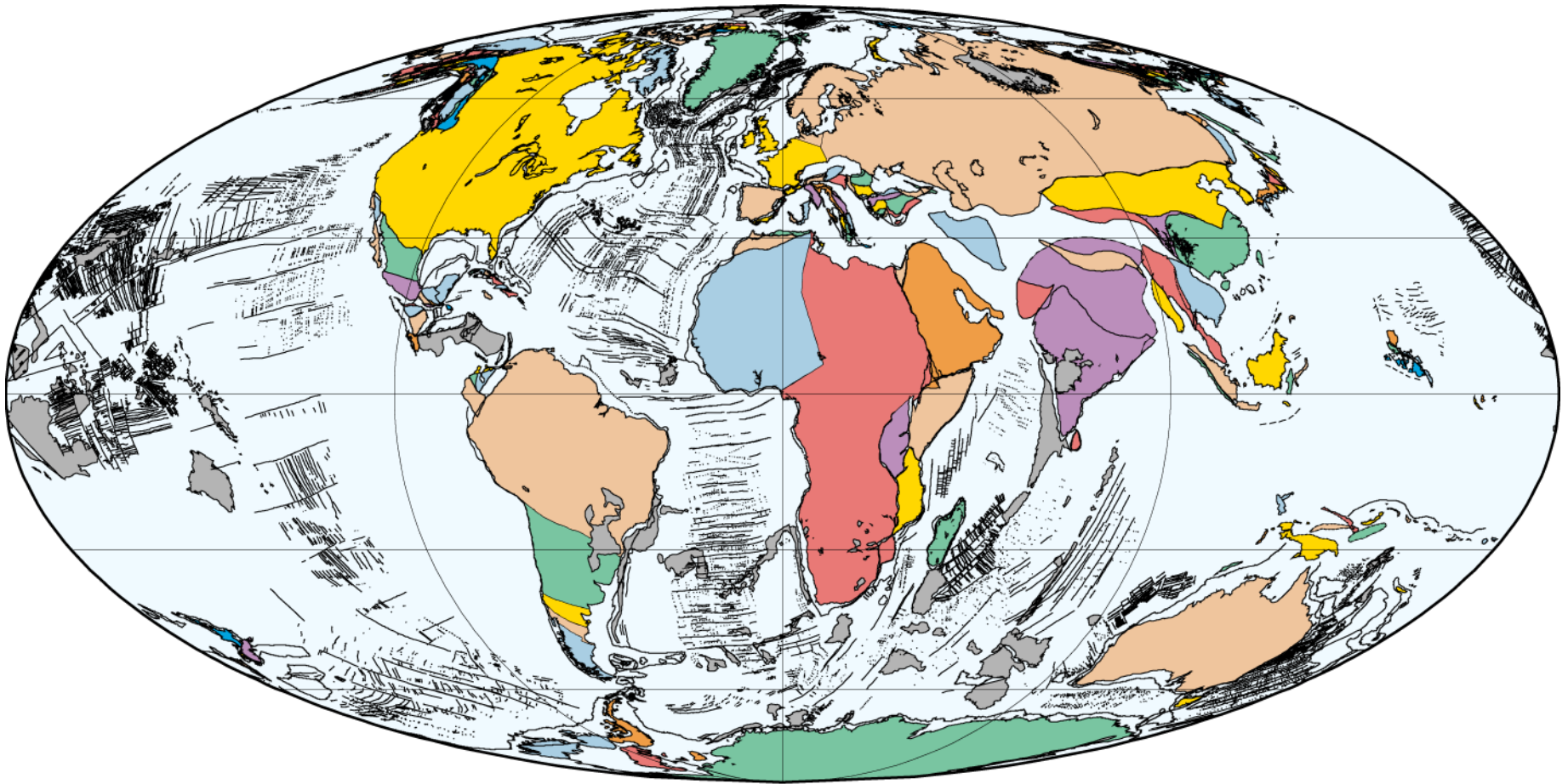
60 Ma  
Late Paleocene

PLATES/UTIG  
August 2002



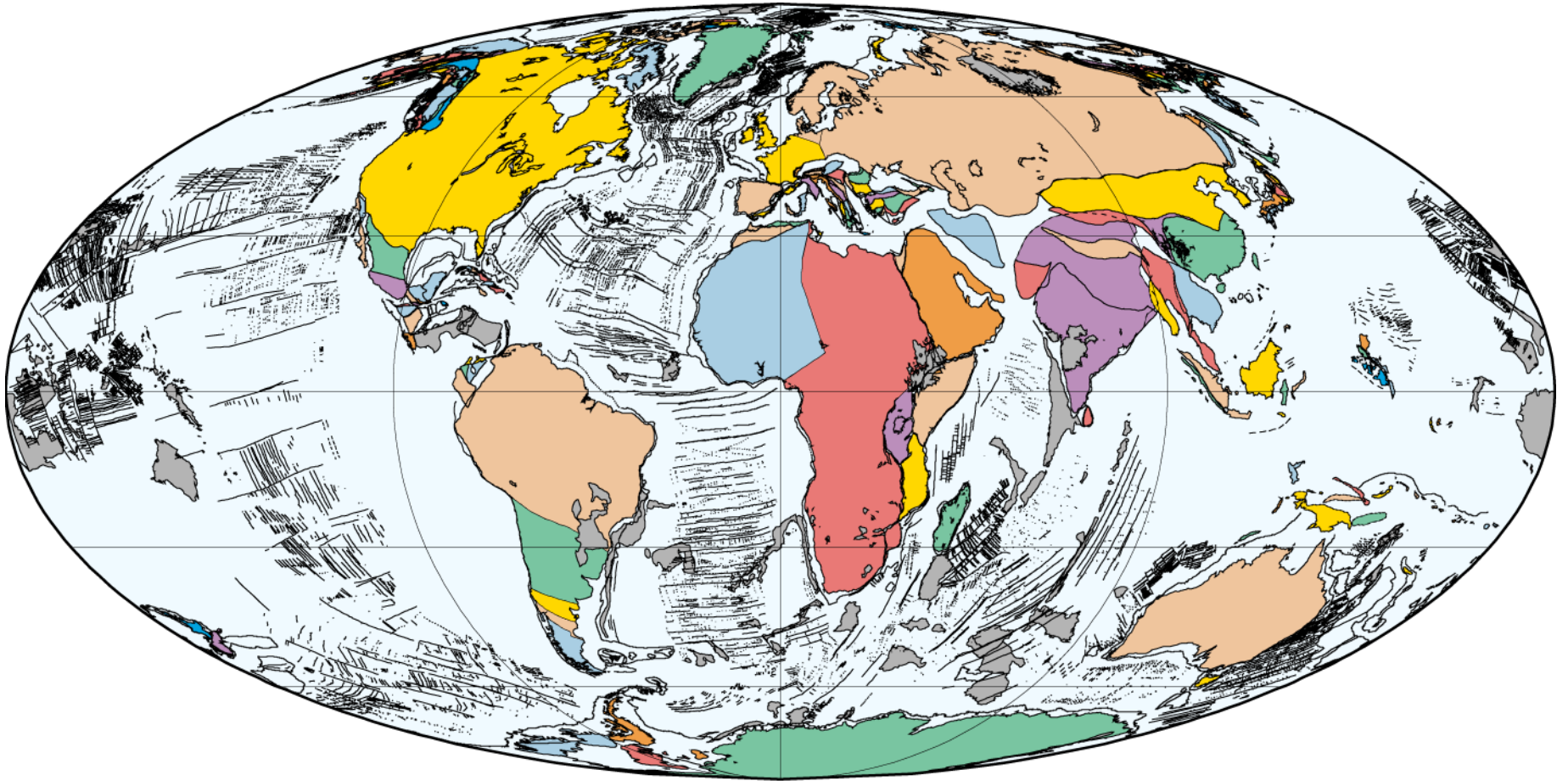
50 Ma  
Early Eocene

PLATES/UTIG  
August 2002



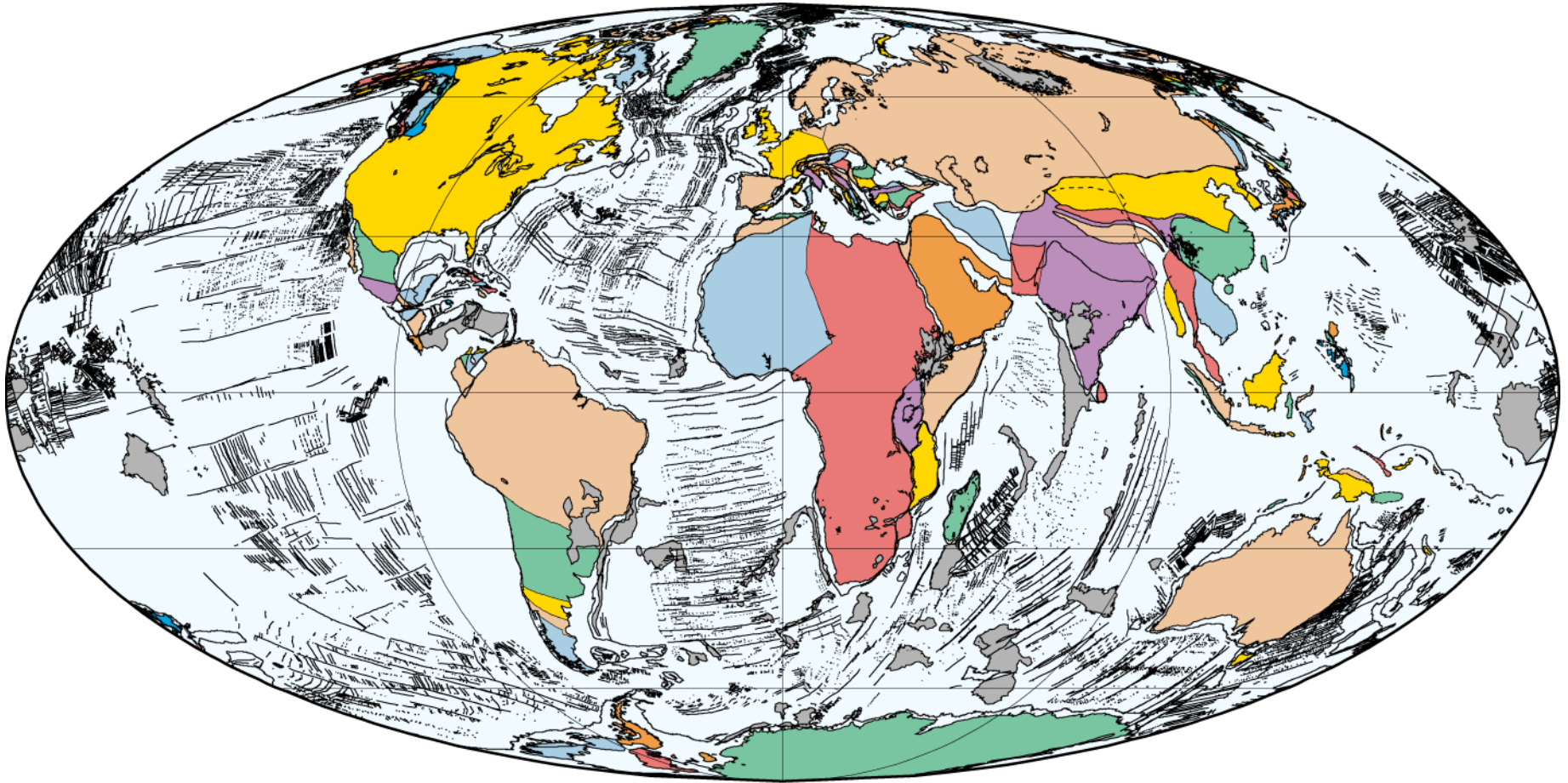
40 Ma  
Middle Eocene

PLATES/UTIG  
August 2002



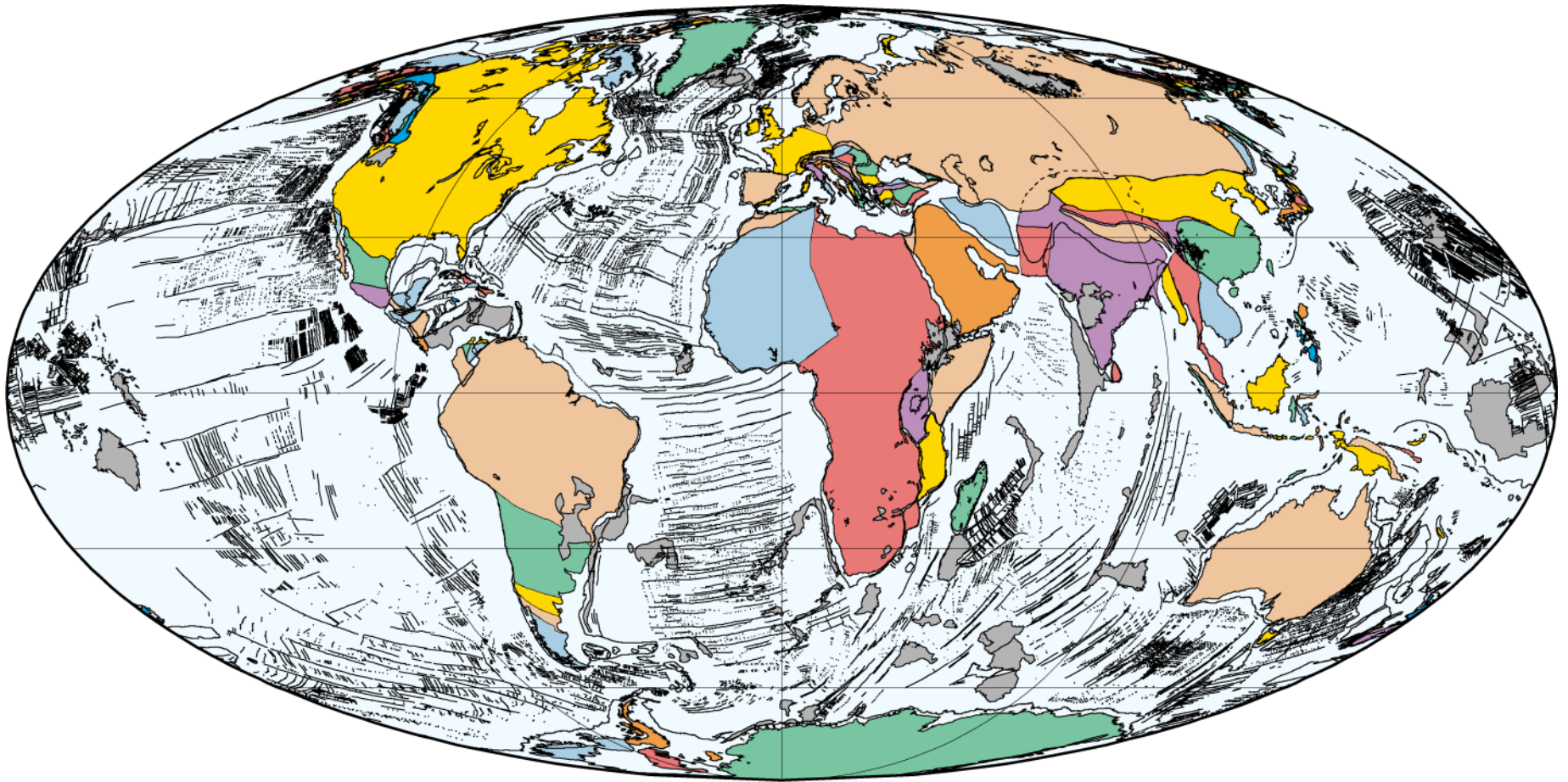
30 Ma  
Early Oligocene

PLATES/UTIG  
August 2002



20 Ma  
Early Miocene

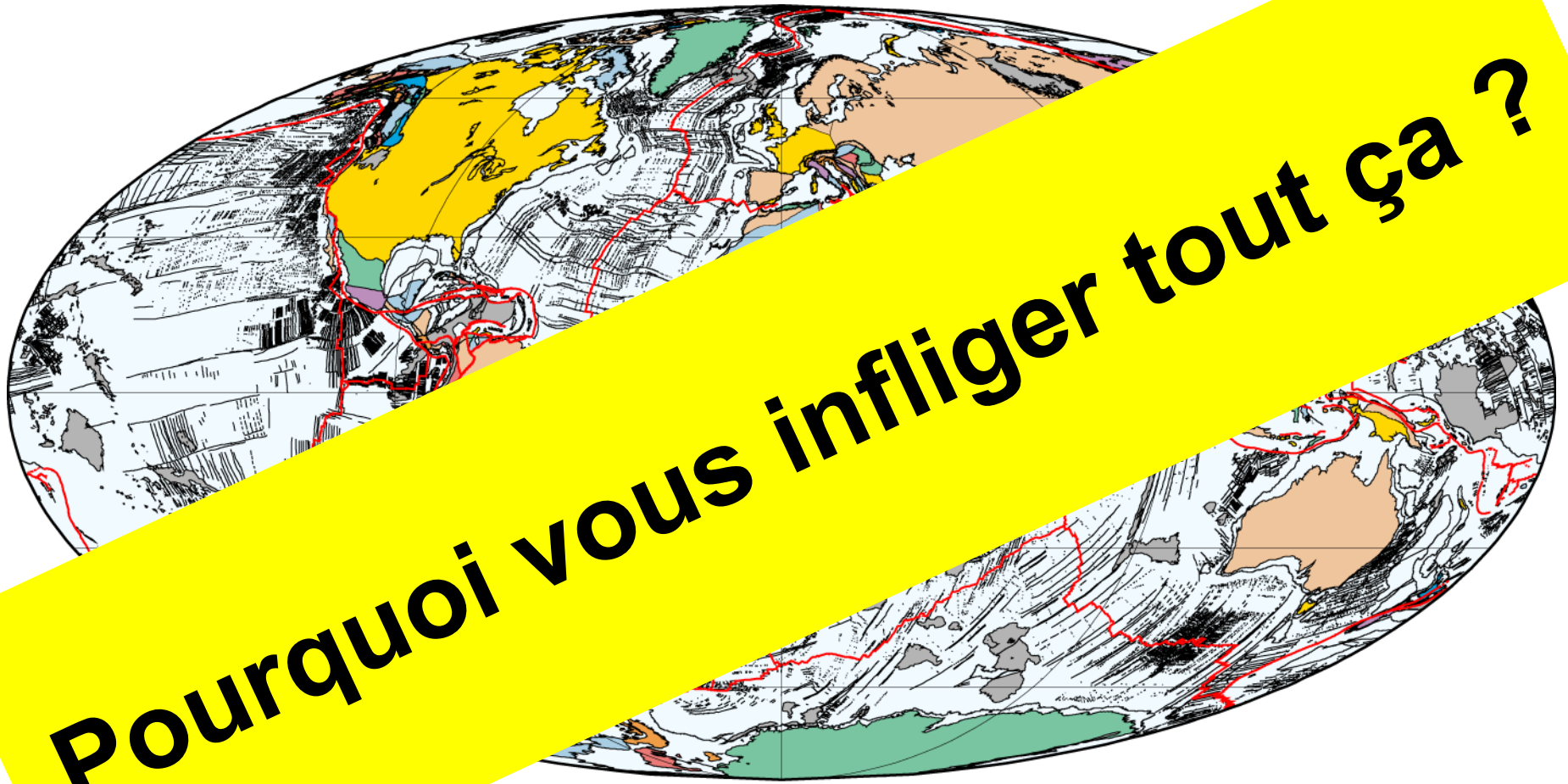
PLATES/UTIG  
August 2002



10 Ma  
Late Miocene

PLATES/UTIG  
August 2002

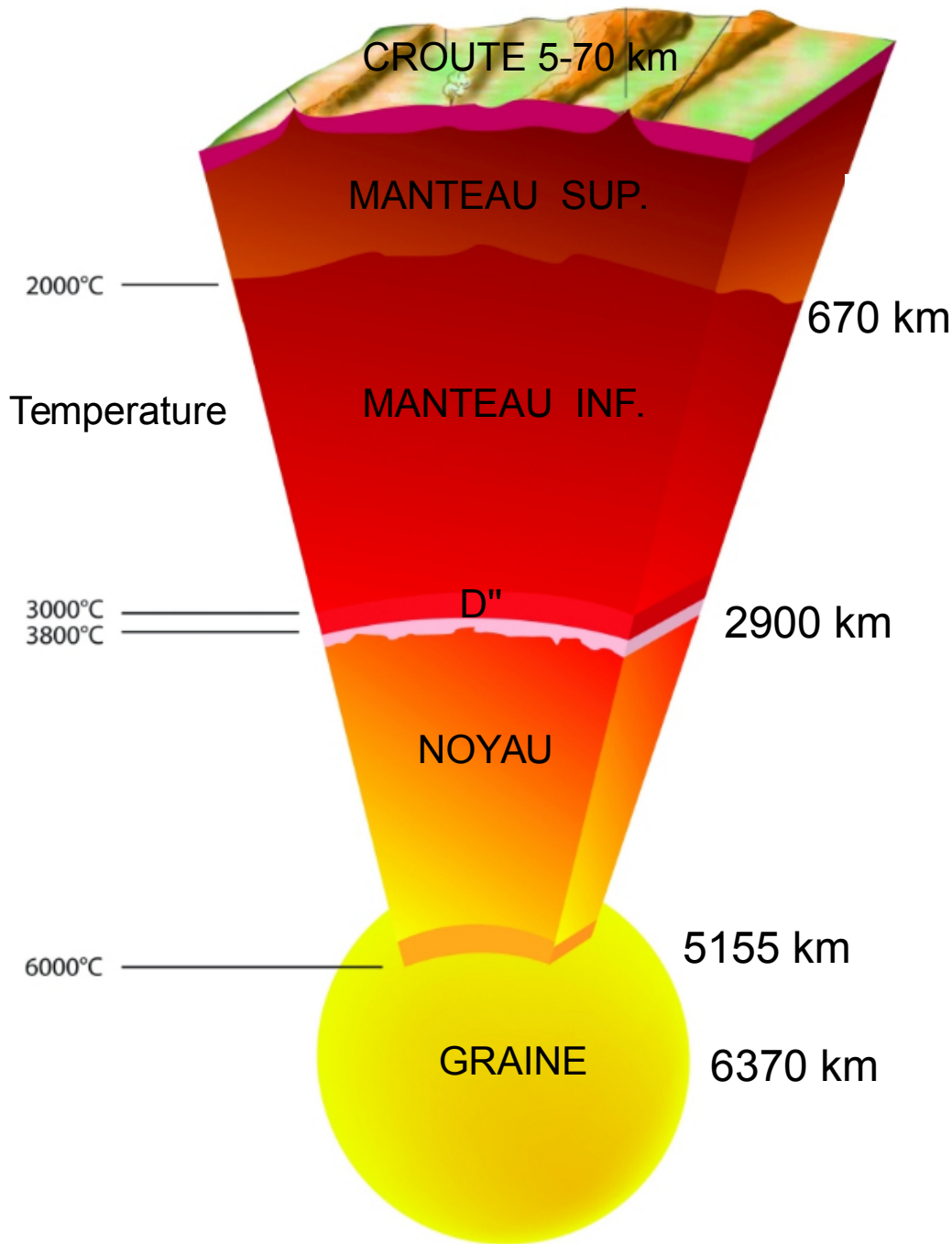




**Pourquoi vous infliger tout ça ?**

0.  
Pre

PLATES/UTIG  
August 2002



**These are surface expressions of mantle convection**

# Mantle convection

## numerical simulations and laboratory experiments

$$Ra = \frac{\rho \alpha \Delta T g D^3}{k \eta}$$

Temperature contrast  $\Delta T = T_{\text{bot.}} - T_{\text{top}} \sim 2500$  K

density  $\rho = 3300\text{-}4000$  kg/m<sup>3</sup>

thermal exp. coeff.  $\alpha = 5 \cdot 10^{-5}$  K<sup>-1</sup>

mantle depth  $D = 2900$  km

thermal diffusivity  $\kappa = 10^{-6}$  m<sup>2</sup>/s

mantle viscosity  $\eta = 10^{21}\text{-}10^{23}$  Pa s

§ **Governing equations** : conservation of mass, momentum, energy

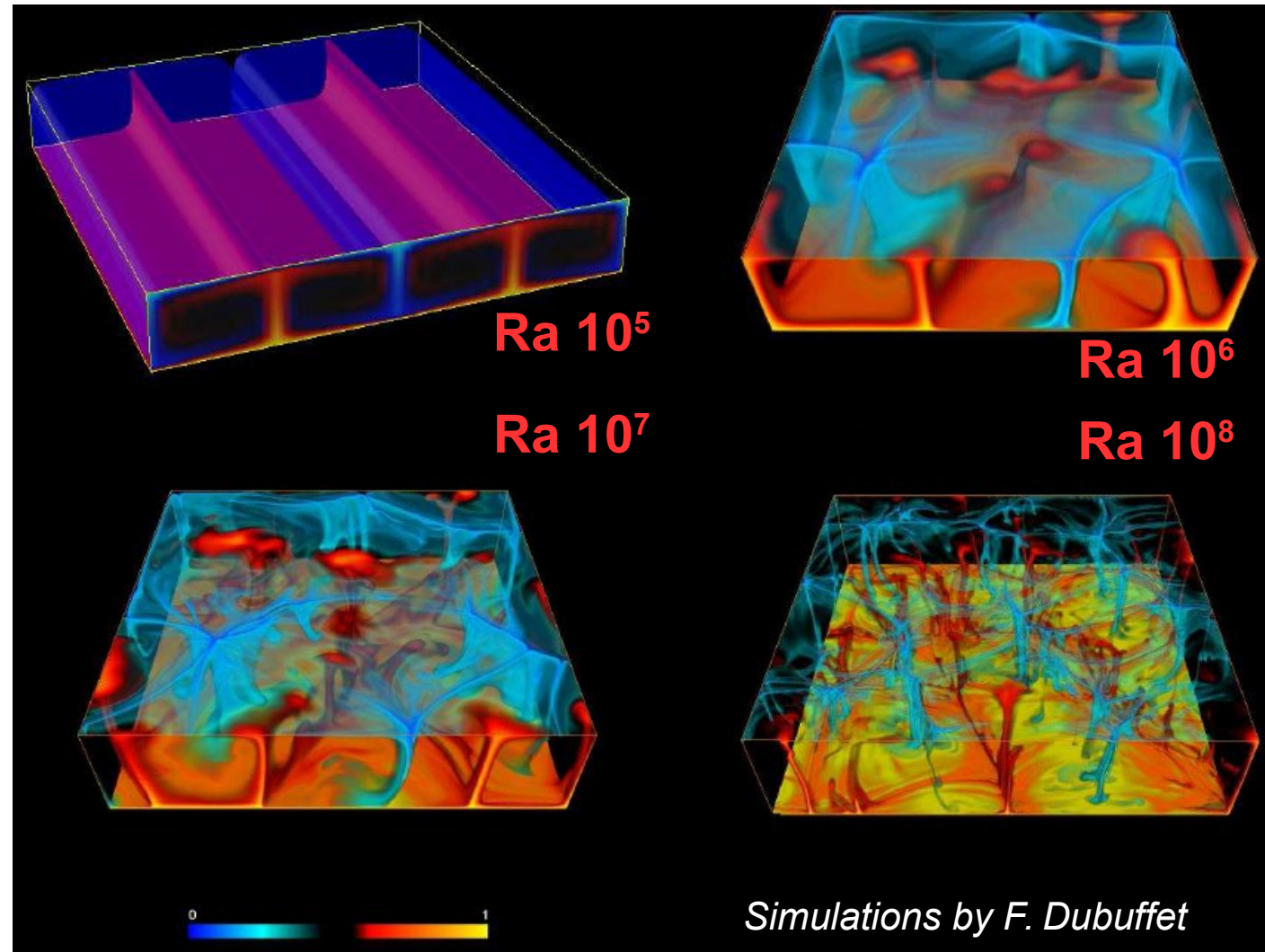
§ For the simplest case solve for a purely thermal, incompressible viscous fluid, cooled from above and heated at the bottom, at infinite Prandtl number (ratio of viscous/thermal diffusion rate is  $\sim 10^{24}$ ).

§ For a more 'realistic' case solve for a compressible viscous fluid ( $\rho$ ,  $\alpha$ ,  $\eta$  are depth dependent), with complex rheology, chemical heterogeneities

# Purely basally heated convection

**Temperature profile** : Temperature variations are confined to two thermal boundary layers (TBL), whose thicknesses and temperature drop are identical. Temperature in the convective fluid is adiabatic.

**Instabilities** : develop from the bottom TBL (hot rising plumes) and from the top TBL (cold downwellings)



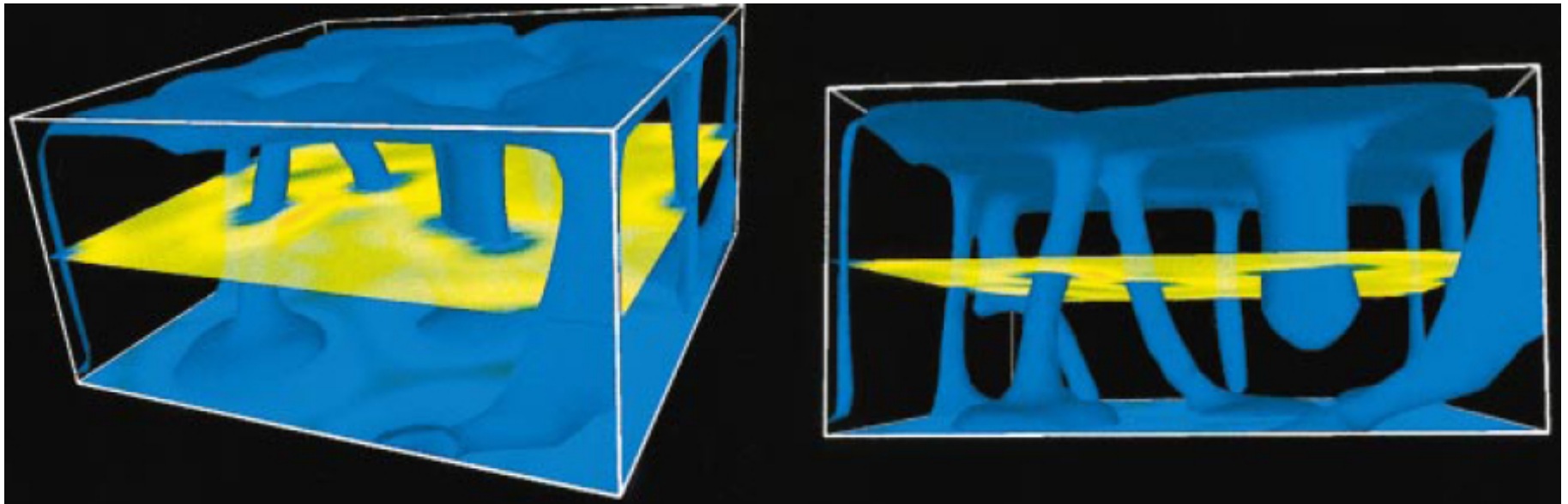
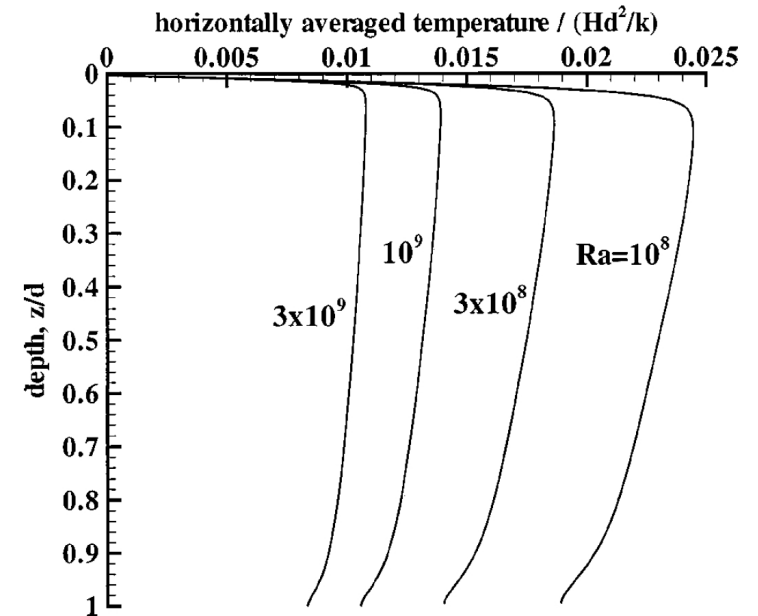
## Rayleigh-Bénard convection:

> $Ra$  leads to a chaotic state of convection, highly time-dependent

# Purely internally heated convection due to radiogenic heating from U, Th, K

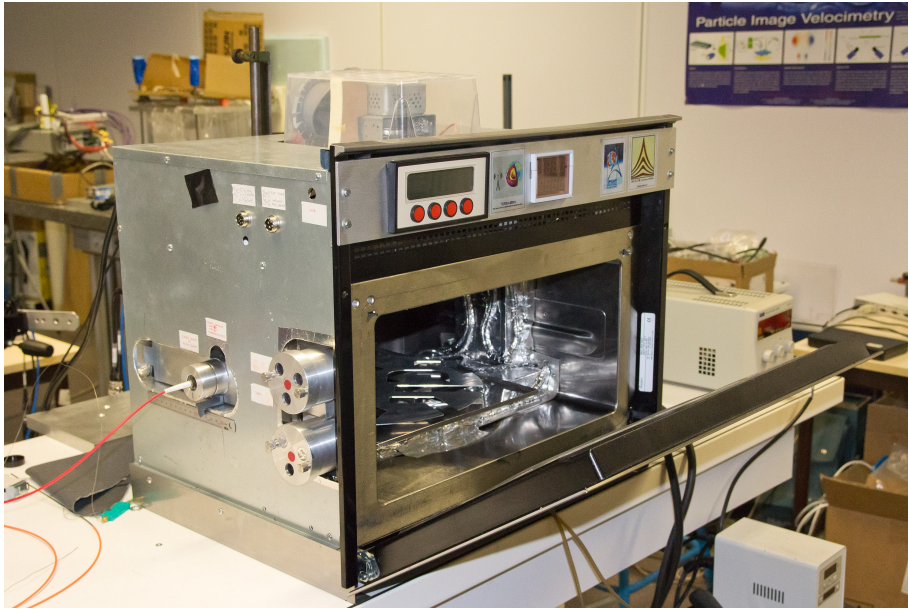
**Temperature profile:** Only a cold, top TBL. The average temperature has a subadiabatic gradient (Parmentier et al., 1994).

**Instabilities:** Develop only from the cold, top TBL. Mantle fluid is rising passively, i.e., without being pushed up by a positive buoyancy

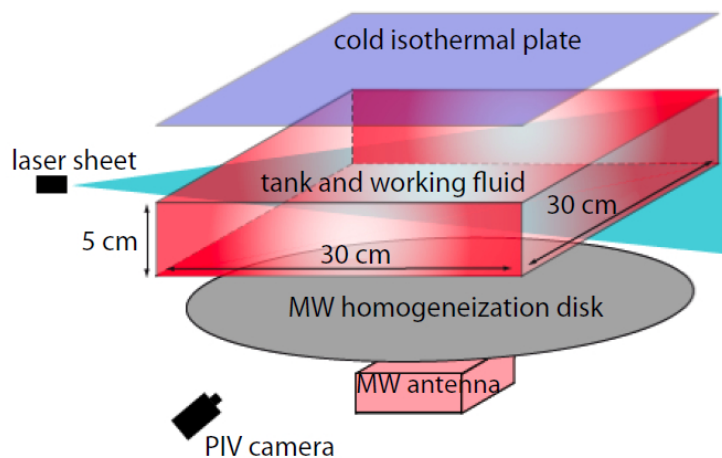


*Simulations by Parmentier & Sotin, 2000*

# Purely internally heated convection with laboratory experiments ? YES, we can !



[Limare et al., 2013]

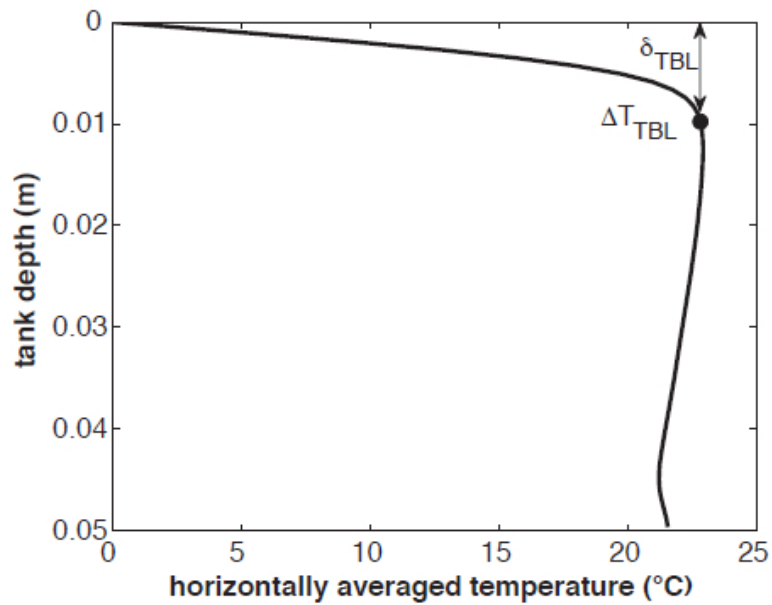
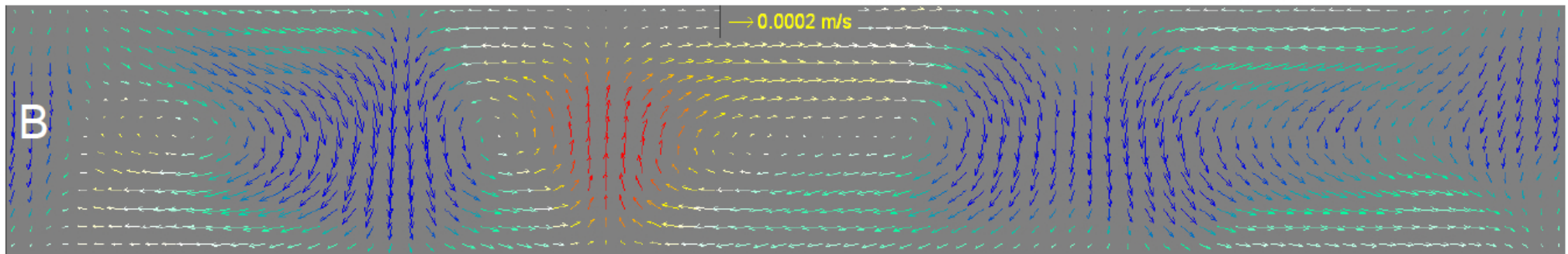
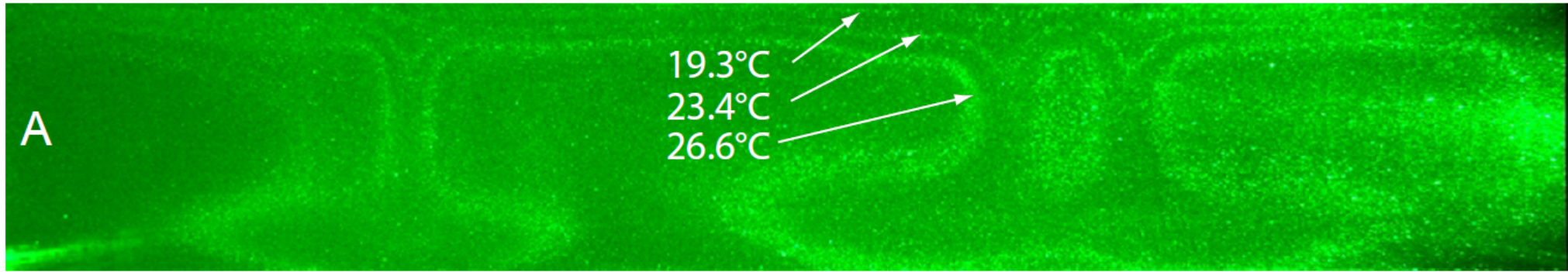


## A challenge :

Uniformly heat 4.5 liters of fluid,  
for several hours, in a microwave  
oven.

Be able to measure temperature  
and velocity field inside the  
convecting fluid (at high  $Ra_H$ )

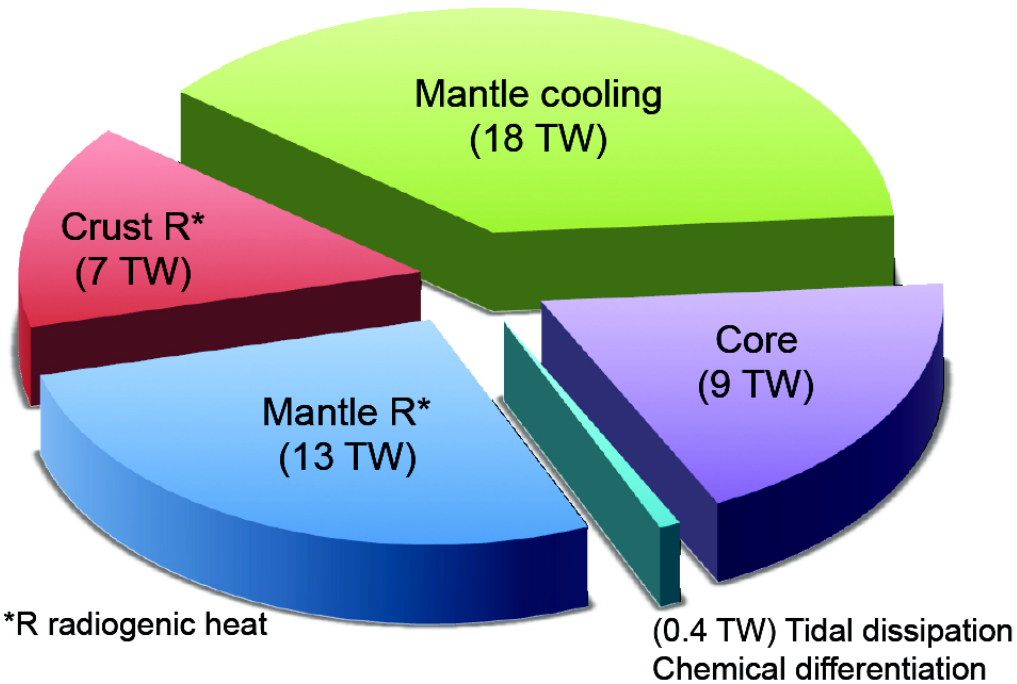
# Purely internally heated convection with laboratory experiments ? YES, we can !



(see Limare's and Kenda's posters)

**Mantle convection and radiogenic  
internal heat production....**

# Earth's surface heat flow $46 \pm 3$ ( $47 \pm 2$ )

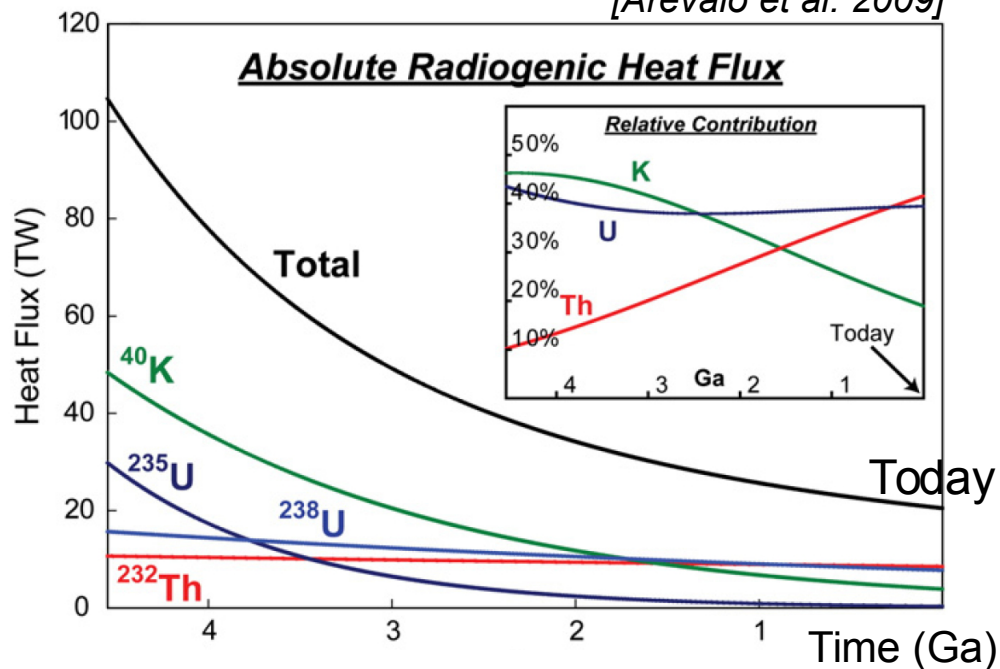


\*R radiogenic heat

(0.4 TW) Tidal dissipation  
Chemical differentiation

after Jaupart et al 2008 Treatise of Geophysics

[Arevalo et al. 2009]



**Present day radiogenic heat flow (TW)**  
13 from the mantle+7 from the crust= 20

$$\text{Urey ratio} = \frac{\text{Radiogenic Power}}{\text{Total Heat flux (46 TW)}}$$

Convective Urey ratio  $13/46=0.28$

## Silicate Earth, today

U=20 ppb, Th=80 ppb, K=280 ppm  
produces 20-21 TW radiogenic heat,  
out of which 7 TW from the crust.

**The Depleted Mantle (DMM), today**  
U=5 ppb, Th=20 ppb, K=100 ppm  
produces only 5 TW. Do we need an  
"enriched reservoir" to arrive at 13TW  
in the mantle?



# A hidden mantle reservoir, enriched in radiogenic elements (and possibly in primordial gases, such as $^3\text{He}$ )

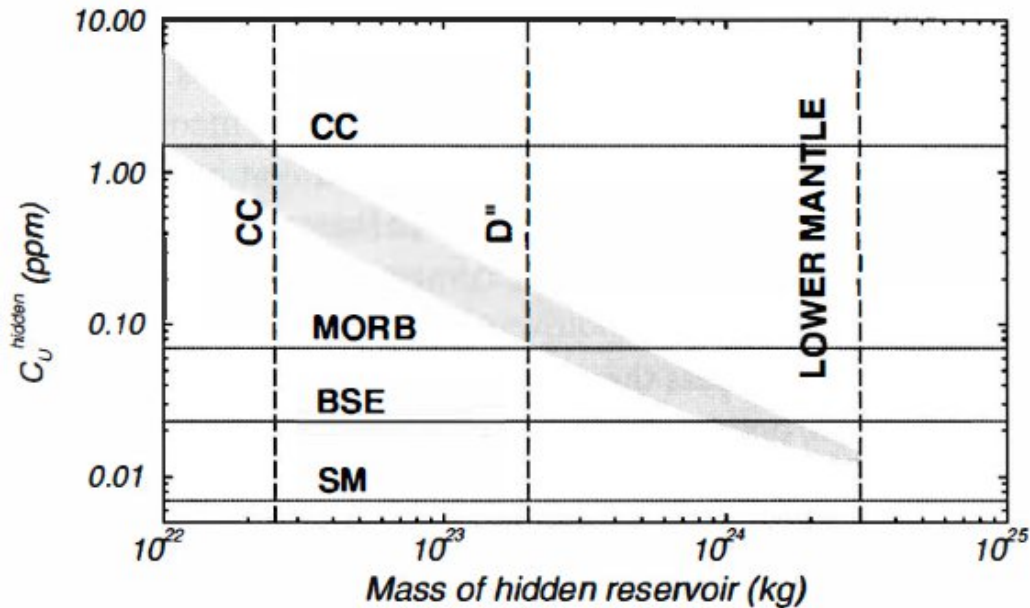
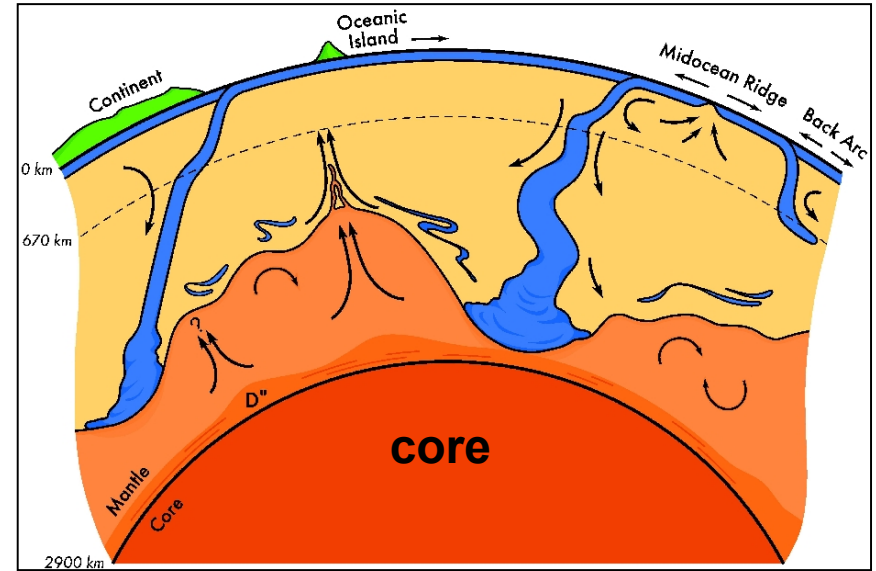


**Figure 1.** The possible concentrations of two lithophile incompatible elements (top uranium, bottom aluminum) in the hidden reservoir as a function of mass of this reservoir are indicated by shadowed areas. To account for the abundance of the incompatible elements in the bulk silicate Earth (BSE), the continental crust (CC) and the shallow mantle (SM) are not enough. A hidden reservoir is necessary with a lithophile incompatible concentration larger than in the shallow mantle. This reservoir could have a rather small volume (like that of  $D''$ ) but be very rich in incompatible elements (with concentrations somewhat similar to that of subducted MORBs). Alterna-

[Ricard and Coltice 2007]



[Kellogg et al. 1999]

**Origin of 'primordial reservoir'**  
from magma ocean crystallization  
from overturn of an early crust  
?

# A hidden mantle reservoir, enriched in radiogenic elements (and possibly in primordial gases, such as $^3\text{He}$ )

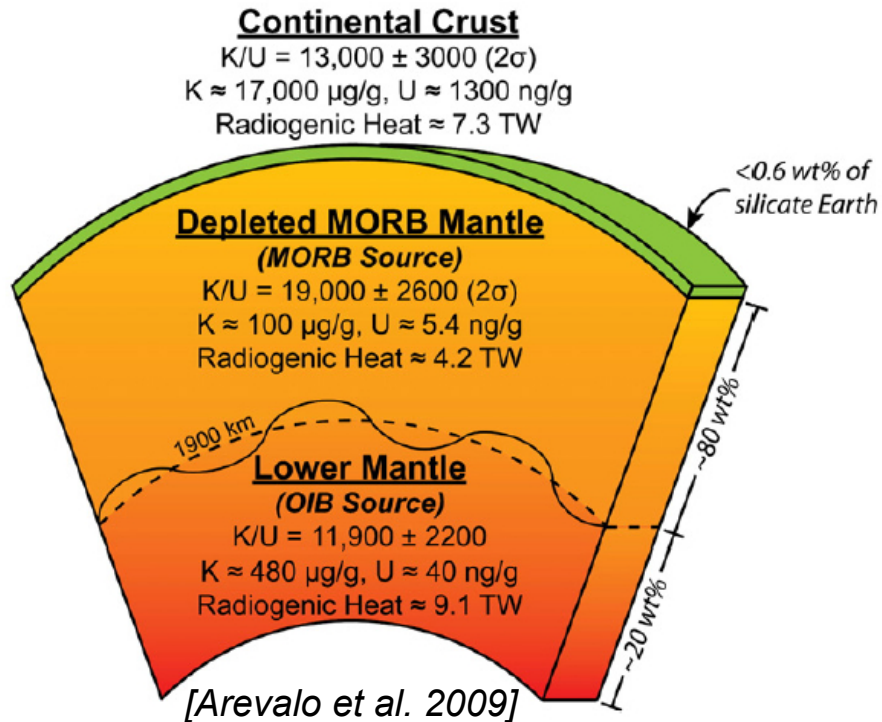
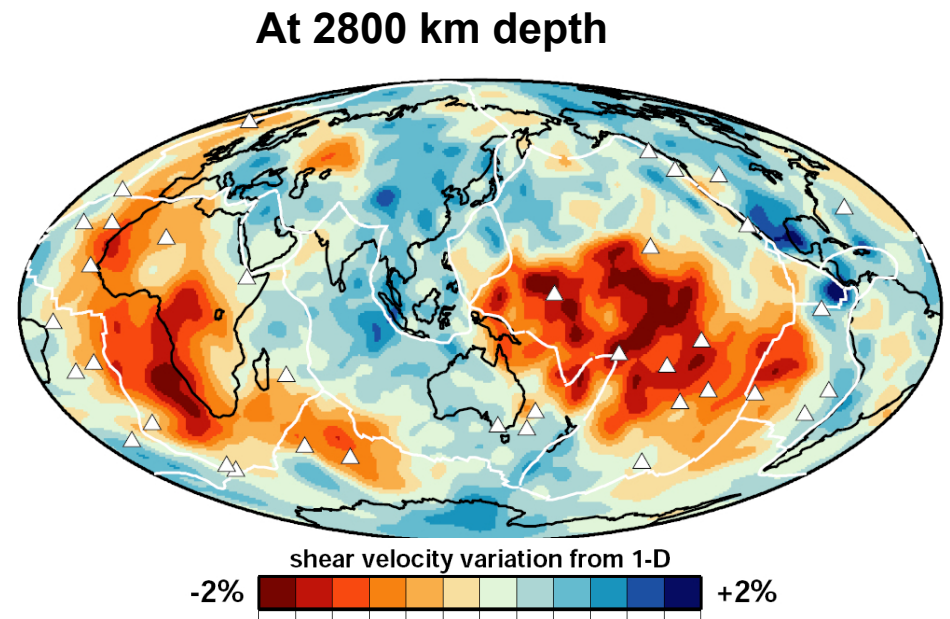


Fig. 7. Composition of and radiogenic heat flow from the continental crust, DMM and OIB source. The estimates of K and U in the continental crust do not take into account the role of the continental lithosphere, though its contribution is considered negligible. The continental crust is assumed to have  $5.6 \mu\text{g/g Th}$ , following the model of Rudnick and Gao (2003), and the DMM  $16 \text{ ng/g Th}$ , following a mantle Th/U ratio of 3.0.

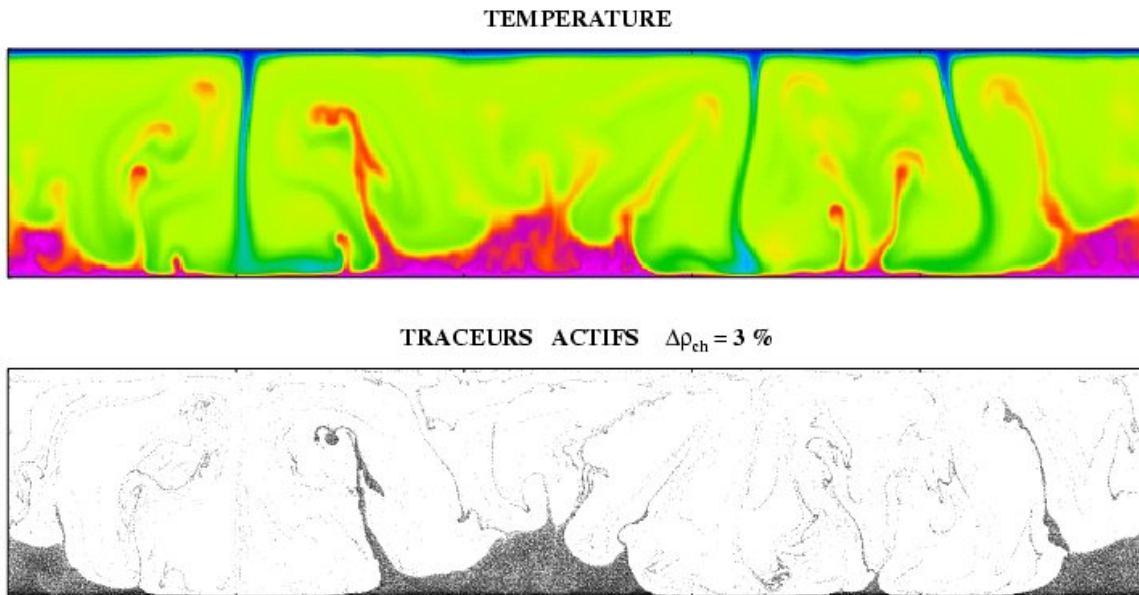
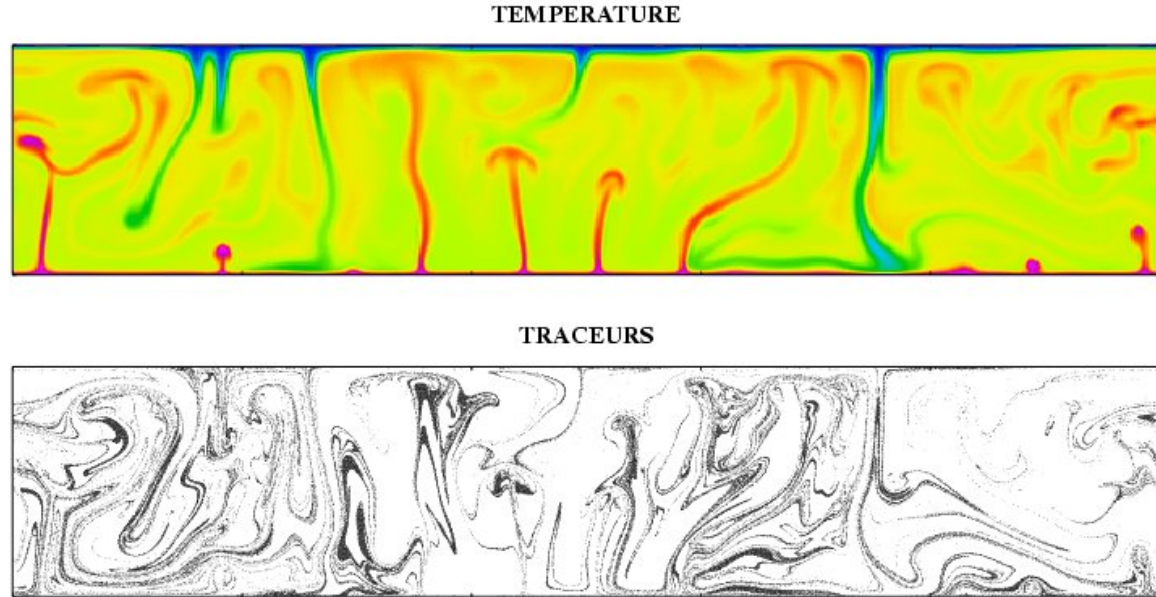
Geochemical considerations, coupled with seismic tomography of the deepest mantle, motivate us to understand the nature and the dynamics of a 'hidden' reservoir.



[Ritsema et al., GJI, 2011]

# Why do we need Thermo-chemical convection ?

A deep layer with the same density as the overlying mantle is easily swept up and 'destroyed' by mantle convection.  
(layer modelled by passive tracers)



Froid 1.00 0.25 0.50 0.75 Chaud 1.00  
Echelle de temperature

Froid 0.00 0.25 0.50 0.75 Chaud 1.00  
Echelle de temperature

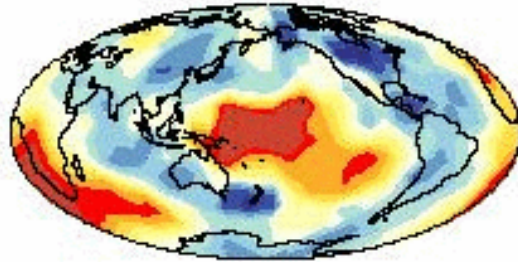
A deep layer which is compositionally denser than the overlying mantle is more stable and forms 'hot piles' of distinct material.  
(layer modelled by active tracers)

[Farnetani, 2002, animations for Palais de la Decouverte]

# Does sismology support a thermo-chemical origin ? (rather than a purely thermal origin)

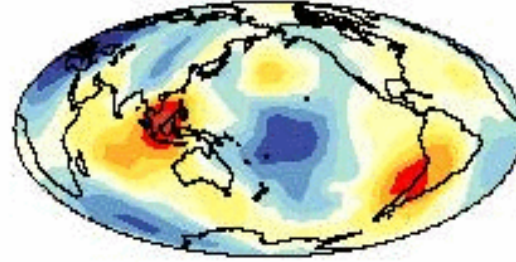
**S-wave**  
 $V_s$

2790 km



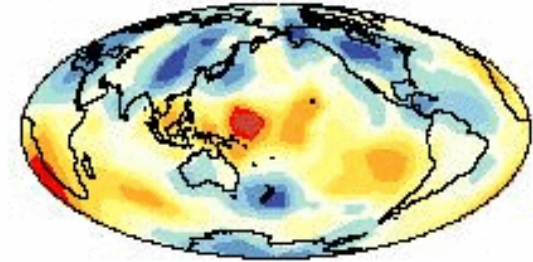
**Bulk sound speed**  
 $V_\phi = (V_p^2 - 4/3 V_s^2)^{1/2}$

2790 km



**P-wave**  
 $V_p$

2790 km

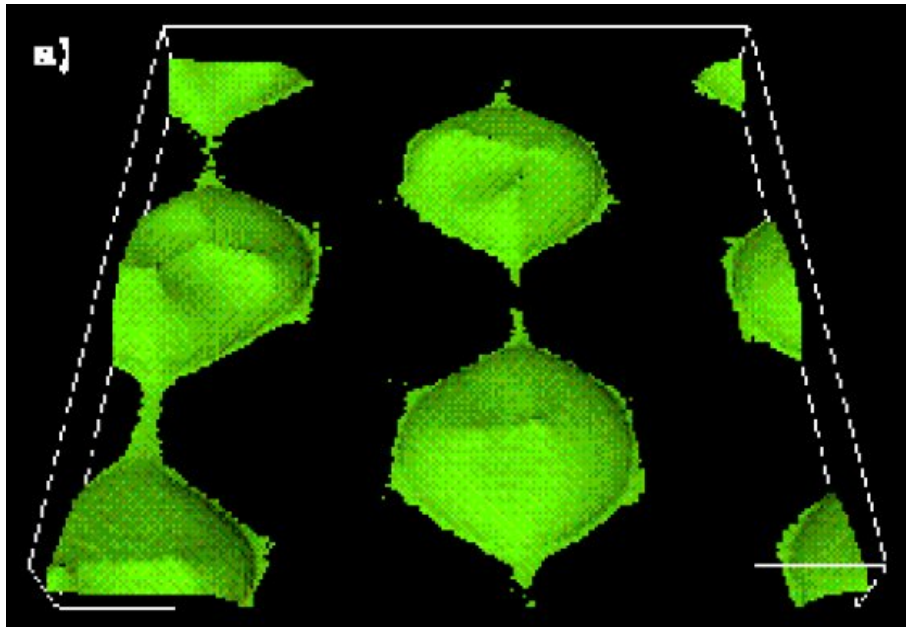
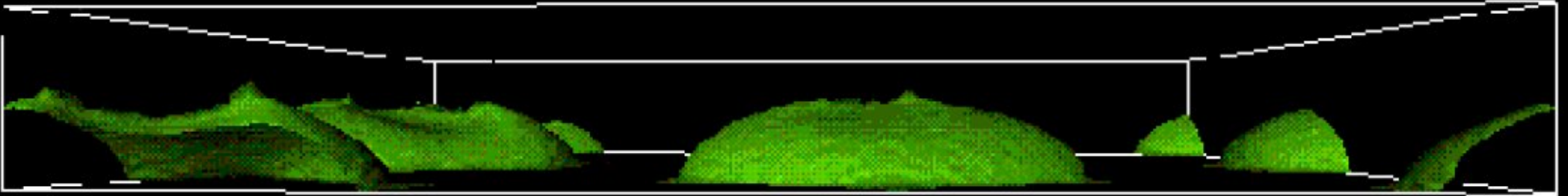


[extracted from Masters et al., 2000]

Anticorrelation between S-wave velocity anomalies and bulk sound speed anomalies suggests a chemical, rather than a purely thermal origin.

# Three-Dimensional Simulations of Mantle Convection with a Thermo-Chemical Basal Boundary Layer: D''?

Paul J. Tackley

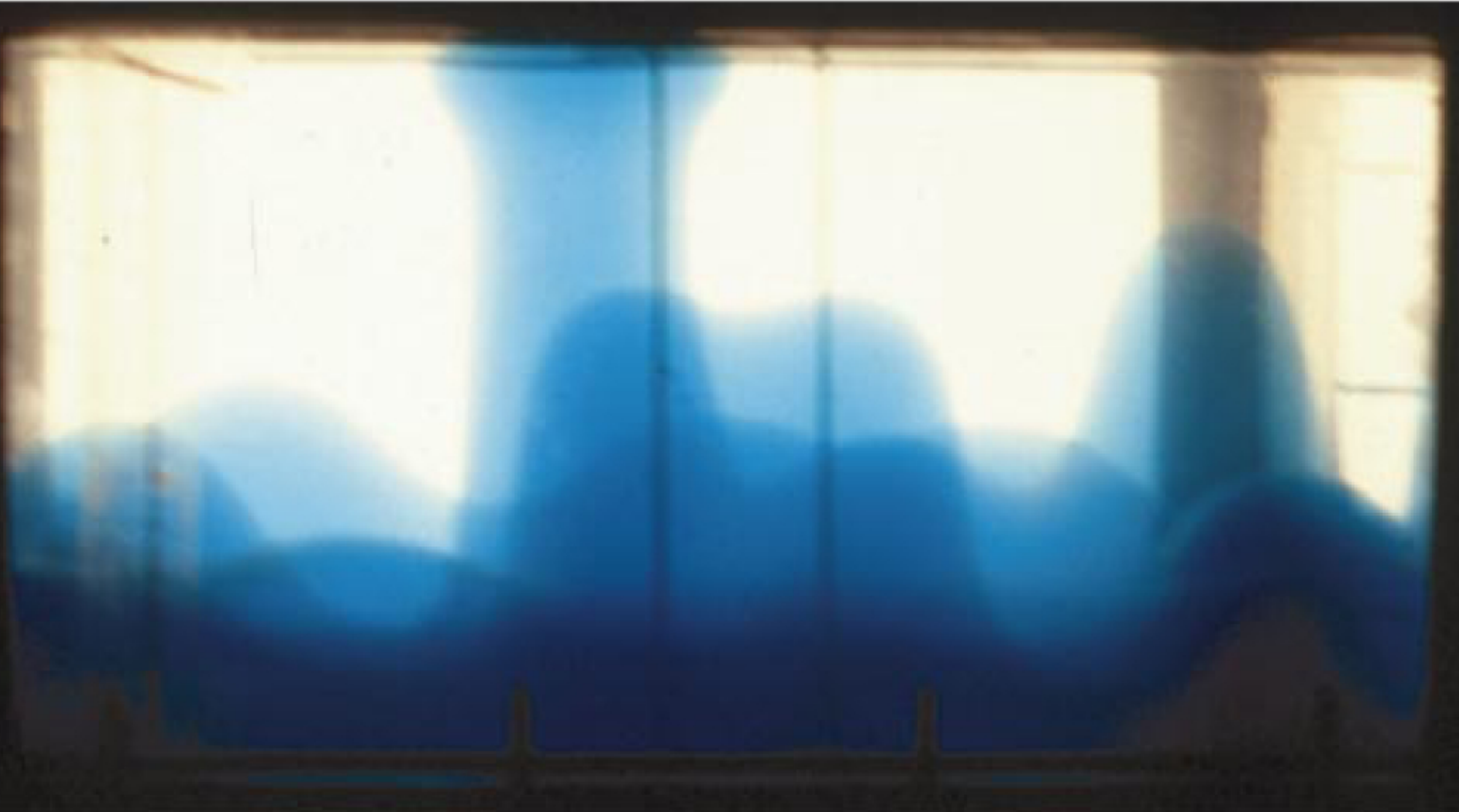


**The first numerical simulations with a compressible mantle and 'primitive' denser material show the survival of 'piles', far from downwellings.**

*[Tackley, 1998]*

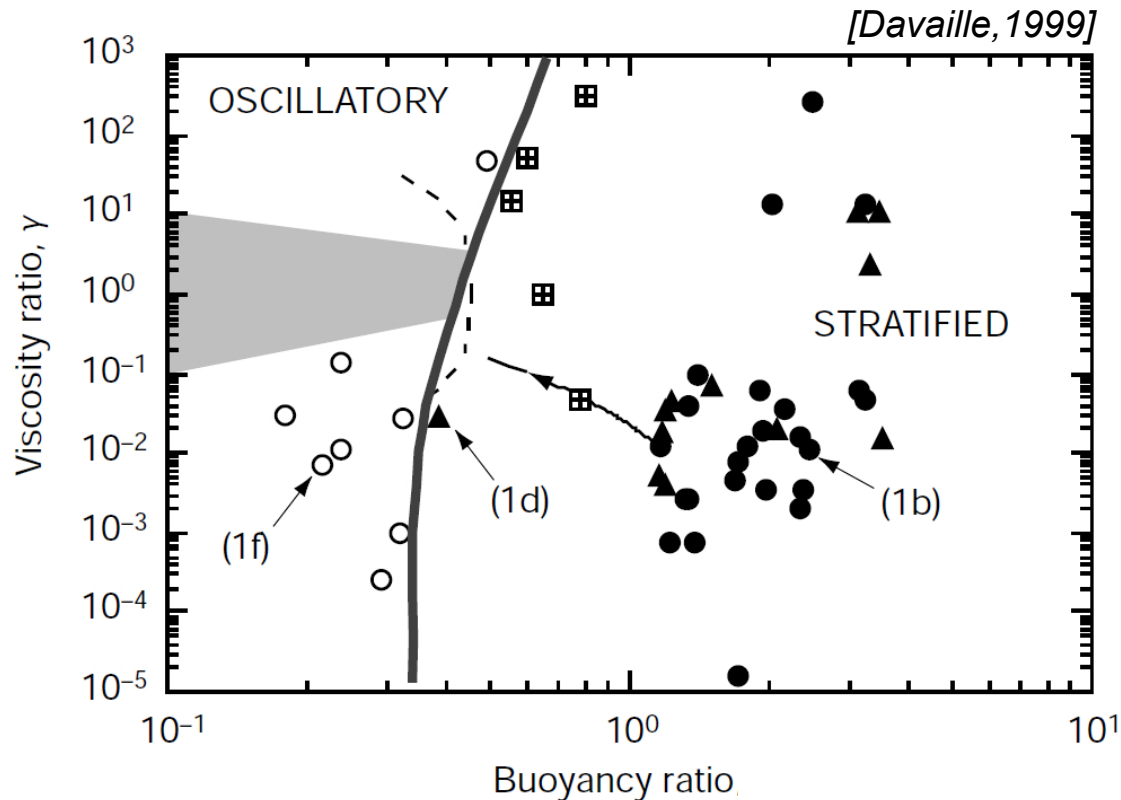
# Simultaneous generation of hotspots and superswells by convection in a heterogeneous planetary mantle

Anne Davaille



[Davaille, 1999]

# Simultaneous generation of hotspots and superswells by convection in a heterogeneous planetary mantle



Fluid dynamics laboratory experiments spanning a whole range of buoyancy ratio, viscosity ratios and thickness of the denser layer.

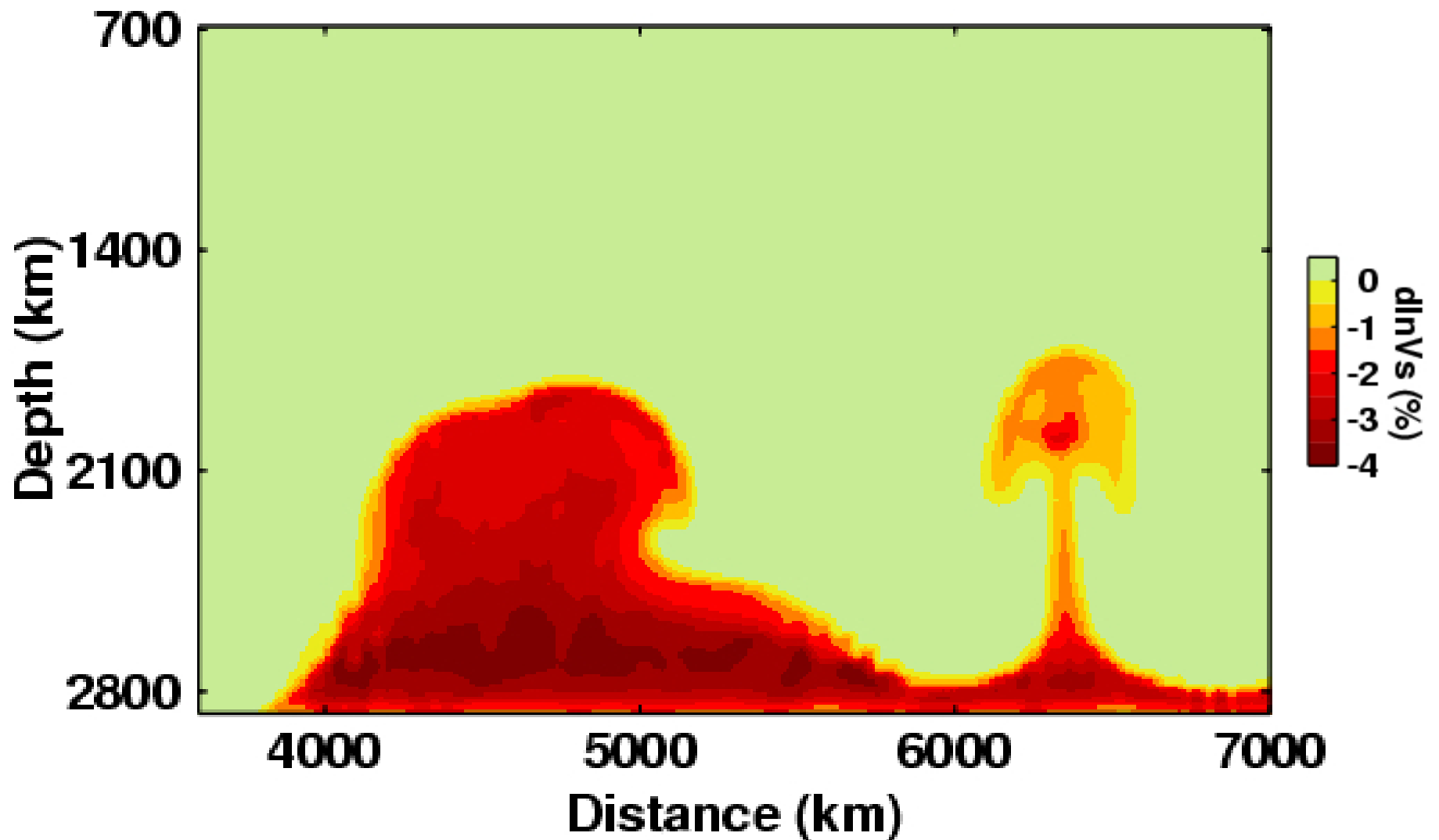
Find large, vertically oscillating domes.

$$\text{Buoyancy ratio} = \frac{\text{Stabilizing chemical density contrast}}{\text{Destabilizing thermal density contrast}}$$

$$= \frac{\Delta\rho_{ch}}{\Delta\rho_{th_s}} = \frac{\Delta\rho_{ch}}{\rho_s \alpha_s \Delta T_{sa}}$$

# Beyond the thermal plume paradigm

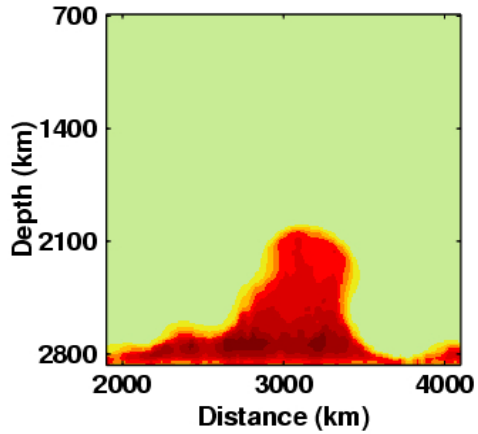
C. G. Farnetani<sup>1</sup> and H. Samuel<sup>2</sup>



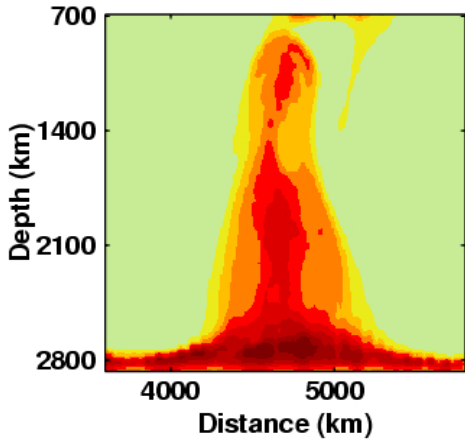
Thermo-chemical convection simulations, 3D compressible mantle.  
We find the coexistence of a great variety of plume shapes.



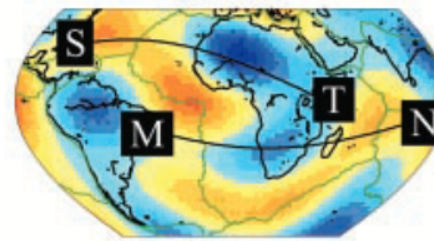
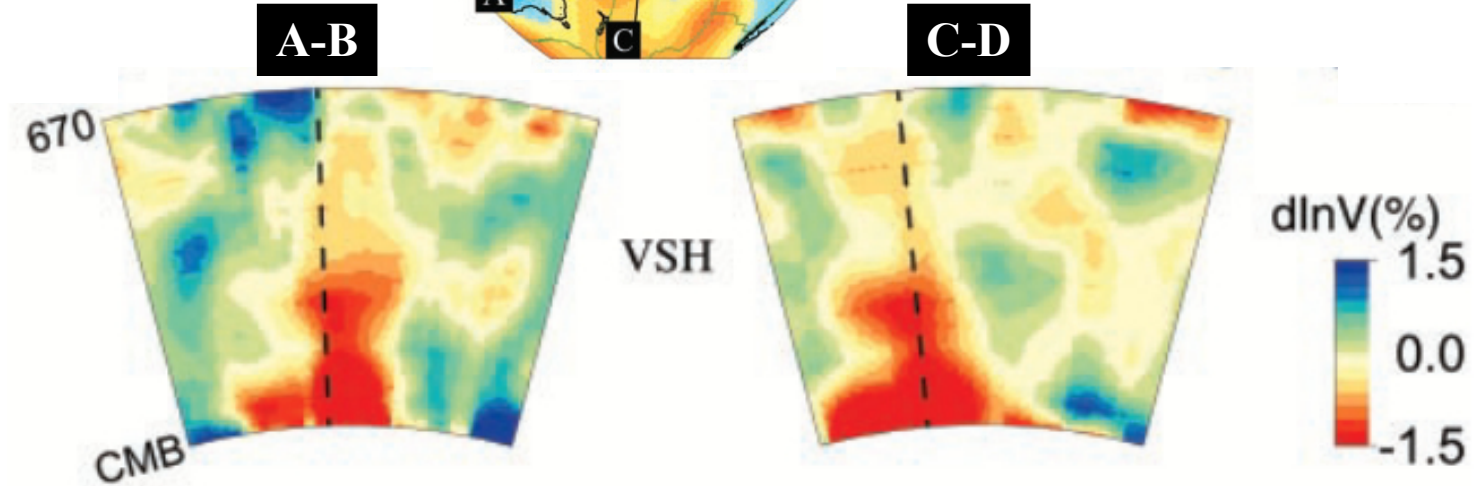
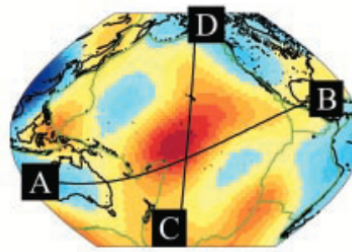
# Plume shapes in the lower mantle



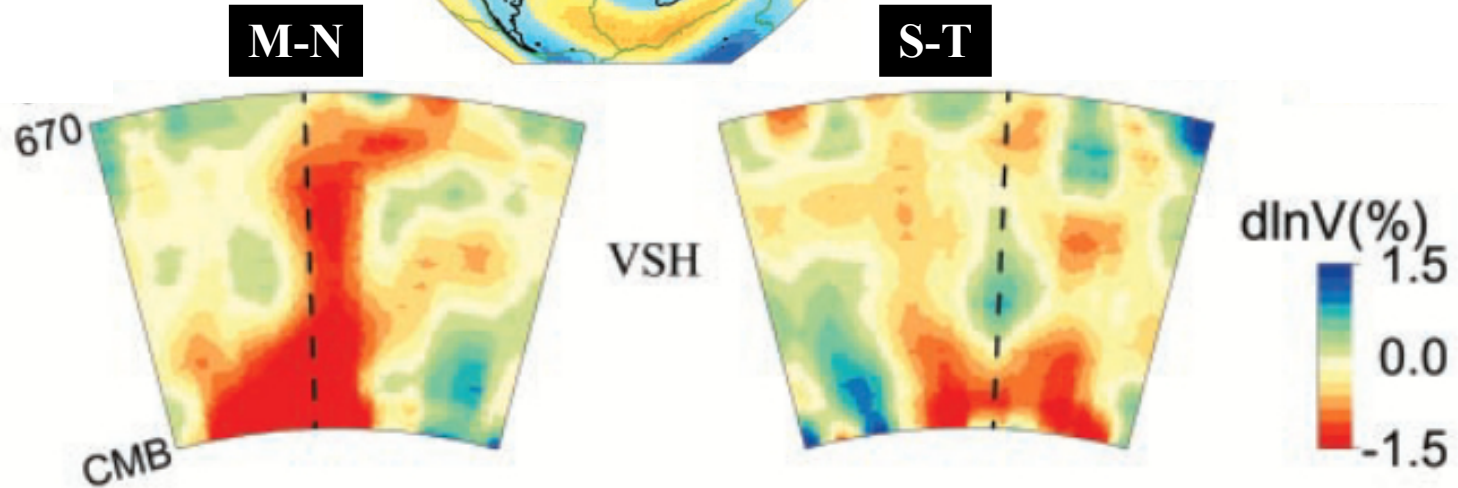
Thermo-chemical convection simulations



[Farnetani & Samuel, GRL, 2005]

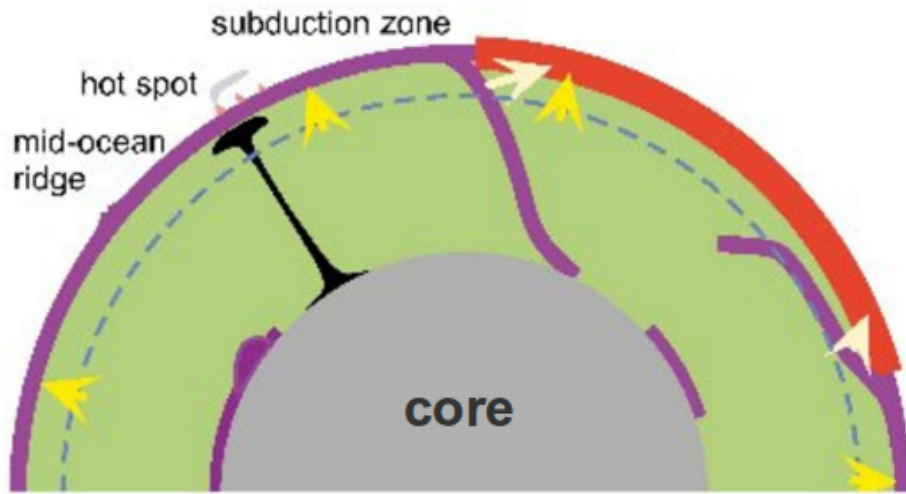


Seismic tomography across Pacific & Atlantic

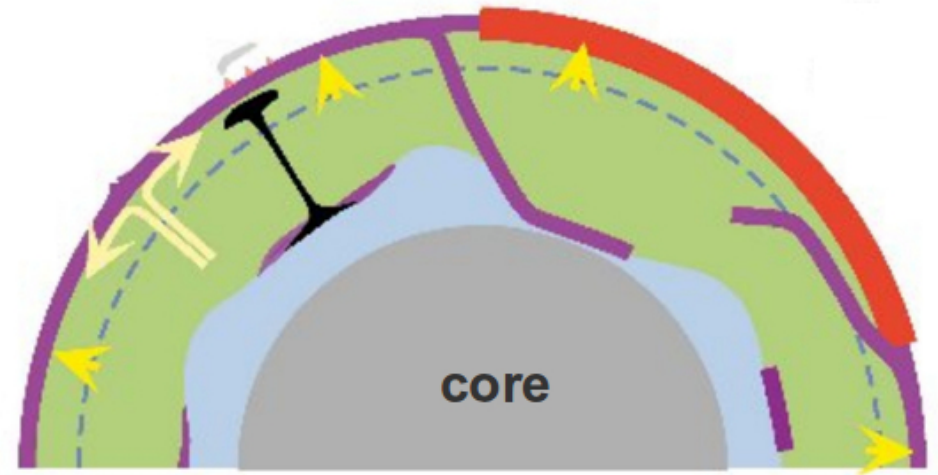


[Romanowicz & Gung, Science, 2002]

## Shift from classical view of whole mantle convection



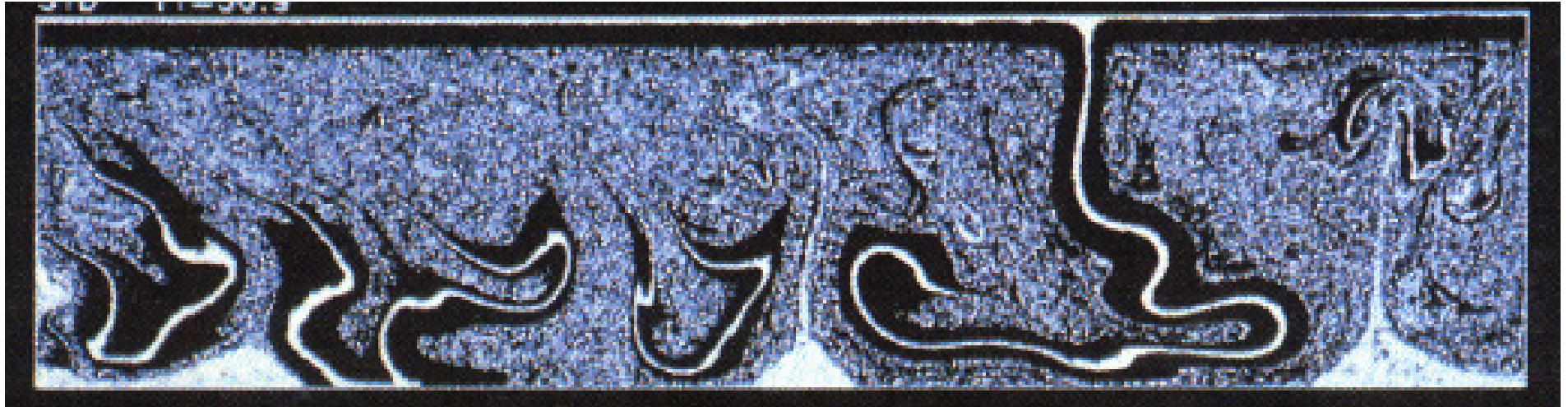
## To thermo-chemical convection with denser material in the lowermost mantle



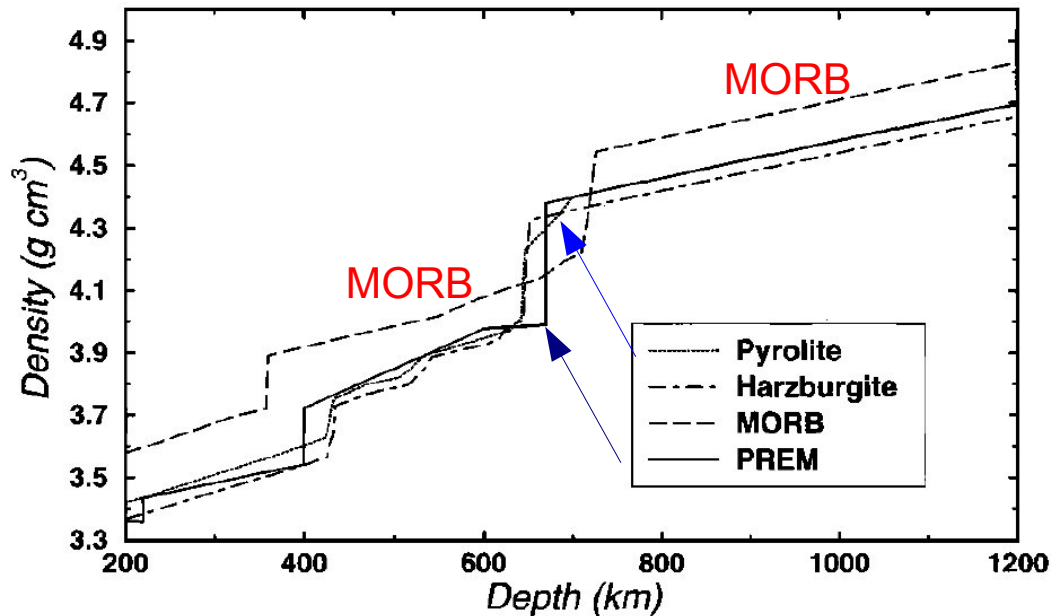
*Albarède and van der Hilst EOS 1999*

**Next : look at the role of**  
**-subducted oceanic crust**  
**-continents**

Subducted oceanic crust (MORB) becomes eclogite which is compositionally denser than the mantle



*Christensen and Hofmann [1994]*



*[Ricard and Coltice 2007, calculation by Matas, 1999]*

## Density vs. Depth

**PREM**

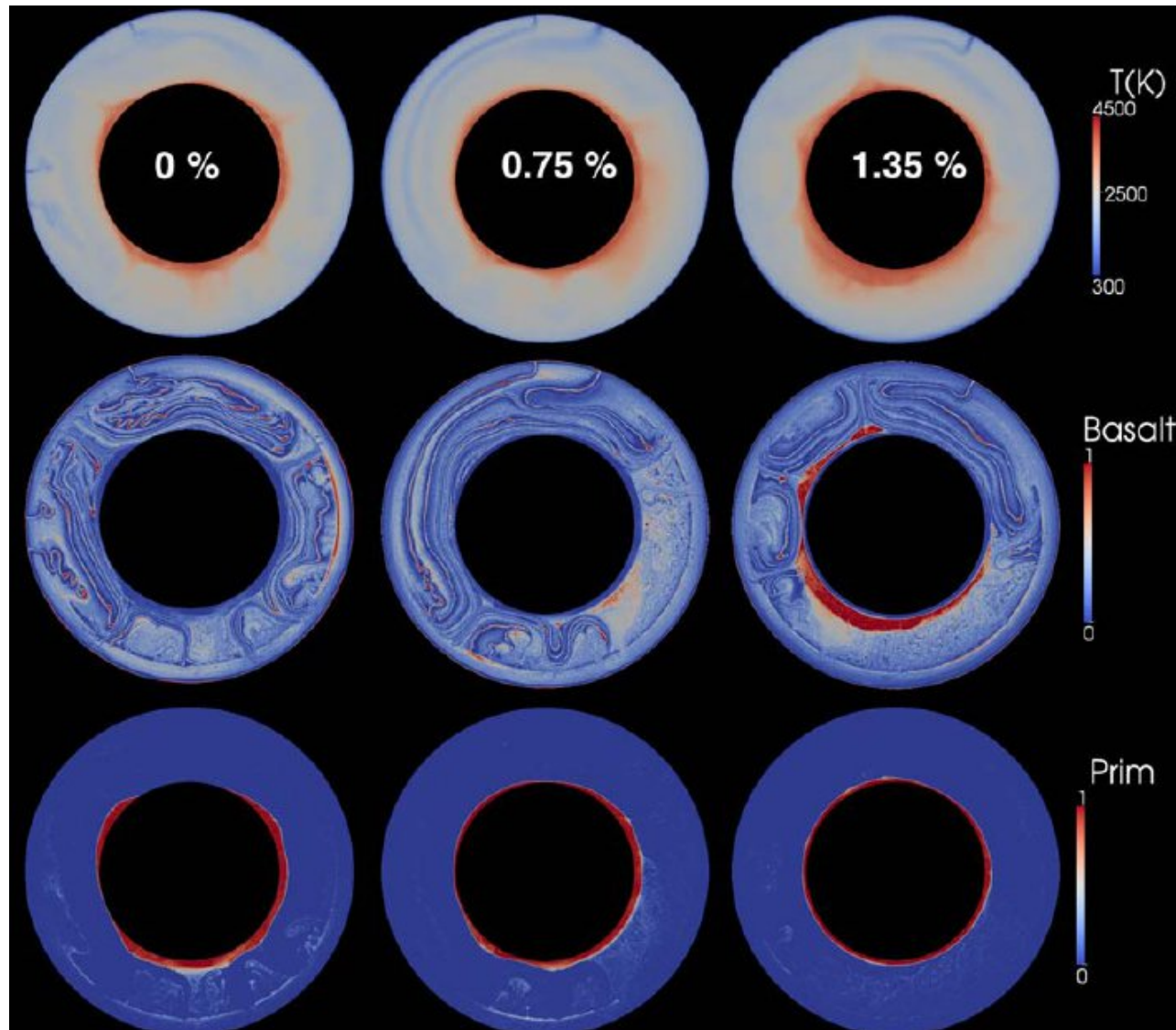
(a close fit to the pyrolite composition)

**MORB**

(subducted oceanic crust, which is ~always denser than PREM)

# Influence of combined primordial layering and recycled MORB on the coupled thermal evolution of Earth's mantle and core

Takashi Nakagawa<sup>1</sup> and Paul J. Tackley<sup>2</sup>



If there is no 'primordial layer', then the core cools too rapidly.

If the 'primordial layer' is global (i.e., covers the whole CMB) then the core cools too slowly.

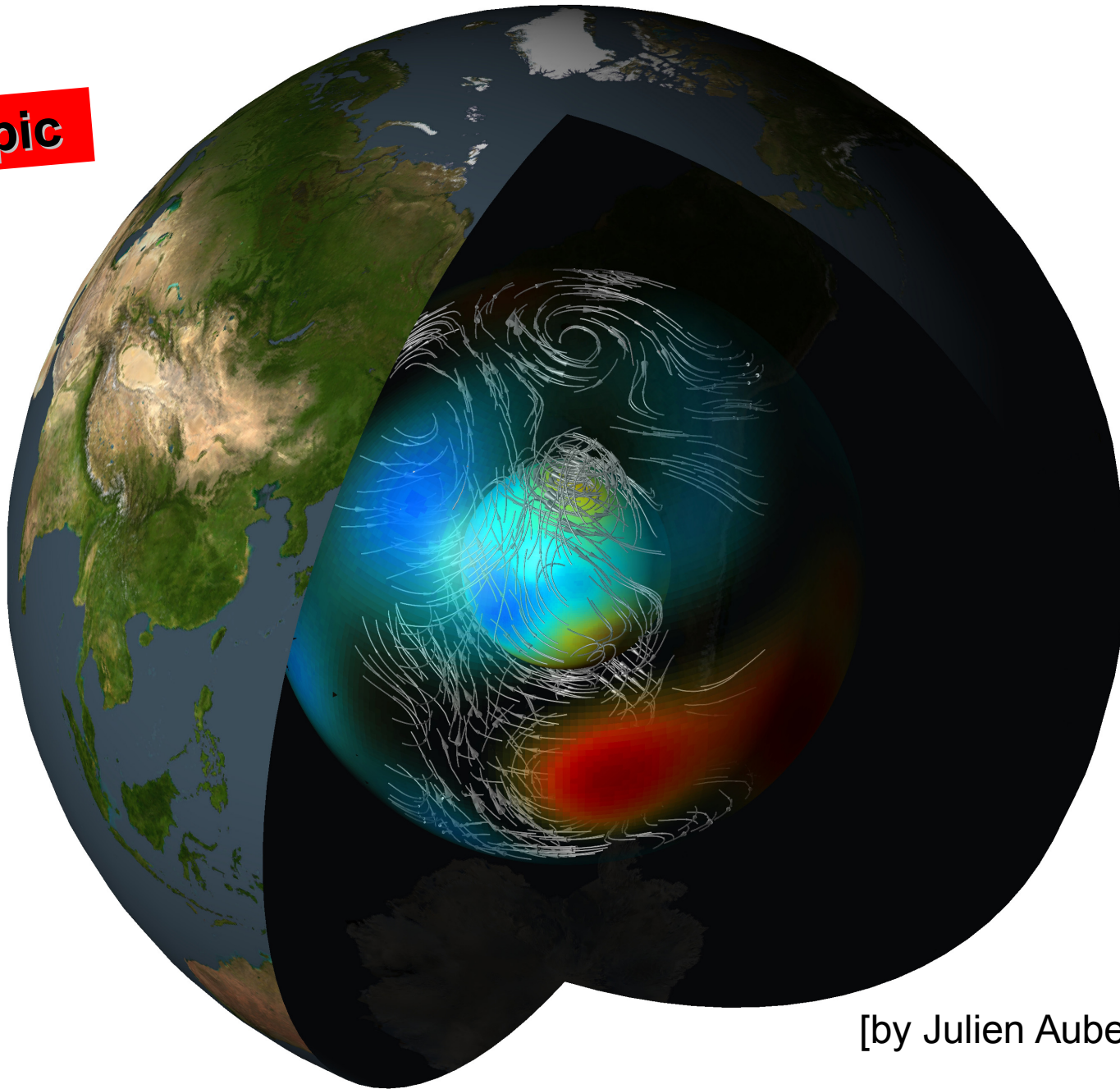
Prefer a spatially intermittent 'primordial layer'.

Predict inner core size ~1200km

**Figure 5.** (top) Thermo-chemical structures at  $t = 4.5$  Gyrs for cases with a primordial layer and three different values of deep-mantle MORB-harzburgite density difference. The primordial-MORB density difference is fixed at  $165 \text{ kg/m}^3$  (about 3% at the CMB). (bottom l

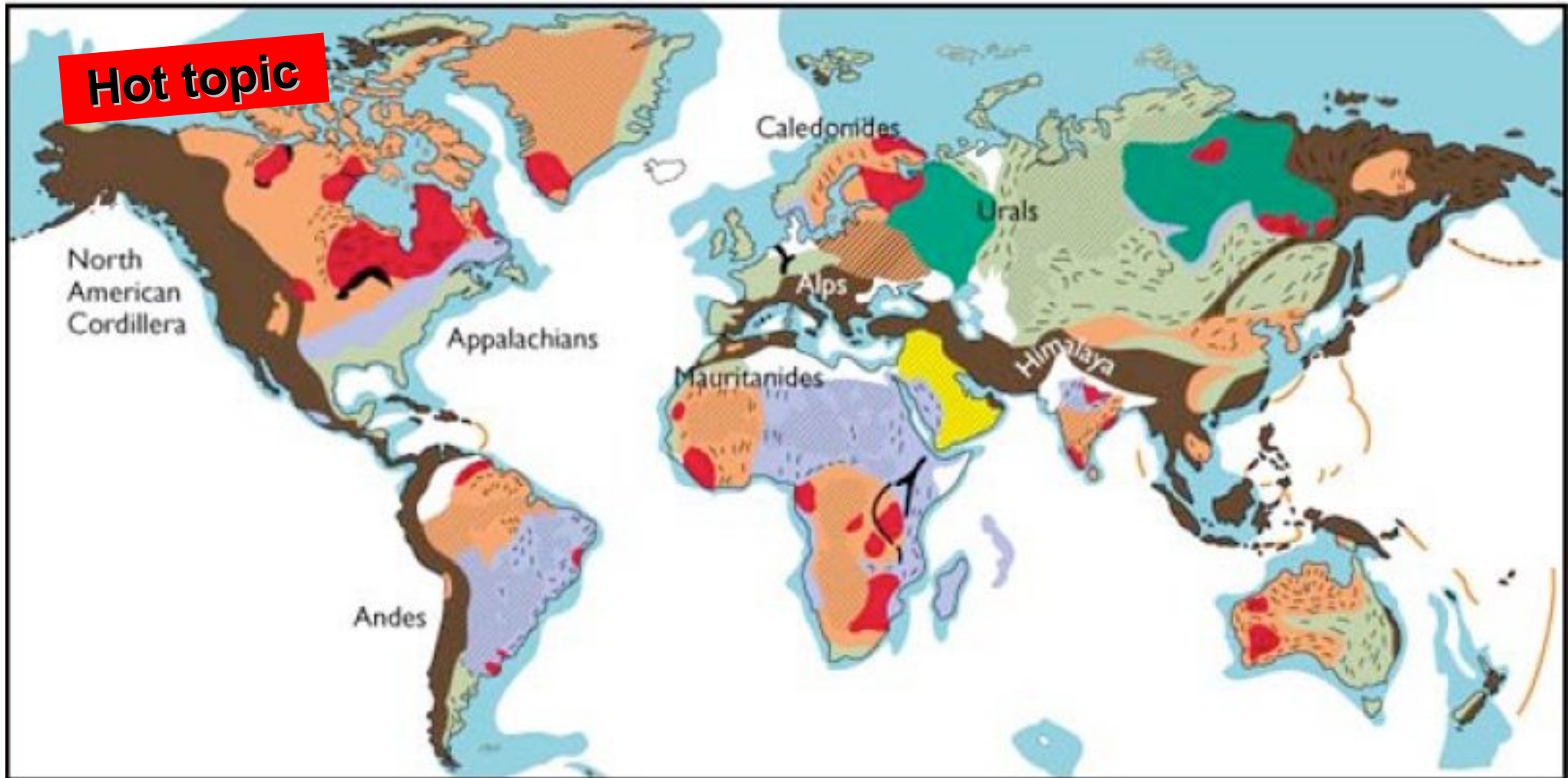
# Future Challenges : coupling between mantle convection and the thermal evolution/dynamics of the core

**Hot topic**



[by Julien Aubert]

# Mantle convection and the role of continents



Age en milliards d'années  
(En bleu = croûte continentale sous-marine)



# Planforms of self-consistently generated plates in 3D spherical geometry

H. J. van Heck<sup>1</sup> and P. J. Tackley<sup>1</sup>

**Simulations explore the effect of lithospheric yield stress (a viscosity reduction at high stress)**

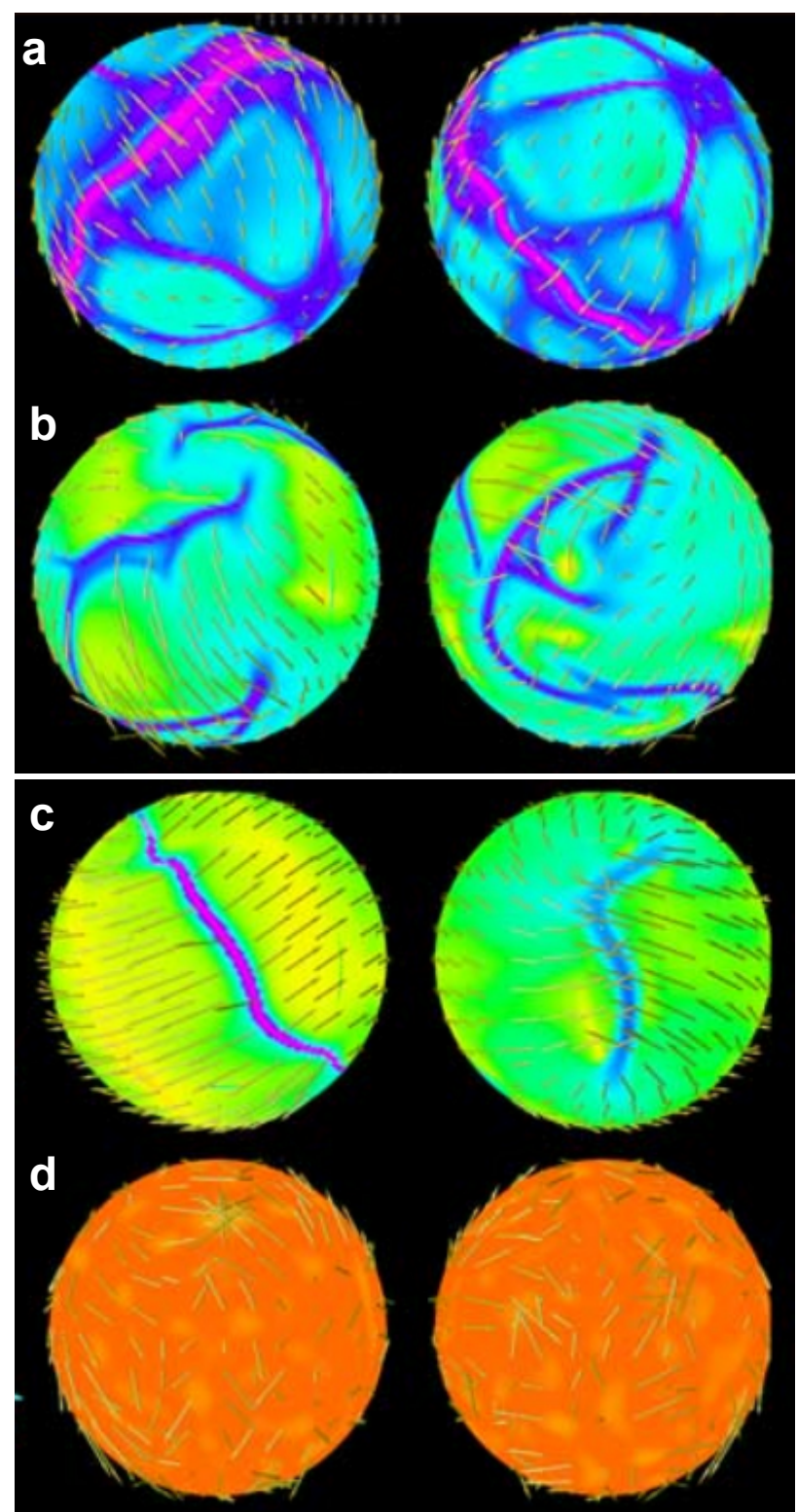
Colors indicate surface viscosity  
blue=weak zones=plate boundaries  
red =rigid zones=plate interior



**a-b : Low-intermediate yield stress**  
Spreading centers, subduction zones and oceanic plates form and are destroyed over time.

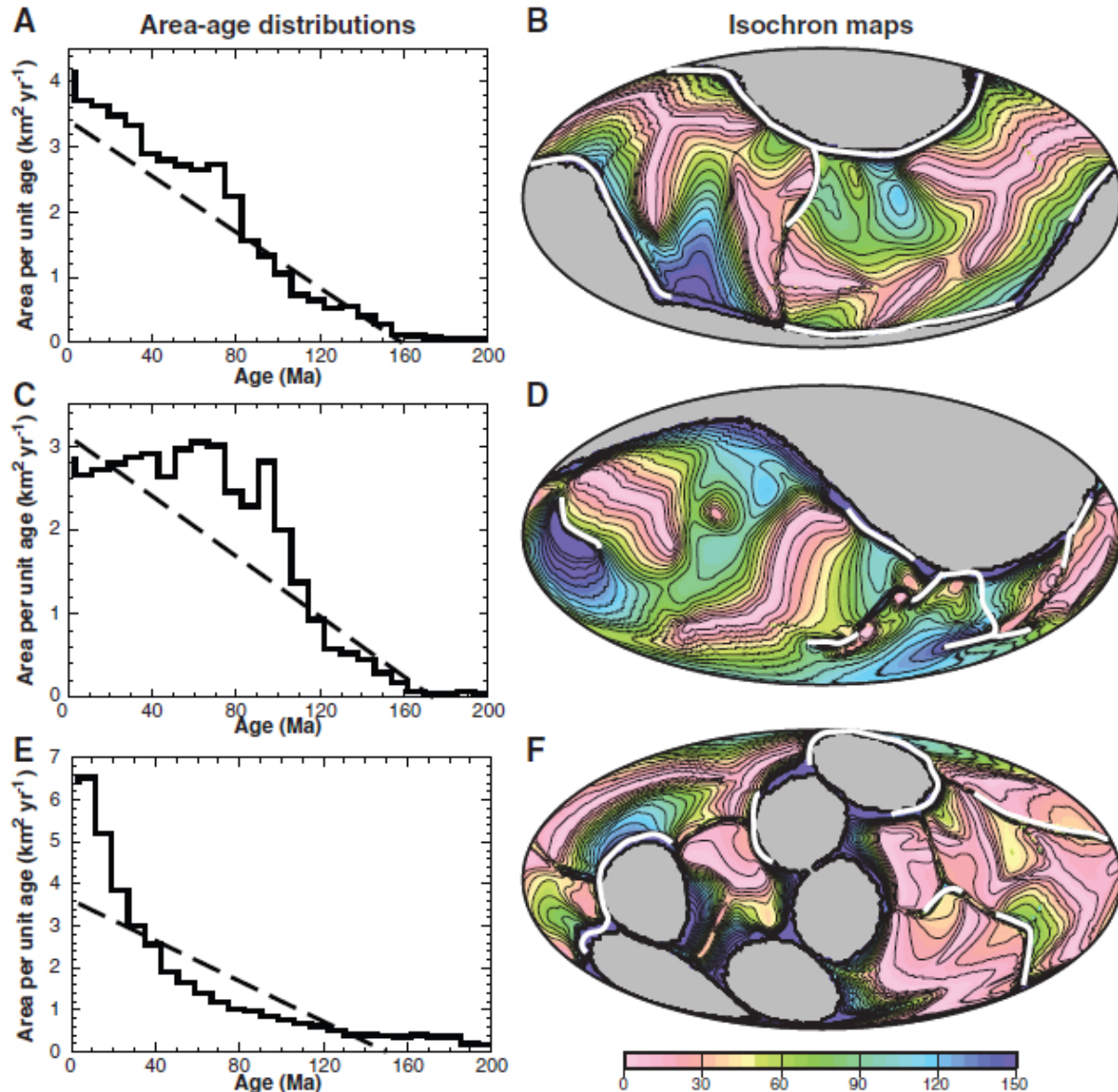
**c : High-intermediate yield stress**  
Elongated upwelling and downwelling form roughly opposite, get two hemispherical 'oceanic plates'.

**d : High yield stress**  
A rigid lid forms.



# Dynamic Causes of the Relation Between Area and Age of the Ocean Floor

N. Coltice,<sup>1,2\*</sup> T. Rolf,<sup>3</sup> P. J. Tackley,<sup>3</sup> S. Labrosse<sup>1,2</sup>



The distribution of seafloor ages is important, since it determines mantle heat loss.

Today we observe a triangular shape of seafloor area-age distribution.

It implies that young, hot oceanic lithosphere can be subducted.

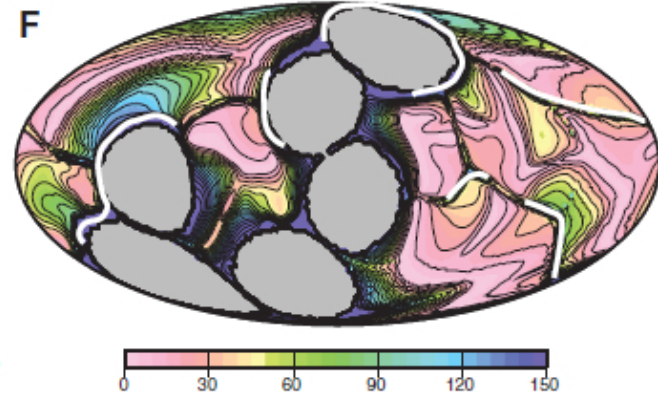
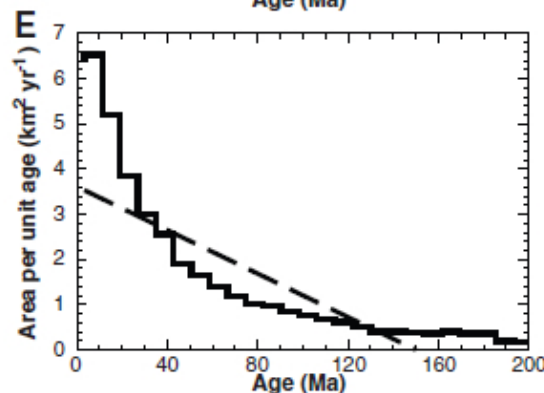
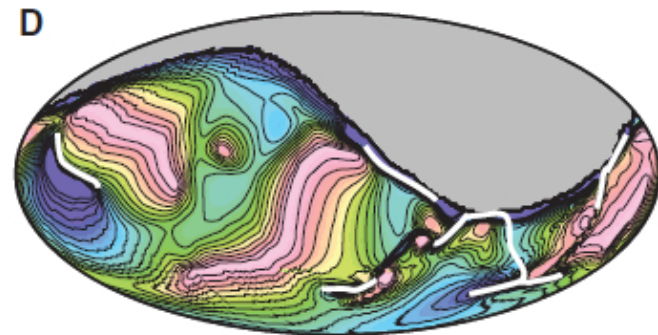
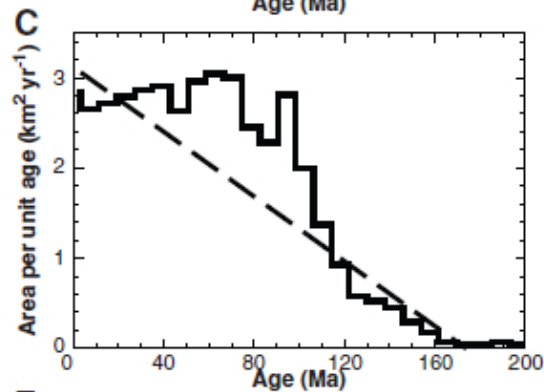
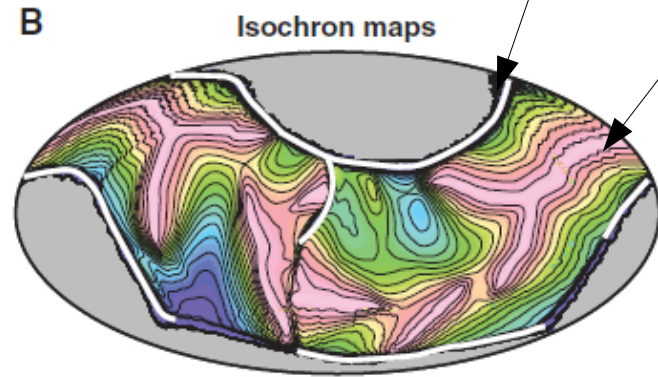
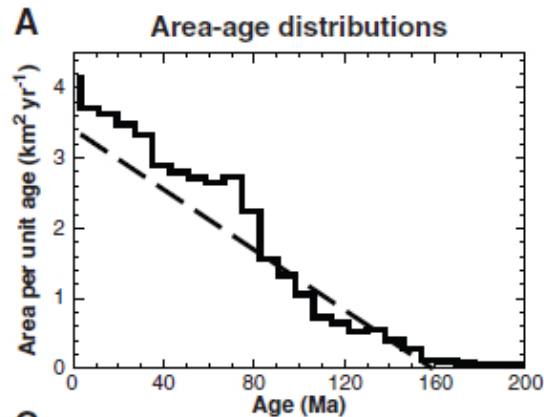
Why it so ?  
Was it so also in the past ?

Numerical simulations !



# Dynamic Causes of the Relation Between Area and Age of the Ocean Floor

N. Coltice,<sup>1,2\*</sup> T. Rolf,<sup>3</sup> P. J. Tackley,<sup>3</sup> S. Labrosse<sup>1,2</sup>



*downwelling*      *spreading ridges*

3 continents 15%+10%+5 % of the surface.

**Find:** Triangular distribution, continents impose the location of subduction

1 supercontinent : 30 % of the surface

**Find:** Flat distribution, seafloor reaches a critical buoyancy before sinking

6 small continents, each 5 % of the surface

**Find:** skewed distribution, large production of new oceanic floor

# Continents and subduction in the laboratory ?

## The initiation of subduction by crustal extension at a continental margin

F. Lévy<sup>★</sup> and C. Jaupart

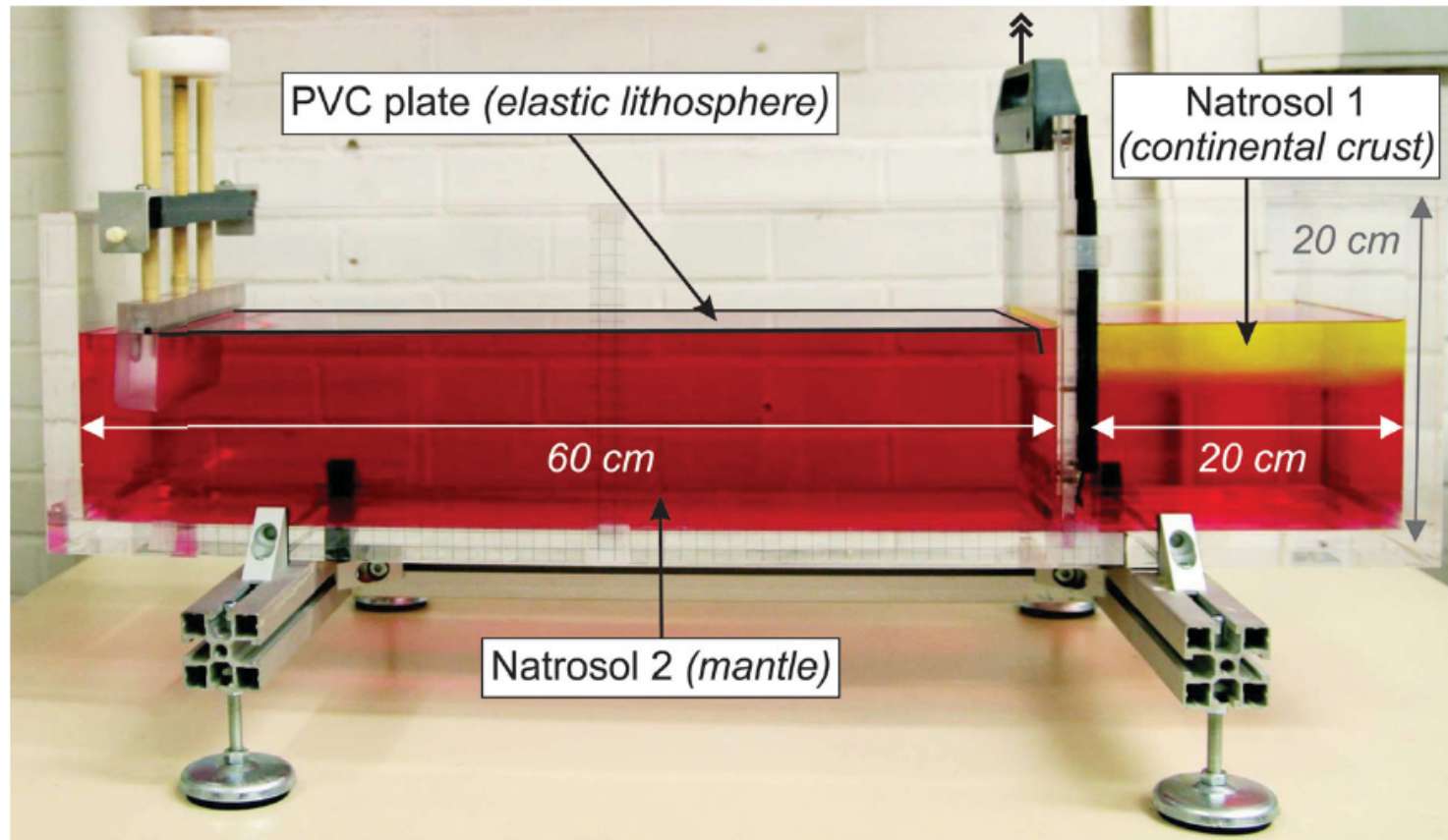
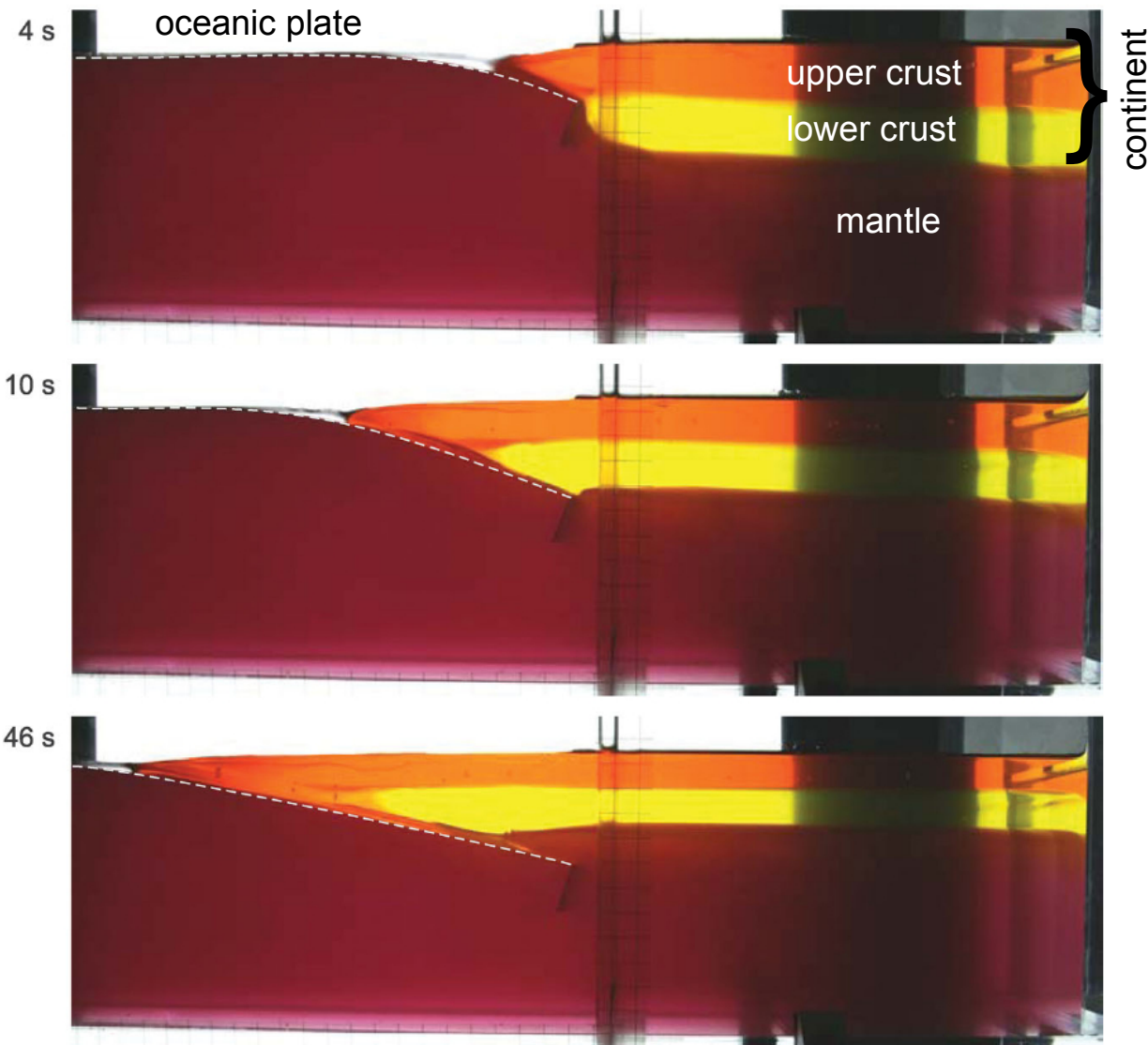


**Figure 1.** Experimental set-up for laboratory experiments. Two different working fluids with different physical properties and elastic sheets of known properties are used. In one set of experiments (Section 2.2), a slightly different set-up is used. A fixed volume of buoyant fluid is released at one end of the plate and spreads over the plate. In a second set of experiments (Section 2.3), using the set-up shown here, a lock initially separates an oceanic-like domain with an elastic plate resting on dense red fluid and a continental-like domain with buoyant viscous yellow fluid on top of the same red fluid. The lock is lifted at time  $t = 0$ , allowing the buoyant fluid to undergo extension in the continental domain and spread over the elastic plate. The tip of the plate has a thick front to prevent leakage of small amounts of buoyant yellow fluid below the plate in the first few seconds of an experiment. In nature, the oceanic plate is thick and does not allow such leakage.



Large topography contrast between continents and oceans drives the spreading of continental crust over oceanic basement.

Loading by continental crust bends the oceanic plate downwards.

Changing from a passive to an active margin does not depend only on the age of the oceanic lithosphere, BUT also on the characteristics of the continental crust

**Figure 5.** Experiment with two buoyant fluid layers mimicking upper and lower crust. Note that the lower liquid (analogous to the lower crust) does not spread over a large distance and is missing from the distal region. The fluid properties are  $\rho_{1u} = 1010 \text{ kg m}^{-3}$ ,  $\rho_{1l} = 1090 \text{ kg m}^{-3}$ ,  $\rho_2 = 1200 \text{ kg m}^{-3}$ ,  $\eta_{1u} = 11.16 \text{ Pa s}$ ,  $\eta_{1l} = 1.67 \text{ Pa s}$  and  $\eta_2 = 3.66 \text{ Pa s}$ . The plate is  $300 \mu\text{m}$  thick.

# Spreading continents kick-started plate tectonics

Patrice F. Rey<sup>1</sup>, Nicolas Coltice<sup>2,3</sup> & Nicolas Flament<sup>1</sup>

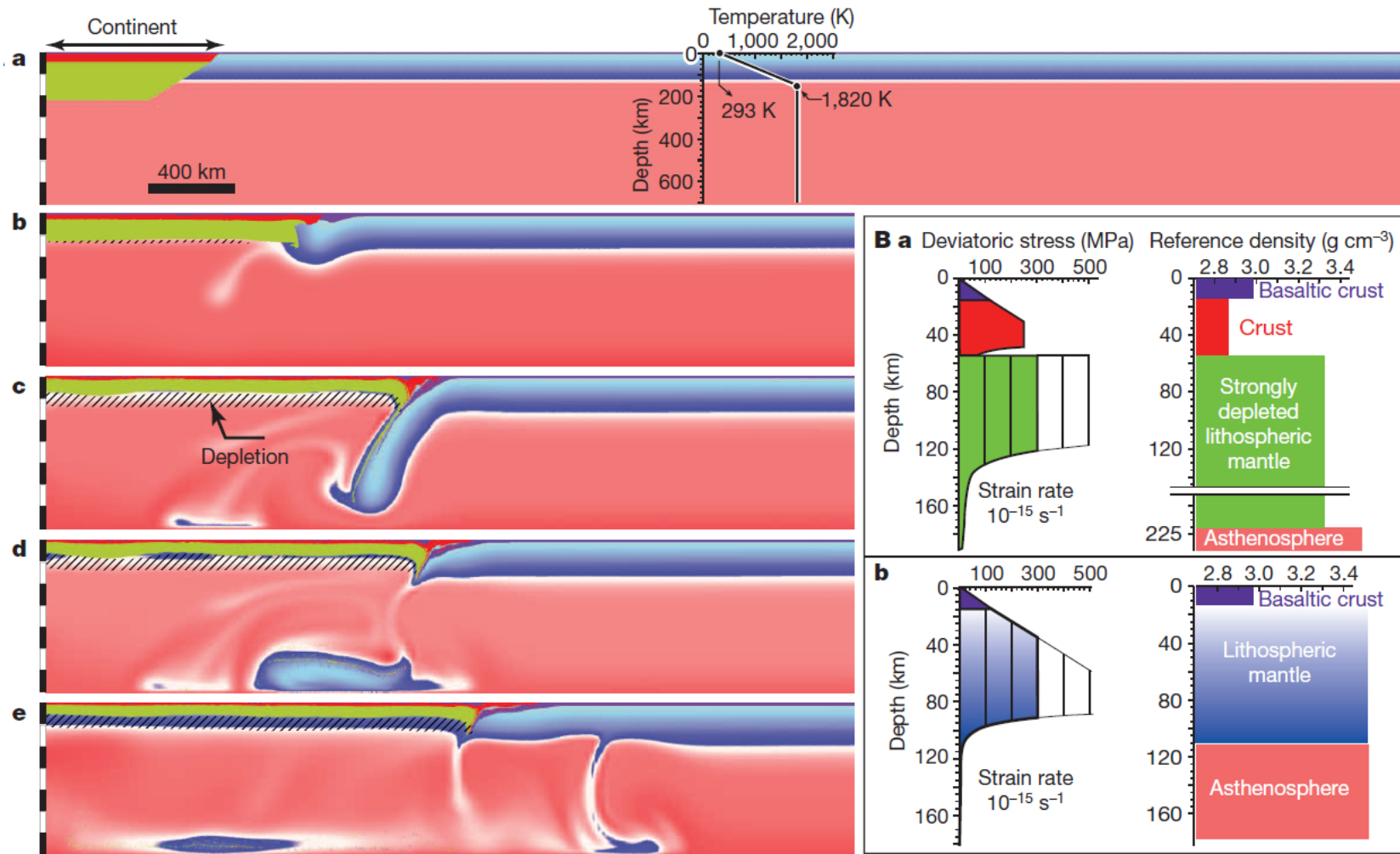


**Figure 1 | Numerical solution of an example of continent collapse leading to subduction.** A, a, Modelling setup (0 Myr). b–e, Computed snapshots for a box 700 km deep and 6,300 km long including a continent 225 km thick with a half-width of 800 km. b, 46.7 Myr; c, 55.3 Myr; d, 57.2 Myr; e, 123.8 Myr. All mantle rocks have a limiting yield stress of 300 MPa. Mantle cooler than 1,620 K is in blue (darker blue is hotter); mantle hotter than 1,620 K is in pink (darker pink is hotter). Regions of depletion due to partial melting of ambient fertile mantle are hatched. B, Compositional structure, reference densities and reference rheological profile for the continent (a) and for the adjacent

lithospheric lid (b). This numerical solution documents the long phase of slow continental spreading leading to the initiation of a slab (A, b and c). Once the slab has reached a depth of ~200 km, slab pull contributes to drive subduction, rollback and continental boudinage (A, c) (in some experiments boudinage leads to rifting) and slab detachment (A, d). In this experiment the detachment of the slab is followed by a long period of thermal relaxation and stabilization during which the thickness of the continent increases through cooling and incorporation of the moderately depleted mantle (A, e).

# Generation of continental rifts, basins, and swells by lithosphere instabilities

Loïc Fourel,<sup>1,2</sup> Laura Milelli,<sup>1,3</sup> Claude Jaupart,<sup>1</sup> and Angela Limare<sup>1</sup>

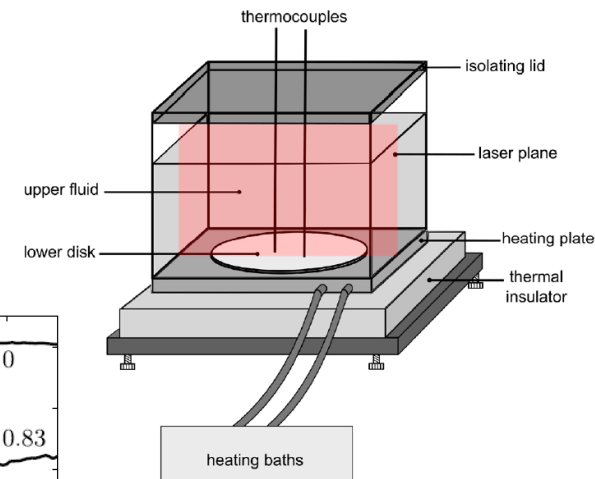
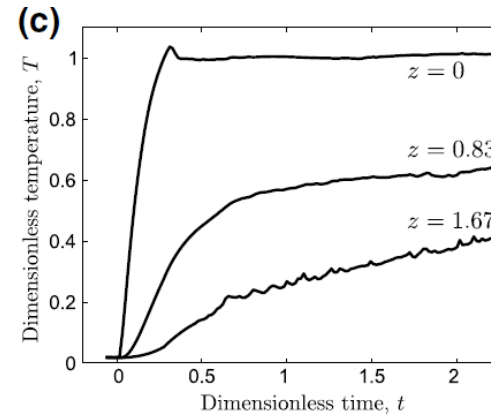
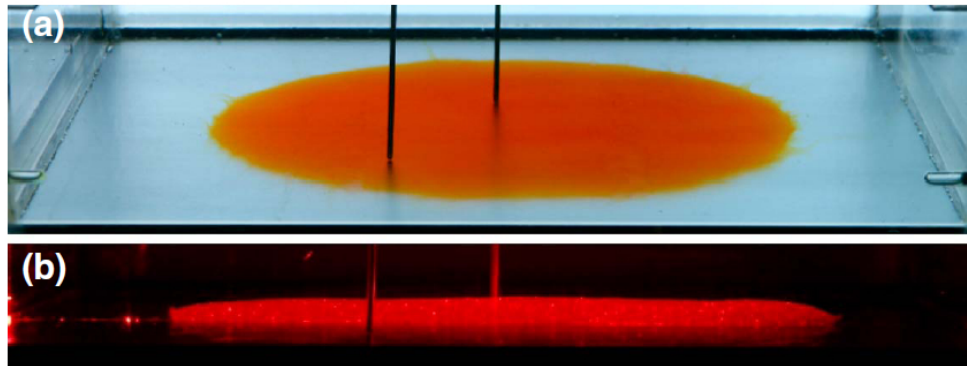


**Figure 5.** Stable experiment ASTICO 30 ( $Ra = 164$ ,  $B = 0.25$ ,  $h_d/R = 0.067$ ). (a) Photograph in normal light. Total width of view is 30 cm. (b) Laser vertical cross section. (c) Time evolution of temperatures at three different depths. Height  $z$  is scaled to the unstable block thickness. Temperature fluctuations are only significant in the ambient fluid and are due to small-scale convection.

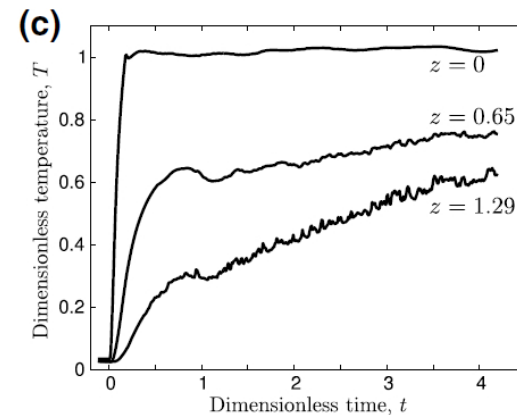
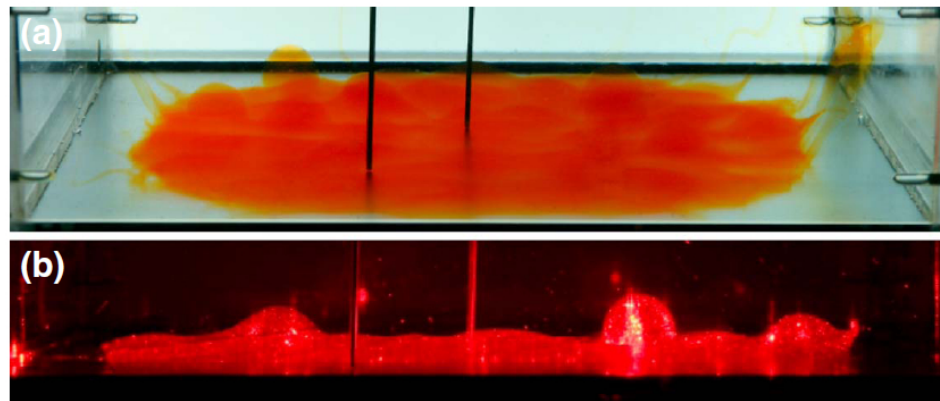
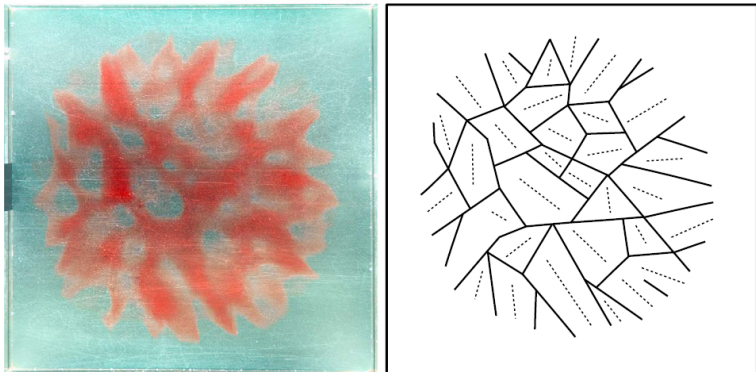
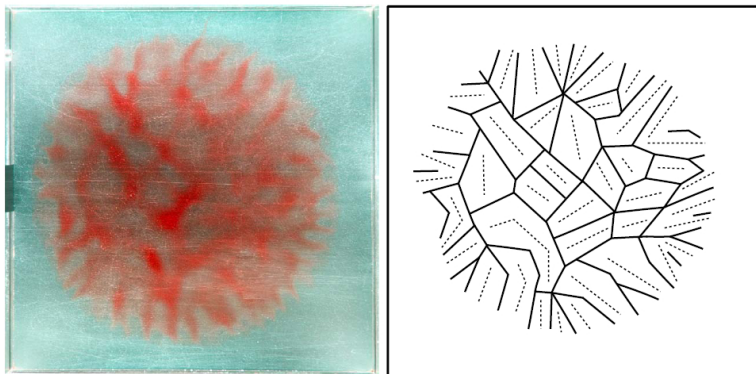
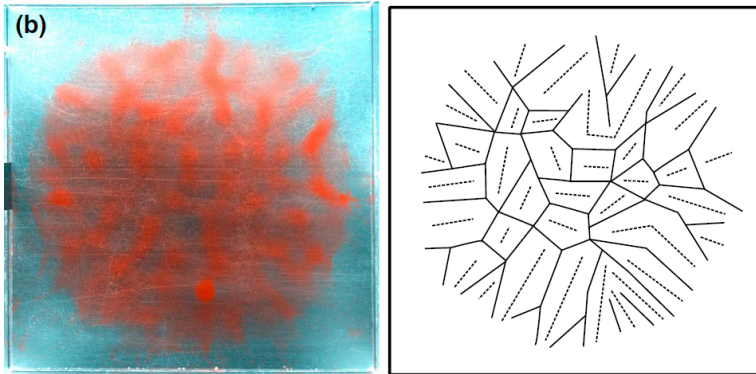
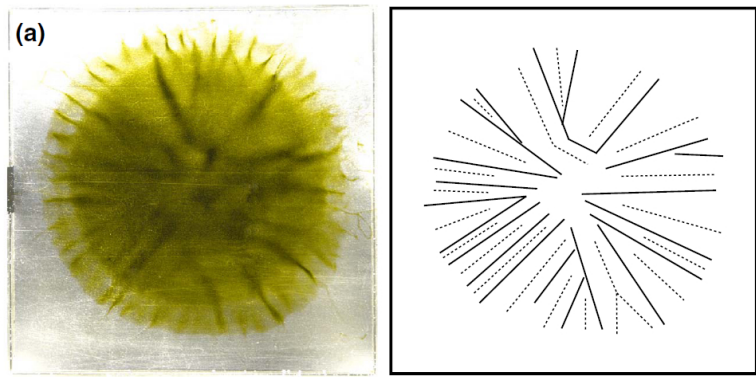
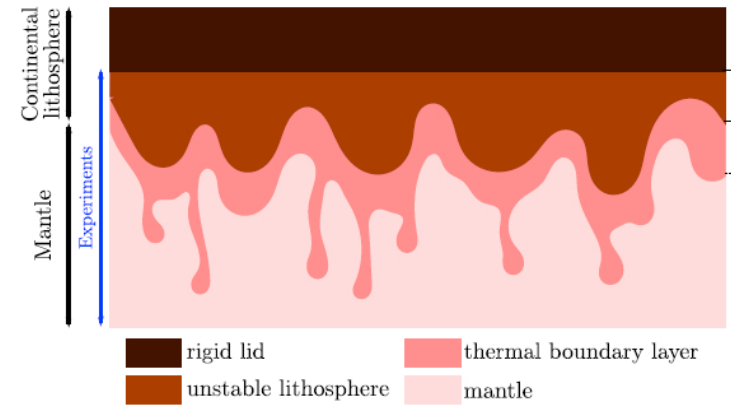


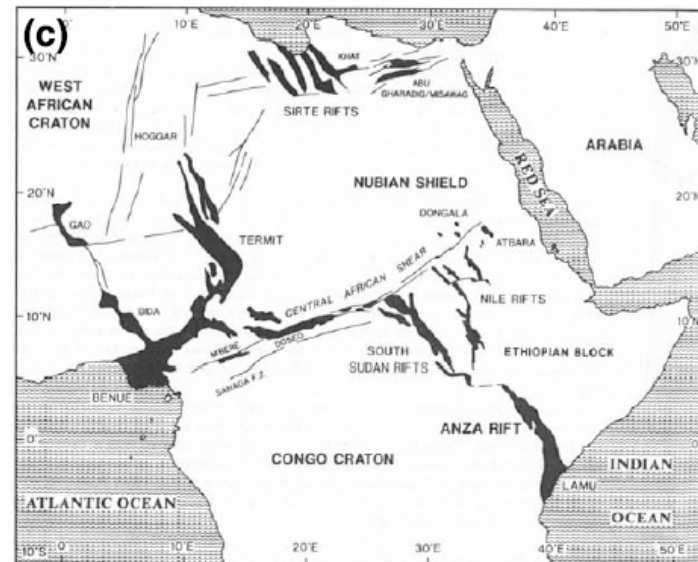
**Figure 6.** Unstable experiment ASTICO 24 ( $Ra = 404$ ,  $B = 0.23$ ,  $h_d/R = 0.066$ ). (a) Photograph in normal light. (b) Laser vertical cross section. (c) Time evolution of temperatures at three different depths. Note the temperature fluctuations that develop at midheight above the tank base, due to thinning of the dense basal block.



Laboratory experiments, planform of instabilities  
 radial spokes at the periphery  
 polygonal cells toward the center



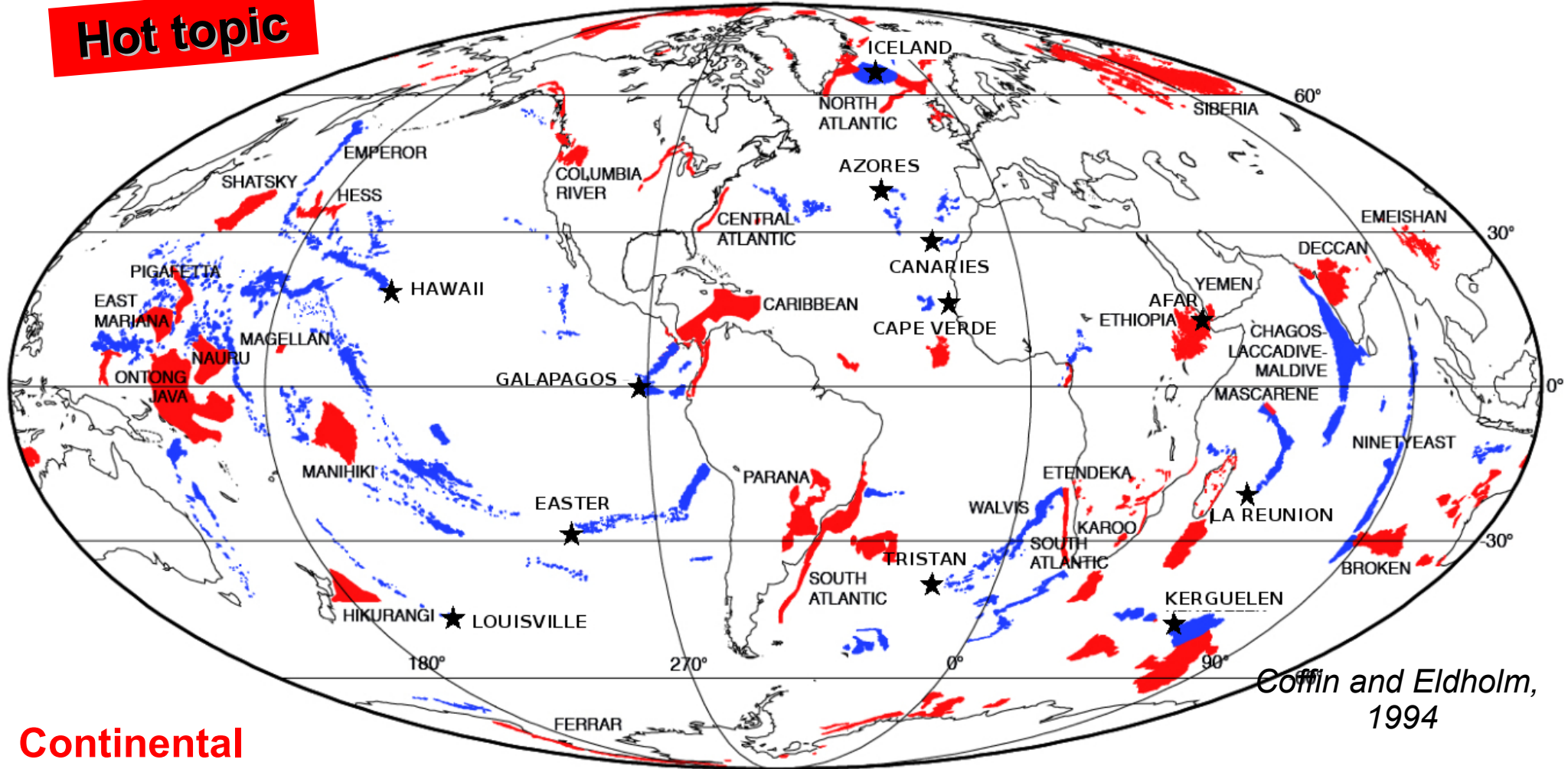
Geological structures in continents  
 linear rifts at 90° form continent/ocean boundary  
 domal uplifts and basins at the interior



The major rifts of Africa between 140 and 70 Myr

# Massive intraplate magmatism

Hot topic



Coffin and Eldholm, 1994

Continental  
Flood Basalt

- 258 Ma : Emeishan Traps
- 250 Ma : Siberia Trapps
- 184 Ma : Karoo, Southern Africa - Ferrar Antarctica
- 125 Ma : Paraná-Etendeka Province
- 65 Ma : Deccan Trapps
- 62 Ma : North Atlantic Tertiary Igneous Province
- 30 Ma : Ethiopian Traps
- 16 Ma : Columbia River



Deccan Traps (65 Ma). Magmatism lasting ~1 Ma.

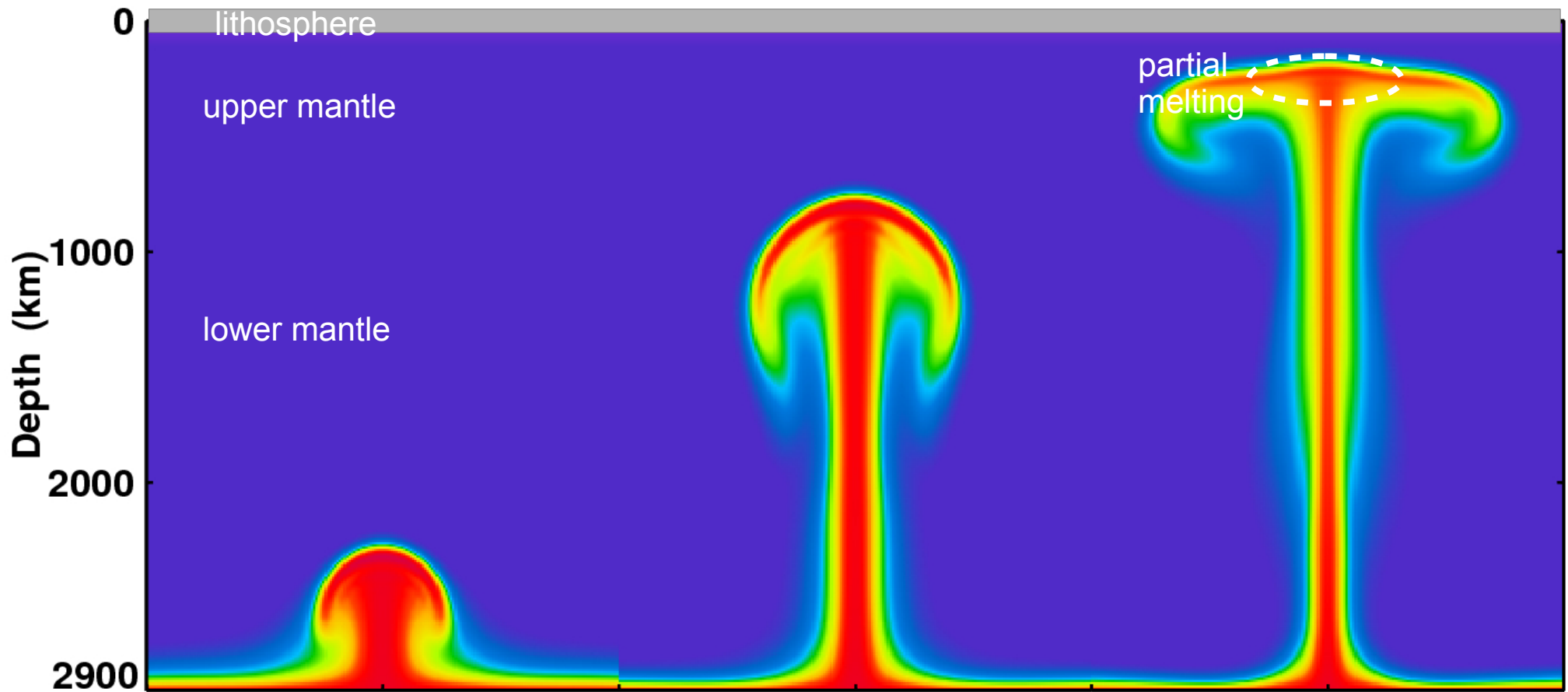
$h_{\max} \sim 2000-2400$  m. Volume  $\sim 1-2 \cdot 10^6$  km<sup>3</sup> Surface 500000 km<sup>2</sup> !

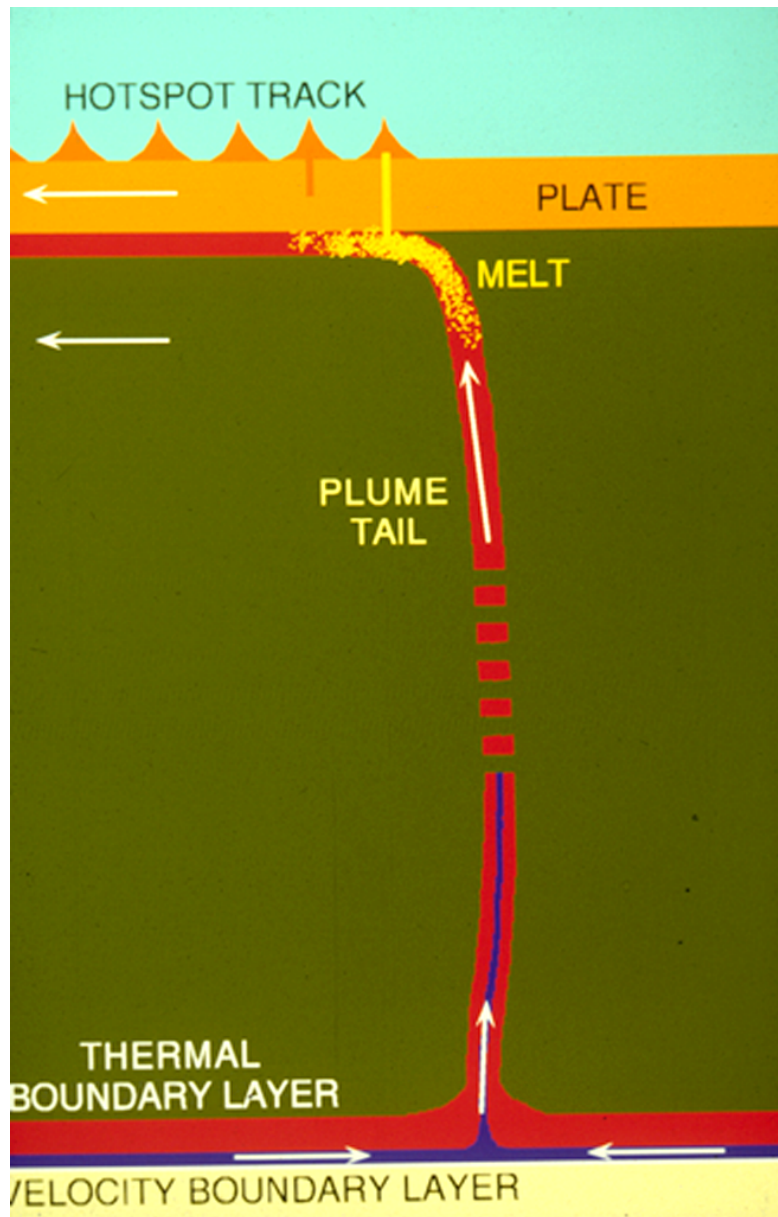
Deccan Traps associated to Reunion hotspot and underlying mantle plume.



# Classical model of a mantle plume

a large head (forms CFB and oceanic plateaux)  
and a narrow tail (forms long-lived hotspot magmatism)

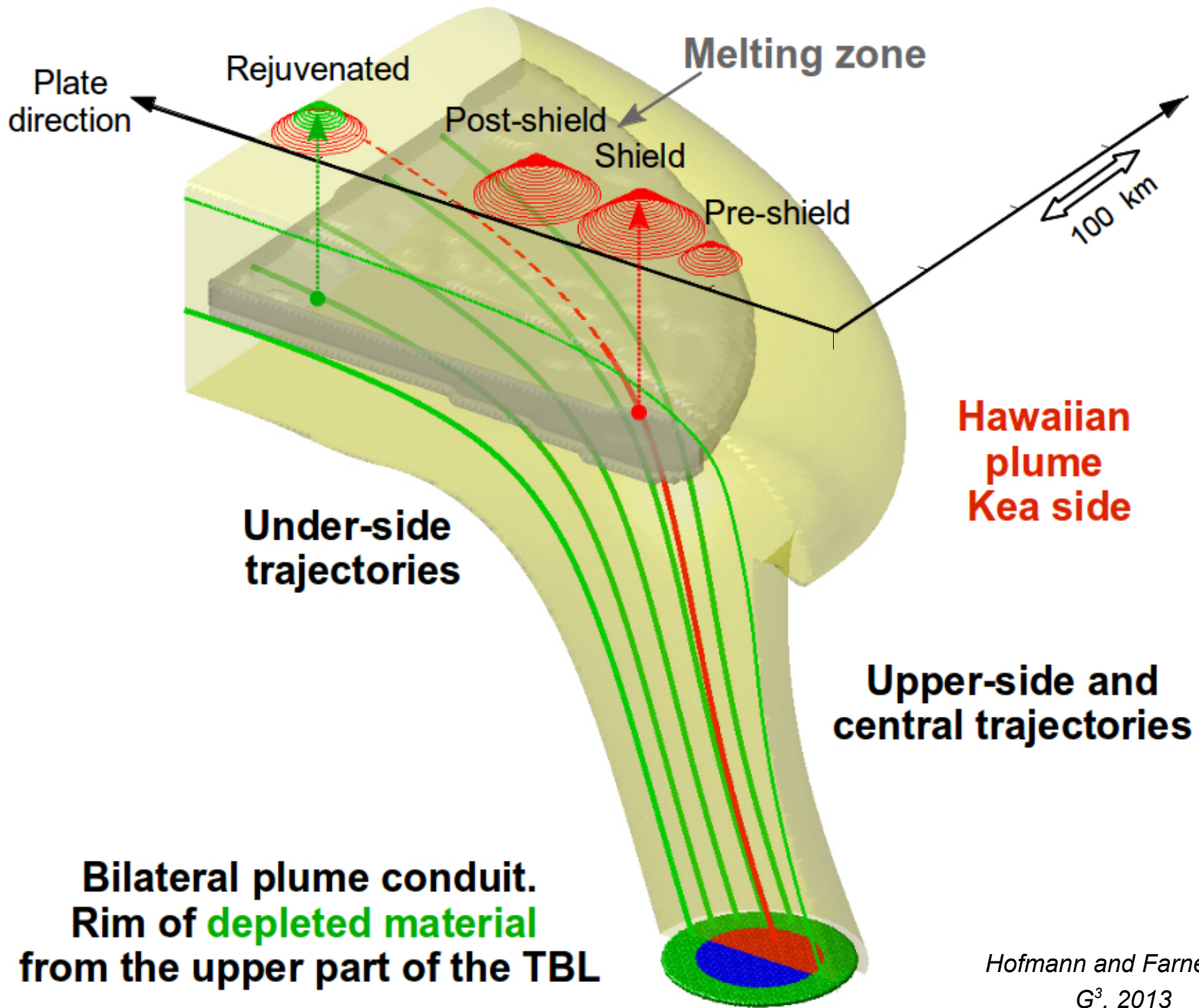


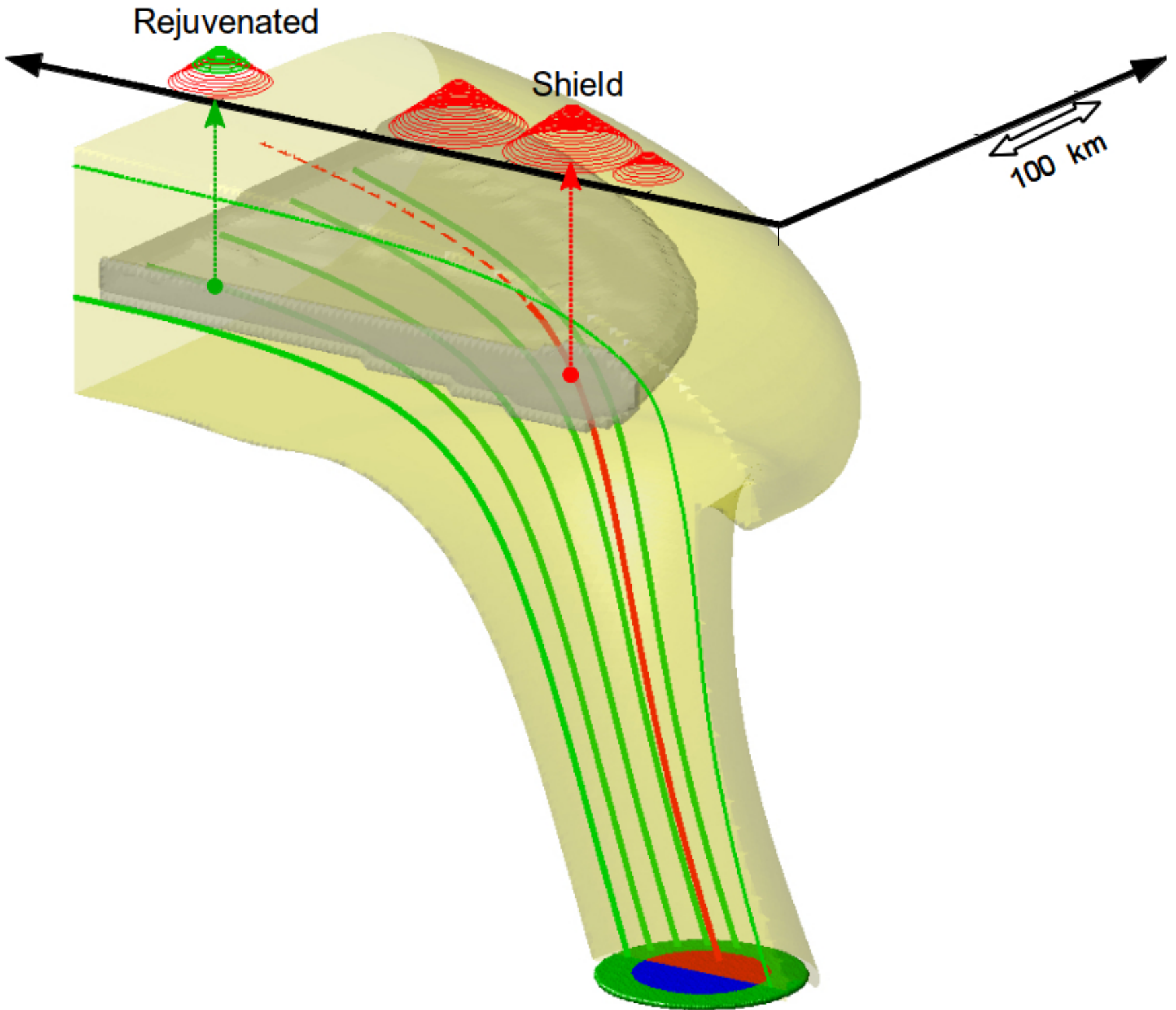


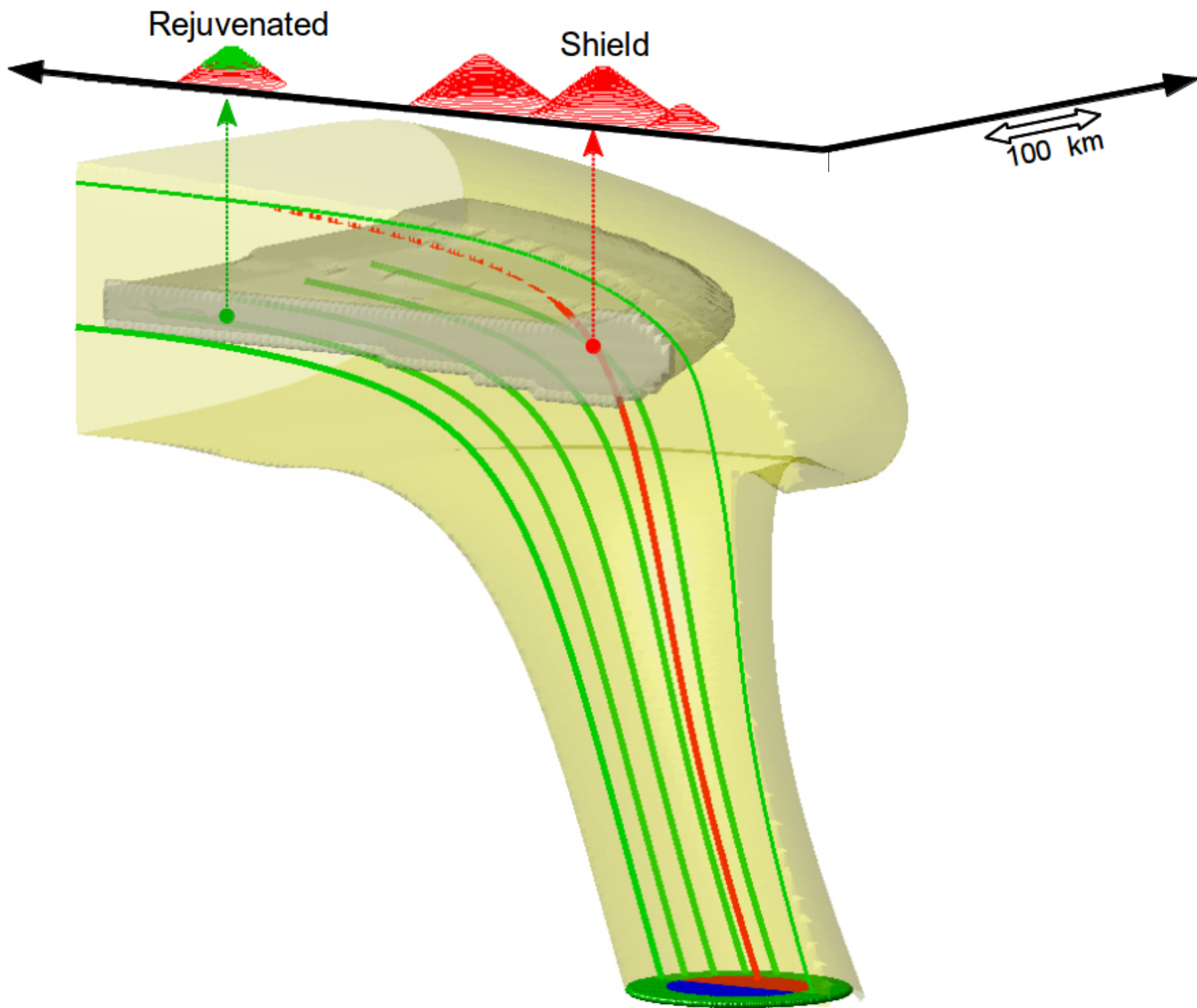
1971, Jason Morgan proposes the existence of a mantle plume beneath the Hawaiian hotspot

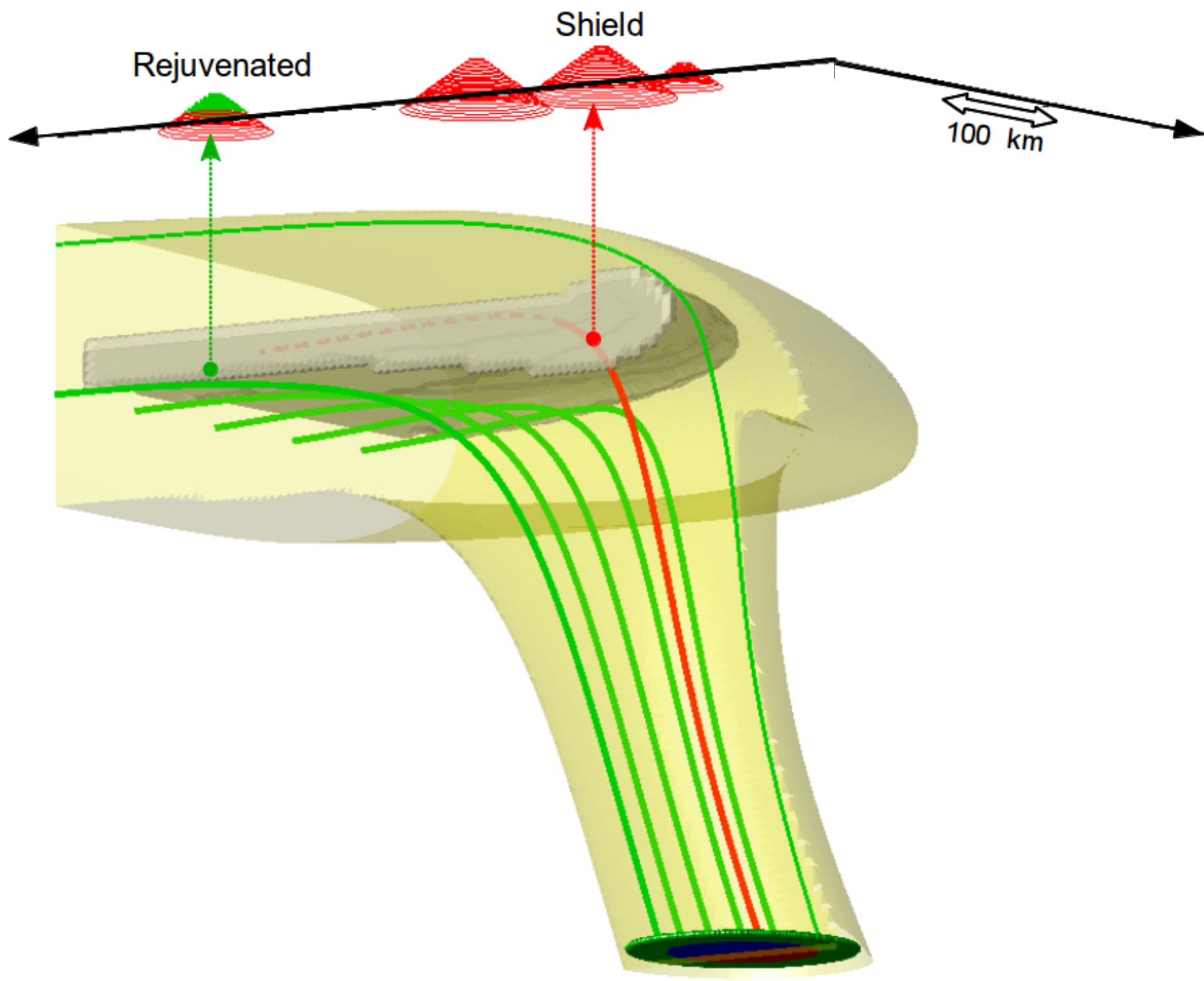


*J. Morgan and G. Bush, 2003*











*Photograph of 1000 m of continuous subaerial flood basalt stratigraphy in the Wrangell Mountains, Alaska. The yellow line marks the contact between Nikolai basalts (~230 Ma) and the overlying Chitistone Limestone. From Greene et al. (2008)*